

Chapter 1

ELEMENTS OF GROUP 1

Peter Hubberstey

1.1	INTRODUCTION	2
1.2	THE ELEMENTS	2
1.2.1	General Properties	3
1.2.2	The Alkali Metals as Solvent Media	4
1.2.3	Metallic Solutions	7
1.2.4	Intermetallic Compounds	8
1.3	MOLTEN SALTS	11
1.3.1	Structural and Thermodynamic Properties	11
1.3.2	Solution Properties	12
1.4	SIMPLE COMPOUNDS OF THE ALKALI METALS	19
1.4.1	Ion Pairs	19
1.4.2	Binary Compounds	21
1.4.3	Ternary Phictides	25
1.4.4	Ternary Oxides and Chalcogenides	25
1.4.5	Ternary Halides	28
1.5	COMPOUNDS OF THE ALKALI METALS CONTAINING ORGANIC MOLECULES OR COMPLEX IONS	33
1.5.1	Acyclic Polyether Complexes	33
1.5.2	Crown Complexes	35
1.5.3	Complexes of Macrocyclic Polyethers of Novel Design	42
1.5.4	Cryptates and Related Complexes	50
1.5.5	Salts of Carboxylic Acids	52
1.5.6	Salts of Nucleotides and Moieties of Biological Significance	56
1.5.7	Multimetal Complexes containing Alkali Metals	59
1.5.8	Lithium Derivatives	60
1.5.9	Sodium Derivatives	64
1.5.10	Potassium, Rubidium and Caesium Derivatives	65
	REFERENCES	68

1.1 INTRODUCTION

As for the 1980 review,¹ the papers abstracted for this and the next Chapter of the present review, have been restricted to those containing some facet of alkali or alkaline earth metal chemistry in which the role of the metal is unique; the application of these metals as simple counter cations is not considered. The data abstracted are such that they are best discussed in a number of subject topics currently of interest and importance; Chapters 1 and 2 are subdivided accordingly. For certain topics, (e.g., molten salts, polyether and cryptate complexes) the chemistry of the two groups of metals is closely interwoven; in these cases, the data abstracted are discussed once only in the appropriate section of this Chapter.

1.2 THE ELEMENTS

The application of lithium and of sodium in energy production and storage technology continually stimulates interest in the chemistry of these metals, their solutions and their intermetallic compounds. Chemical aspects of the role of liquid sodium as coolant in the fast breeder reactor and that of liquid lithium as a candidate for use as coolant/tritium breeder in the thermonuclear reactor were considered at the second international conference on 'Liquid Metal Technology in Energy Production' (April 1980, Richland, Wa., U.S.A.). Subjects covered for both liquid metals included corrosion and mass transfer, containment material compatibility and structural integrity, impurity monitoring and control together with basic physical chemistry. Similarly, the development of battery systems using lithium and sodium based electrodes has led to a large number of papers, primarily in the Journal of the Electrochemical Society, in which facets of the chemistry of these metals and of their intermetallic compounds are described. Systems which are considered include low temperature lithium-thionyl chloride or sulphuryl chloride cells and moderate temperature lithium or sodium-transition metal oxide or chalcogenide cells; aspects of chemistry covered include electrode-electrolyte compatibility studies, alkali metal incorporation in transition metal oxides or chalcogenides and the introduction of novel electrode materials constructed from Zintl phases based on lithium or sodium.

Since the majority of the papers published in these two fields are technologically oriented, they are of only peripheral interest

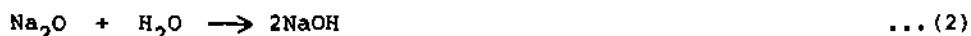
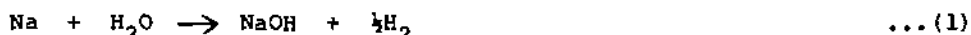
to the average inorganic chemist and hence will not be considered in detail. The specialist reader is referred to the Proceedings of the Conference² and the appropriate volume of the Journal of the Electrochemical Society.³ There are, however, a number of papers of more general interest; these have been abstracted and are reviewed, as appropriate, in the following subsections.

1.2.1 General Properties

A linear semi-empirical relationship has been shown to hold between the electron affinity of the alkali metals and the ionisation enthalpy of the neighbouring alkaline earth metal.⁴ Using this relationship, the electron affinity of francium has been calculated as $45.4 \pm 0.2 \text{ kJ.mol}^{-1}$.⁴

Three papers have been published during the period of this Report in which the combustion of alkali metals is considered.⁵⁻⁷ The relative behaviour of sodium and of potassium has been studied.⁵ Although theoretical analyses based on presently available kinetic data predict that potassium burns faster than sodium, it was observed experimentally that the two metals burned at similar rates.⁵

A novel method for the analysis of the combustion residues of a sodium fire have been proposed.⁶ By hydrolysing the residues, equations (1)-(3), titrating the NaOH so formed and simultaneously



measuring the volume of gases evolved and the $\text{H}_2:\text{O}_2$ ratio, their exact composition can be determined. The method has been tested on commercial sodium, Na_2O and Na_2O_2 and has been applied successfully to various sodium fires. It is recognised that the presence of NaO_2 may be a potential source of error. Thermodynamic calculations⁷ of the composition of the gas phase in equilibrium with burning sodium, however, suggest that NaO_2 cannot be formed in equilibrium with Na and Na_2O or Na_2O_2 and hence it will not be present in combustion residues obtained at normal pressure.

In a related study, the kinetics of alkali metal (Li, Na, K, Cs)

ionisation in an atmospheric pressure $\text{CO/O}_2/\text{N}_2$ flame of known temperature ($T=1930\text{K}$) have been redetermined⁸ using an r.f. resonance method.⁹

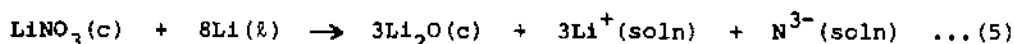
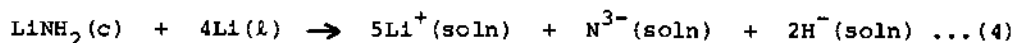
The feasibility of the preparation of high purity silicon by reaction of sodium with SiF_4 has been demonstrated.¹⁰ The reaction is commercially attractive in view of the relatively inexpensive starting materials, SiF_4 being obtained from H_2SiF_6 by precipitation and decomposition of Na_2SiF_6 .

The existence of $\text{Li}(\text{NH}_3)_4$ has been postulated from the results of a study of the Li-NH_3 diagram.¹¹ It is thought to melt congruently forming eutectics with solid NH_3 (at 88.80K) and with solid lithium (at 88.91K); although the eutectic compositions are unknown at present it seems likely that they are very close to $x_{\text{Li}}=0.2$, the stoichiometric composition of $\text{Li}(\text{NH}_3)_4$.

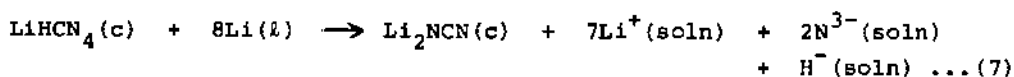
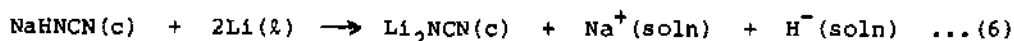
1.2.2 The Alkali Metals as Solvent Media

The solvent properties of liquid lithium and of liquid sodium have been the subject of two reviews.^{12,13} In both papers, it is emphasised that the major difference between the two solvents lies in the dominant reactive species: in liquid lithium it is dissolved nitrogen (Li_3N), but in liquid sodium it is dissolved oxygen (Na_2O). Thus, whereas transition metals readily form binary or ternary oxides in liquid sodium, in liquid lithium, they form corresponding nitrides. Indeed, the formation of oxides in liquid lithium is restricted to the lanthanide elements and, even then, only in the absence of Li_3N .

The solution chemistry of liquid lithium has been extensively studied¹²⁻¹⁹ during the past year. A summary of chemical interactions between non-metals dissolved in liquid lithium has been presented.¹² Whereas hydrogen (LiH) reacts with neither nitrogen (Li_3N) nor carbon (Li_2C_2), reaction between Li_3N and Li_2C_2 occurs at 673K to form Li_2NCN . Similarly Li_3N reacts with silicon ($\text{Li}_{22}\text{Si}_5$) to form an, as yet, unidentified ternary nitride, but not with germanium ($\text{Li}_{22}\text{Ge}_5$). In an attempt to extend and corroborate these observations, the stabilities of a number of salts of heteronuclear polyatomic anions (LiNH_2 , LiNO_3 , NaNHCN and LiHCN_4) towards lithium has been ascertained at 750K using a resistivity technique to monitor the species formed in solution.¹⁴ Whereas LiNH_2 and LiNO_3 undergo complete dissociation, equations (4) and (5), NaNHCN and LiHCN_4 only undergo partial dissociation,



equation (6) and (7), Li_2NCN being formed as a stable product.¹⁴



A number of these experimental observations have been theoretically corroborated in a thermochemical analysis ($500 \leq T/K \leq 1500$) of the Li-O-H, Li-O-C and Li-N-C systems.¹⁵ Metallurgical phase diagrams reveal that the compounds LiOH, Li_2CO_3 and LiCN cannot coexist with lithium and that interactions between Li_2O , LiH and Li_2C_2 will be negligible. Conversely, Li_2NCN has been shown to be stable to liquid lithium and hence strong interaction is expected to occur between Li_3N and Li_2C_2 .¹⁵

Nitride formation has been observed to be the primary feature of corrosion of several transition metals in liquid lithium.^{13,16,17} The corrosion of titanium, zirconium, vanadium, niobium and tantalum plates immersed in static lithium containing high Li_3N concentrations has been studied at 923K;¹³ X-ray powder diffraction analysis of the corroded surfaces showed the formation of binary or ternary nitrides. Resistivity studies of the reaction of chromium plates with Li_3N dissolved in liquid lithium have shown that at $T \geq 773\text{K}$ and at $x_{\text{N}} \geq 0.0005$, Li_3N attacks the chromium to produce a surface deposit which is tentatively suggested to be a ternary lithium-chromium-nitride.¹⁶ Preliminary compatibility studies between AISI 316 stainless steel plates and liquid lithium at 923K correlated a slight increase in plate weight with a reduction of the nitrogen content of the liquid metal.¹⁷

The stability of boron nitride towards lithium has been ascertained using an electrochemical method;¹⁸ reaction was observed to occur with the formation of Li_3N and an unidentified lithium boride.

The solubilities of silicon ($0.00 \leq x_{\text{Si}} \leq 0.0165$) and of germanium ($0.00 \leq x_{\text{Ge}} \leq 0.0872$) in liquid lithium have been determined by the

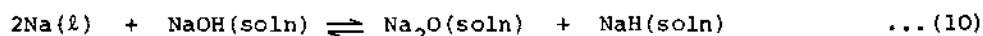
resistivity technique;¹⁹ they can be represented, in part, by equations (8) and (9). X-ray powder diffraction studies show that the compounds $\text{Li}_{22}\text{Si}_5$ and $\text{Li}_{22}\text{Ge}_5$ precipitate from dilute

$$\ln x_{\text{Si}} = 5.548 - 6775/T \quad 500 \leq T/K \leq 700 \quad \dots (8)$$

$$\ln x_{\text{Ge}} = 5.459 - 6630/T \quad 530 \leq T/K \leq 715 \quad \dots (9)$$

solutions of silicon and of germanium in liquid lithium. The resulting point of $\text{Li}_{22}\text{Ge}_5$ (934K) and the lithium-rich eutectic horizontal (453.5K) have been established by thermal methods and used to augment the Li-Ge phase diagram ($0.00 \leq x_{\text{Ge}} \leq 0.20$).¹⁹

Results have been reported for sodium solutions containing a number of diverse solutes, including non-metals,^{20,21} metals²² and metal oxides.²³ The kinetics of the decomposition of NaOH in liquid sodium, equation (10), have been determined ($573 \leq T/K \leq 773$)



by monitoring the variation in concentration of the dissolved decomposition products using electrochemical oxygen and hydrogen meters.²⁰ The kinetics of the gettering of dissolved oxygen (by uranium foil) and of dissolved hydrogen (by yttrium foil) have been determined similarly.²⁰ Equilibrium measurements on the Na-U-O system have been used to derive thermodynamic data for the formation of Na_3UO_4 , the ternary oxide in equilibrium with UO_2 and sodium containing dissolved oxygen; the data are reported in section 1.4.4.²⁰

In an independent, yet complementary investigation, the solubility of UO_2 (and of PuO_2) in liquid sodium has been determined experimentally ($948 \leq T/K \leq 1083$).²³ The results exhibit considerable scatter and appear to be dependent on the oxygen content of the sodium; at 1073K and an oxygen concentration of < 1 wppm O, a maximum solubility value of 0.06 wppm UO_2 (0.02 wppm PuO_2) is quoted. It is tacitly assumed that $\text{UO}_2(\text{PuO}_2)$ is the soluble species. As pointed out earlier, however, $\text{Na}_3\text{UO}_4(\text{Na}_3\text{PuO}_4)$ is also present as a solid phase in this system and may be the soluble species especially at higher oxygen concentrations. This duplicity of dissolved species is probably responsible for the observed scatter in the data and their dependence on oxygen

concentration.²³

Preliminary compatibility studies have also been effected between commercially available UO_2 ceramics and liquid sodium;²⁴ no deterioration of the UO_2 was observed, even after 100 hours immersion in sodium at 1173K. Comparative studies were undertaken on ceramics based on ThO_2 , MgO and Al_2O_3 .²⁴ Whereas ThO_2 , like UO_2 , did not appear affected after 100 hours exposure at 1173K, the MgO - and Al_2O_3 -based ceramics exhibited discoloration of the surface and marked deterioration in structural integrity.

Electrochemical studies of carbon activity in liquid sodium solutions ($T=913\text{K}$) strongly suggest that carbon dissolves as C_2 units and in accordance with Henry's Law.²¹ The results also give an approximate value (16 wppm C) for carbon solubility in sodium with respect to graphite at 913K. Similar studies have also shown that the carbon formed (together with hydrogen and methane) as a product of the reaction of mineral oil with liquid sodium readily dissolves in the liquid metal increasing its carbon activity.²¹

The solubility of iron in liquid sodium containing very low levels of oxygen has been determined by a radio-tracer technique;²² it can be represented by equation (11). Preliminary solubility

$$\log S(\text{wppm Fe}) = 4.720 - 4116/T \quad 658 \leq T/\text{K} \leq 997 \quad \dots(11)$$

data have also been reported for manganese in liquid lithium;²² they lie in the range from 0.1 to 10 wppm Mn ($623 \leq T/\text{K} \leq 923$). As in the case of UO_2 (PuO_2) the solubility data for both iron and manganese are susceptible to the presence of oxygen in the liquid sodium. They increase markedly with increase in oxygen concentration, presumably owing to the formation of more soluble oxygenated species.²²

1.2.3 Metallic Solutions

Chemical short range ordering (i.e., pseudo compound formation) in liquid phase binary metallic solutions has been studied in a number of laboratories.²⁵⁻³⁰ Thermodynamic investigations of liquid Li-Ag ,²⁵ Li-Pb ,²⁵ Na-Hg ,²⁶ and Na-Tl ²⁷ solutions have provided evidence for ordering in these systems. The excess stabilities of Li-Ag and of Li-Pb solutions exhibit maxima at $\text{Li}_{0.5}\text{Ag}_{0.5}$ and $\text{Li}_{0.80}\text{Pb}_{0.20}$.²⁵ Similar maxima occur in the heat

capacities of liquid Na-Hg²⁶ and of Na-Tl²⁷ solutions at Na_{0.33}Hg_{0.67} and Na_{0.50}Tl_{0.50}; the compositions at which these maxima occur can be correlated with the stoichiometries of the intermetallic compounds, LiAg, Li₂₂Pb₅, NaHg₂ and NaTl. The thermodynamic properties of the Na-Hg solutions were measured not only as a function of temperature and composition but also as a function of pressure. In principle, all the thermodynamic properties of a liquid binary metal solution A_xB_{1-x} can be determined using this method, providing they are known for the pure components A and B.

Entropy data for liquid Na-Pb solutions, which exhibit anomalous behaviour at Na_{0.8}Pb_{0.2} have been successfully calculated using the theory of the entropy of mixing of compound-forming liquid solutions on the basis of the pseudobinary mixture of hard spheres model.²⁸

The origin of the short range ordering phenomenon, is thought to be ionic in nature. Indeed, theoretical studies of M-Au (M = Li, Na, K, Rb, Cs) liquid solutions have been undertaken²⁹ using a tight-binding model which includes short range order and charge transfer in a self-consistent way. The model accounts satisfactorily for both the metallic conductivity of Li_{0.50}Au_{0.50} and the ionic conductivity of Cs_{0.50}Au_{0.50}. Transfer of electronic charge from potassium to sodium has even been shown to be a possibility in Na-K liquid solutions.³⁰

1.2.4 Intermetallic Compounds

Wen and Huggins^{31,32} have undertaken a comprehensive emf study of the thermodynamic properties of the intermetallic compounds formed in the Li-Ga³¹ and Li-Sn³² systems; materials such as these are presently being considered for use as either reactants or mixed conducting matrices in lithium-based battery electrodes. Coulombic titration curves showed that three compounds exist in the Li-Ga system (nominal compositions Li₂Ga, Li₃Ga₂, LiGa) and that six compounds exist in the Li-Sn system (nominal compositions Li₂₂Sn₅, Li₇Sn₂, Li₁₃Sn₅, Li₅Sn₂, Li₇Sn₃ and LiSn). Thermodynamic data for the intermediate phases are collected in Table 1. The existence of Li₂Ga, Li₃Ga₂ and LiGa was further substantiated by X-ray powder diffraction analysis. Evidence for Li₅Ga₄ was not obtained in either the coulombic or the structural study.³¹ Schafer et al,³³ however, have prepared single crystals of this material; X-ray diffraction studies indicate that it has a structure intermediate

Table 1. Thermodynamic data (688K) for the intermediate phases in the Li-Ga³¹ and Li-Sn³² systems.

Phase	$-\Delta H_f^0(X,c,688K)$ kJ mol ⁻¹	$-\Delta S_f^0(X,c,688K)$ J K ⁻¹ mol ⁻¹	$-\Delta G_f^0(X,c,688K)$ kJ mol ⁻¹
Li ₂ Ga	-	-	62
Li ₃ Ga ₂	-	-	115
LiGa	-	-	51
Li ₂₂ Sn ₅	220	75.6	168.0
Li ₇ Sn ₂	197	63.1	153.6
Li ₁₃ Sn ₅	165	52.8	128.7
Li ₅ Sn ₂	159	49.7	124.8
Li ₇ Sn ₃	151	47.7	118.2
LiSn	70	25.8	52.2

between those of LiGa and Li₃Ga₂ (Figure 1).

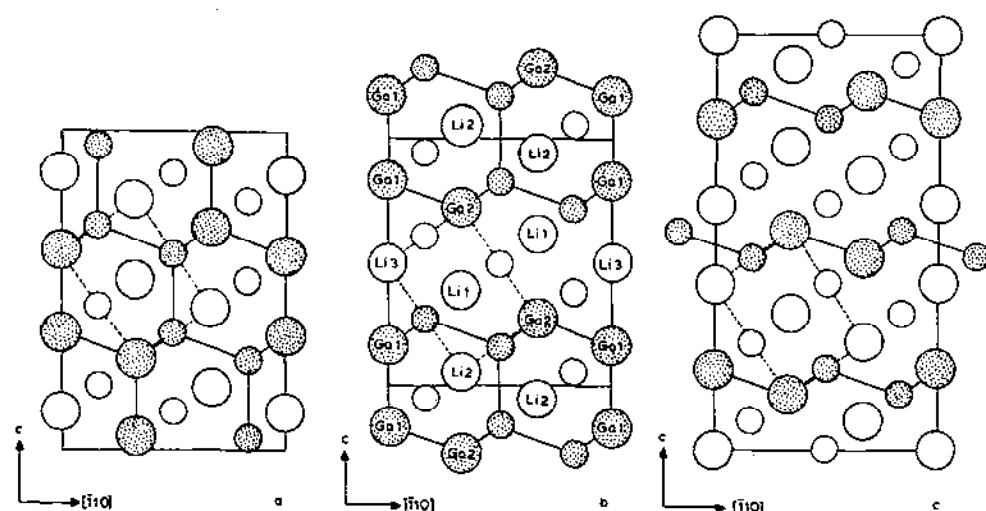


Figure 1. Projection onto the (110) plane of the unit cells of (a) LiGa (in a pseudo-rhombohedral setting), (b) Li₅Ga₄ and (c) Li₃Ga₂ (reproduced by permission from Z. anorg. allg. Chem., 474(1981)221).

Table 2. Unit cell parameters for binary and ternary intermetallic phases.

Phase	Symmetry	Space Group	a/pm	b/pm	c/pm	$\beta/^\circ$	Reference
Li_2Ga	orthorhombic	Cmcm	456.2	954.2	436.4	-	31
Li_3Ga_2	rhombohedral	$\text{R}\bar{3}\text{m}$	436.7	-	1389.6	-	31
LiGa	cubic	(NaTl)	621.3	-	-	-	31
Li_5Ga_4	hexagonal	$\text{P}\bar{3}\text{m}1$	437.5	-	825.7	-	33
RbGa_3	tetragonal	$\text{I}\bar{4}\text{m}2$	631.5	-	1500.0	-	34
RbGa_7	monoclinic	$\text{C}2/\text{m}$	1143.2	660.3	1025.9	111.85	35
$\alpha\text{-Li}_2\text{ZnGe}$	cubic	(Li_3Bi)	614.8	-	-	-	36
$\beta\text{-Li}_2\text{ZnGe}$	hexagonal	$\text{P}\bar{3}\text{m}1$	432.6	-	1647.0	-	36
$\text{Rb}_4\text{Au}_7\text{Sn}_2$	rhombohedral	$\text{R}\bar{3}\text{m}$	680.1	-	2909.0	-	37

Phase transitions in Li_2ZnGe have been studied by X-ray diffraction and d.t.a. methods.³⁶ The transition from $\beta\text{-Li}_2\text{ZnGe}$ (hexagonal- Na_3As structure) to $\alpha\text{-Li}_2\text{ZnGe}$ (cubic- Li_3Bi structure) occurs at 775K with $\Delta H_{\text{trans}}^\circ = 4.5 \text{ kJ mol}^{-1}$; $\alpha\text{-Li}_2\text{ZnGe}$ melts at 1058K with $\Delta H_{\text{m}}^\circ = 39.9 \text{ kJ mol}^{-1}$. Pertinent crystallographic data are included in Table 2, together with unit cell parameters for $\text{Rb}_4\text{Au}_7\text{Sn}_2$.³⁷

Fascinating observations have been made when Zintl phases have been extracted into ethylene diamine containing the cryptate, C222.³⁸⁻⁴⁰ ¹¹⁹Sn-n.m.r. studies of the solutions resulting from contact of Na_xSn alloys ($1 \leq x \leq 2$) with ethylenediamine in both the presence and absence of C222 indicate the presence of the naked cluster, Sn_4^{2-} . Similarly Na-Sn-Tl, Na-Sn-Ge and Na-Sn-Te alloys give rise to the heteroatomic naked clusters, TlSn_8^{5-} , nido- $\text{Sn}_{9-x}\text{Ge}_x^{4-}$ ($0 \leq x \leq 9$) and SnTe_4^{4-} , respectively. The complexes are thought to be polyhedral cluster anions, with the exception of SnTe_4^{4-} which appears to be a classical Sn-centred tetrahedral tellurostannate anion.³⁸ The fluxional behaviour of Sn_4^{2-} in solution has been predicted from ab initio calculations.³⁹ Extraction of KSn_2 with ethylenediamine containing C222 gave, inter alia, black plate-shaped crystals which analysed as $[\text{K}(\text{C}222)]_2.\text{Sn}_4.\text{en}$; $[\text{Na}(\text{C}222)]_2.\text{Ge}_4$ has also been synthesised.⁴⁰ Single crystal X-ray diffraction studies have shown the salts to contain the complex cryptate cation $[\text{M}(\text{C}222)]^+$ and the 18-electron, tetrahedral cluster

anions, Sn_4^{2-} and Ge_4^{2-} .⁴⁰

1.3 MOLTEN SALTS

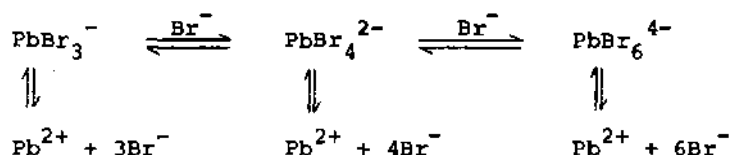
Recent interest in molten salt chemistry has centred on their structural characteristics and on the behaviour of dissolved solutes. The change of emphasis noted in the previous Report⁴¹ has been maintained, there being a higher number of papers extracted for the solution properties subsection vis-a-vis the structural and thermodynamic properties subsection.

1.3.1 Structural and Thermodynamic Properties

The structure of molten NaCl has been reinvestigated using X-ray diffraction methods.⁴² The first peak position in the radial distribution curve occurs at 273pm. This value is consistent with that (275pm) obtained in an earlier X-ray diffraction analysis⁴³ and the summation of the cation and anion radii (276pm); it is inferred that the value (260pm) obtained by neutron diffraction methods⁴⁴ is low and should not be used as evidence of coincidence with the computer-simulation calculations.

Thermodynamic parameters of NaCl-KCl,⁴⁵ NaCl-AlCl₃,⁴⁶ NaCl-NiCl₂,⁴⁷ KCl-CdCl₂,⁴⁸ MBr (M=K,Rb,Cs)-PbBr₂⁴⁹ and LiI-NdI₃⁵⁰ molten salt mixtures have been determined by vapour phase,^{45,46,50} calorimetric⁴⁸ and electrochemical^{46,47,49} methods. With the exception of the NaCl-KCl mixtures, the thermodynamic data have been used to derive structural characteristics. Substantial evidence is provided for the stabilisation and structural ordering of the NaCl-AlCl₃,⁴⁶ NaCl-NiCl₂⁴⁷ and KCl-CdCl₂⁴⁸ melts near the stoichiometric compositions NaAlCl₄, Na₂NiCl₄ and KCdCl₃, respectively; a model based on alkali metal cations and discrete complex anions has been proposed for these systems.⁴⁷

The results for the MBr-PbBr₂ system⁴⁹ indicate that a number of complex ions, including PbBr_3^{2-} , PbBr_4^{2-} and possibly PbBr_6^{4-} , are present in the melts and that a series of equilibria exist as shown in scheme 1:

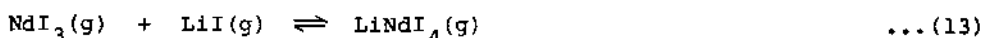


Scheme 1

Similarly, the results for the LiI-NdI_3 system⁵⁰ indicate that iodine is present in three different anionic environments - terminal, bridged and free - under equilibrium conditions, equation (12).



Different species are present in the gas phase equilibrium, equation (13), above these liquids.



The salient features of the thermodynamic analysis of the NaCl-KCl system⁴⁵ are the small negative deviations from ideality observed in the liquid state and the large positive deviations from ideality in the solid state; the latter are attributed to the strain energy which arises from the difference in radii between Na^+ and K^+ .⁴⁵

Raman spectra have been recorded for Li_2SO_4 ,^{51,52} Na_2SO_4 ,⁵¹ Na_2CO_3 ,⁵¹ K_2CO_3 ,⁵¹ NaClO_3 ,⁵¹ melts and for $\text{Li}_2\text{SO}_4\text{-K}_2\text{SO}_4$,^{51,52} $\text{Li}_2\text{CO}_3\text{-K}_2\text{CO}_3$,⁵¹ and $\text{NaClO}_3\text{-AgClO}_3$,⁵¹ molten mixtures as a function of temperature and, where appropriate, composition. The symmetric stretching frequencies (ν_1) of the anions in these melts have been combined with literature data for other oxyanions and have been correlated with the polarizing power and polarizability of the cation.⁵¹ The asymmetric stretching frequency (ν_3) of the SO_4^{2-} anion is split in Li_2SO_4 and $\text{Li}_2\text{SO}_4\text{-K}_2\text{SO}_4$ melts, indicating the presence of structures with C_{3v} and C_s , rather than T_d , symmetry;⁵² these findings are in agreement with models proposed from X-ray diffraction studies.⁵³

Pressure-composition-temperature data have been collected for the LiCl-LiH system by measuring equilibrium hydrogen pressures in a Sievert's apparatus.⁵⁴ The system follows Sievert's Law:

$$P_{\text{H}_2}^{\frac{1}{2}} = k \cdot x_{\text{LiH}}/x_{\text{LiCl}} \quad \dots(14)$$

for compositions below 10 mol % LiH .⁵⁴

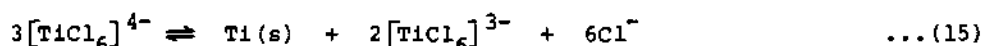
1.3.2 Solution Properties

The solvent properties of a wide range of molten salts have been studied; although halides and nitrates predominate as reaction media,

some data have been reported for carbonates, sulphates and pyrosulphates.

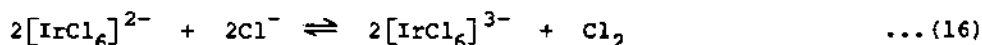
Solubility data for NiO and Co_3O_4 in molten NaCl (1100K) have been determined⁵⁵ by coulombic titration of the respective chlorides (NiCl_2 , CoCl_2) with electrochemically generated oxide ion. Analysis of the data is complicated by competitive reactions which result in the formation of Na_2O_2 , NaNiO_2 and NaCoO_2 .⁵⁵

Electronic absorption spectroscopic studies of the coordination chemistry of titanium halides in LiCl-KCl eutectic ($658 \leq T/K \leq 1185$)⁵⁶ and NaCl-KCl eutectic containing varying amounts of KF ($963 \leq T/K \leq 1023$)⁵⁷ have been undertaken. In LiCl-KCl melts, Ti(III) ions are present in an octahedral $[\text{TiCl}_6]^{3-}$ -tetrahedral $[\text{TiCl}_4]^-$ coordination equilibrium, the equilibrium favouring $[\text{TiCl}_4]^-$ at elevated temperatures. Although Ti(II) ions are octahedrally coordinated $[\text{TiCl}_6]^{4-}$ in this solvent a disproportionation equilibrium, equation (15), is established as evidenced by the



formation of a metallic film. In NaCl-KCl melts, Ti(III) ions form tetragonally distorted octahedral $[\text{TiCl}_6]^{3-}$ complexes with νD_{4h} symmetry. As the concentration of KF is increased, mixed coordination species $[\text{TiCl}_x\text{F}_{6-x}]^{3-}$ are obtained until at $\text{KF}:\text{Ti(III)}$ ratios in excess of 100, the trigonally distorted octahedral $[\text{TiF}_6]^{3-}$ complex with νD_3 symmetry is formed.⁵⁷

Chlorination of iridium in molten KCl or LiCl-KCl eutectic leads to a mixture of $[\text{IrCl}_6]^{3-}$ and $[\text{IrCl}_6]^{2-}$ in the ratio $\text{Ir(III)}:\text{Ir(IV)} = 2:1$;⁵⁸ this is thought to be indicative of the establishment of an intramolecular redox equilibrium, equation (16).



Reactions of FeS electrodes in LiCl-KCl melts of varying composition (673K)⁵⁹ and in LiF-LiCl-LiBr (0.22-0.31-0.47) molten salt (700K)⁶⁰ have been elucidated by a combination of phase studies, cyclic voltammetry and emf measurements. In LiCl-KCl melts,⁵⁹ six electrochemical and four chemical reactions were established; they involved the formation of either Li_2FeS_2 or $\text{LiK}_6\text{Fe}_{24}\text{S}_{26}\text{Cl}$. The experiments using LiF-LiCl-LiBr as solvent were undertaken to ascertain the free energy of formation of

Li_2FeS_2 ; ⁶⁰ $\Delta G_F^\circ(\text{Li}_2\text{FeS}_2, \text{C}, 700\text{K}) = -524.9 \text{ kJ mol}^{-1}$ - this is equivalent to a free energy of formation from Li_2S and FeS of -1.9 kJ mol^{-1} at 700K. ⁶⁰

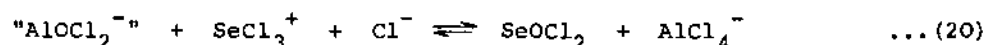
The deposition characteristics of gadolinium from LiF-LiCl-GdF_3 (0.18-0.80-0.02), $\text{LiF-BaF}_2\text{-GdF}_3$ (0.75-0.10-0.15) and LiF-GdF_3 (0.75-0.25) electrolytes have been evaluated. ⁶¹ The morphology of the deposited gadolinium differed with the electrolyte, plate-like, block-like and needle-like crystals being obtained from the three molten salts, respectively. ⁶¹

The corrosion behaviour of platinum, gold, tin oxide and glassy carbon electrodes immersed in LiCl-KCl eutectic at 723K has been assessed by electrochemical characterisation of the $\text{UO}_2^{2+}/\text{UO}_2^+$ couple using normal pulse polarography. ⁶² Whereas platinum and gold electrodes corroded in the melt, tin oxide and glassy carbon electrodes were inert. The structural integrity of vanadium-titanium-aluminium-molybdenum (0.90-0.08-0.01-0.01) alloy electrodes immersed in molten LiCl-KCl eutectic has also been ascertained. ⁶³

Several features of the chemistry of chloroaluminate melts have been elucidated. ^{56,64-70} The solubility of NaCl in NaCl-AlCl_3 melts at 448K has been found to be $x_{\text{NaCl}} = 0.50209$ by potentiometric measurements with chlorine/chloride electrodes. ⁶⁴ Furthermore in the $p\text{Cl}$ range of 3.885-5.034, the measured potential of these electrodes could be rationalised by a combination of three reactions, equations (17)-(19). ⁶⁴ Solution of SeCl_4 in this melt in the $p\text{Cl}$



range 1.183-4.662 leads to SeCl_3^+ . ⁶⁴ Under basic conditions ($p\text{Cl} < 2.58$) and in the presence of oxide impurity (formulated as " AlOCl_2^- ") SeCl_3^+ reacts to form SeOCl_2 (equation (20)). Under acidic conditions ($p\text{Cl} > 2.58$) no reaction occurs, the oxide



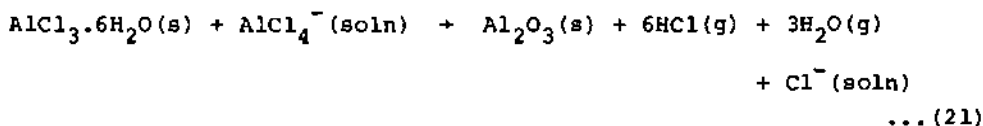
impurity existing in the form of the oxochloroaluminium compound. ⁶⁴

Electronic absorption spectroscopic studies of the coordination

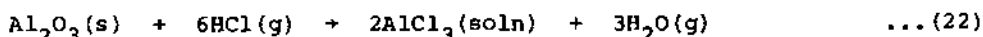
chemistry of titanium halides in KCl-AlCl_3 melts ($1.00 \leq x_{\text{AlCl}_3} \leq 0.49$; $471 \leq T/K \leq 894$) have been effected.⁵⁶ Although Ti(III) ions are octahedrally coordinated $[\text{TiCl}_6]^{3-}$ in pure AlCl_3 and in KCl-AlCl_3 melts with $x_{\text{AlCl}_3} \geq 0.67$, octahedral $[\text{TiCl}_6]^{3-}$ -tetrahedral $[\text{TiCl}_4]^-$ coordination equilibria are established at lower AlCl_3 contents. Ti(II) ions adopt octahedral coordination $[\text{TiCl}_6]^{4-}$ in AlCl_3 and in KCl-AlCl_3 melts with $x_{\text{AlCl}_3} \geq 0.51$. The situation is complicated, however, by a disproportionation equilibrium which occurs for $x_{\text{AlCl}_3} \leq 0.6$ and which culminates at $x_{\text{AlCl}_3} = 0.49$ where Ti(II) ions are unstable and the spectrum of Ti(III) ions in an octahedral-tetrahedral coordination equilibrium is obtained.⁵⁶

Oxidation reactions of aluminium,^{65,66} sulphur⁶⁷ and iodine⁶⁸ have been studied in NaCl-AlCl_3 melts. The kinetics of the oxidation of aluminium to AlCl_3 in equimolar NaCl-AlCl_3 melt ($620 \leq T/K \leq 780$) using PbCl_2 , CdCl_2 or CuCl_2 have been shown to be first order.⁶⁵ In the presence of chlorine gas the halogen carrier (e.g. PbCl_2) can be recovered in good yield.⁶⁶ U.v.-visible and e.s.r. spectroscopic studies ($405 \leq T/K \leq 523$) of the electro-oxidation of sulphur in acidic NaCl-AlCl_3 ($0.37-0.63$) melts clearly show⁶⁷ that the oxidation of S_8 to SCl_3^+ is very complex; suggested intermediates included diverse polymeric sulphur cations and SCl_2 .⁶⁷ Resonance Raman and u.v.-visible spectroscopic studies, together with thin layer coulometry, have shown⁶⁸ that whereas oxidation of iodine to ICl proceeds via I_2^+ in acidic NaCl-AlCl_3 ($0.37-0.63$) melts, oxidation in basic NaCl-AlCl_3 ($0.50-0.50$) melts leads directly to ICl .

Low temperature ($373 \leq T/K \leq 393$) dehydration of $\text{AlCl}_3 \cdot 6\text{H}_2\text{O}$ in MCl-AlCl_3 ($\text{M} = \text{Li, Na, K}$) melts is not possible owing to the thermal decomposition of the hexahydrate into Al_2O_3 , equation (21).⁶⁹ At higher temperatures ($673 \leq T/K \leq 773$), however, the alumina so



formed is reactive to overpressures of HCl and readily forms the anhydrous chloride, equation (22).

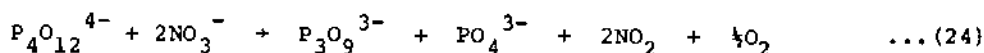
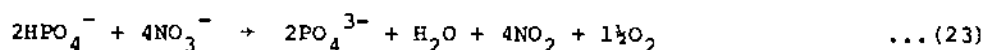


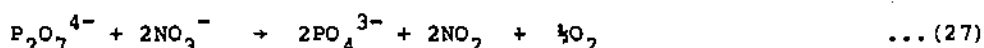
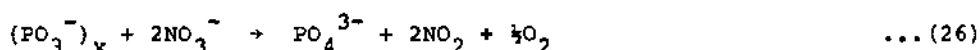
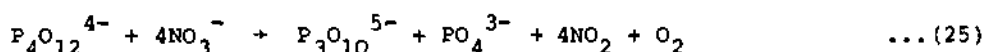
Electrodeposition and dissolution processes occurring on aluminium surfaces submerged in LiCl-AlCl_3 (0.5075-0.4925) molten salts have been elucidated.⁷⁰ The major surface product, LiAl , is formed predominantly by a deposition process rather than an implantation mechanism. Similar studies were also conducted using NaCl-AlCl_3 (0.5025-0.4975) melts;⁷⁰ unfortunately the role of dissolved oxygen species in this melt complicates the interpretation of the deposition and dissolution data.

The application of chloroantimonates as molten salt solvents has also been investigated.^{71,72} The solubility of antimony metal in molten CsCl-SbCl_3 ($0.00 < x_{\text{CsCl}} < 0.80$; $678 < T/K < 915$) has been determined.⁷¹ Isothermal solubility data pass through a maximum at $x_{\text{CsCl}} \approx 0.3$. It is postulated that this behaviour is due to the formation of chlorophilic and chlorophobic species. Whereas both species are thought to exist in melts rich in SbCl_3 , the chlorophilic species is stabilised in melts rich in CsCl .⁷¹

Electronic absorption spectra of solutions of a number of transition metal chlorides (MCl_3 ($M = \text{Ti, V, Cr, Fe}$) and MCl_2 ($M = \text{Mn, Co, Ni}$)) have been studied⁷² in KCl-SbCl_3 (0.08-0.92) melts and compared with similar data for SbCl_3 melts. The predominant coordination geometry observed is octahedral; it is only in the case of Mn(II) and Co(II) that tetrahedral coordination geometries are observed. The Co(II) system exhibits an octahedral-tetrahedral coordination equilibrium which is dependent on the chloride content of the melt.⁷²

The solution chemistry of molten nitrates has been the subject of several papers; solvents considered include KNO_3 ,⁷³ $\text{LiNO}_3\text{-KNO}_3$,⁷⁸ eutectic,^{74,75} equimolar $\text{NaNO}_3\text{-KNO}_3$,^{76,77} $\text{NaNO}_3\text{-Ba(NO}_3)_2$ eutectic⁷⁹ and $\text{KNO}_3\text{-Ba(NO}_3)_2$ eutectic.⁷⁹ Cryoscopic studies⁷³ of solutions of diverse phosphates in molten KNO_3 suggest that whereas the polyanions $\text{P}_3\text{O}_{10}^{5-}$ and $\text{P}_3\text{O}_9^{3-}$ are stable, the simple phosphates and classical metaphosphates dissociate with the formation of the stable PO_4^{3-} anion, and in some cases, $\text{P}_3\text{O}_{10}^{5-}$ or $\text{P}_3\text{O}_9^{3-}$. The reactive phosphates appear to act as Lux-Flood acids abstracting O^{2-} from NO_3^- forming PO_4^{3-} , NO_2 and O_2 , equations (23)-(27).⁷³





Electronic absorption spectroscopic studies⁷⁴ of the solutions formed by dissolution of TlF_3 and of $\text{Co}(\text{NO}_3)_2$ in molten LiNO_3 - KNO_3 eutectic containing KF indicate the formation of the tetrahedral complexes, $[\text{TlF}_4]^-$ and $[\text{CoF}_4]^{2-}$. Similar studies⁷⁵ of molten LiNO_3 - KNO_3 eutectic containing KN_3 and either $\text{Co}(\text{II})$, $\text{Ni}(\text{II})$ or $\text{Cu}(\text{II})$ salts gave evidence for the formation of transition metal azido complexes.

Thermodynamic parameters of diverse equilibria pertaining in molten NaNO_3 - KNO_3 ,^{76,77} and in molten MNO_3 - $\text{Ba}(\text{NO}_3)_2$ ($\text{M} = \text{Na}, \text{K}$)^{78,79} have been evaluated. Stability constants for $[\text{Ca}(\text{IO}_3)]^+$, $[\text{Ca}(\text{IO}_3)_2]$, $[\text{Ag}(\text{MoO}_4)]^-$, $[\text{Ag}_2\text{MoO}_4]$ and $[\text{Ag}(\text{MoO}_4)_2]^{3-}$ and thermodynamic data for the associated equilibria have been determined in molten equimolar NaNO_3 - KNO_3 ($523 < T/\text{K} < 613$) by Holmberg et al. from potentiometric and solubility measurements.^{76,77} A continuous range of solid solutions $[(\text{Ag}_x\text{Na}_{1-x})_2\text{MoO}_4]$ ($1 < x < 0.4$) was observed at 553K; these solids can be considered to be regular cationic substitutional solutions with an interaction parameter of $9.6 \pm 0.5 \text{ kJ mol}^{-1}$.⁷⁷ Gupta et al.⁷⁸ have evaluated thermodynamic parameters of the formation of CdI^+ and of CdI_2 in molten KNO_3 - $\text{Ba}(\text{NO}_3)_2$ (0.876 - 0.124) eutectic ($568 < T/\text{K} < 608$) and of the equilibrium between AgCl_2^- , AgBr_2^- and AgClBr^- (equation (28)) in molten NaNO_3 - $\text{Ba}(\text{NO}_3)_2$ (0.942 - 0.058) eutectic ($623 < T/\text{K} < 673$) from



concentration cell emf data. The equilibrium constant for equation (28) corresponds to a slight stabilisation of the mixed complex.

The kinetics of the CO_2/O_2 reaction in molten Li_2CO_3 - K_2CO_3 eutectic have been elucidated⁷⁹ using an electrolytic cell containing porous NiO electrodes; the reported reaction orders are complex and do not correlate with any of the proposed reaction mechanisms.

Solubility data for NiO and CoO in molten Na_2SO_4 (1200K) have

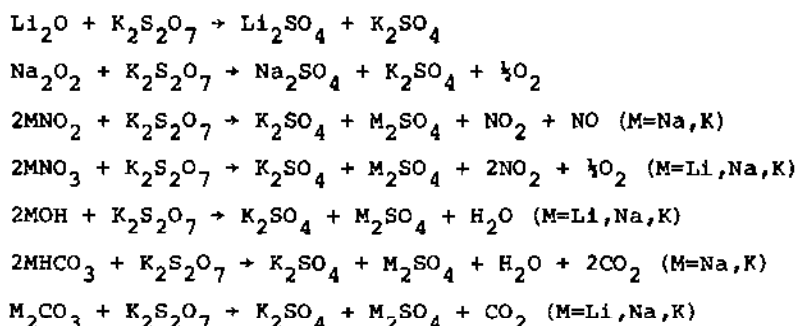
been measured by coulombic titration of NiSO_4 and CoSO_4 with electrochemically generated oxide ion.⁵⁵ Analysis of the data was complicated by competitive reactions leading to the formation of Na_2O_2 , NaNiO_2 and NaCoO_2 .

Anion-cation interactions in molten equimolar Na_2SO_4 - K_2SO_4 have been investigated using both electronic and vibrational spectroscopic methods.⁸⁰ Addition of Al^{3+} ions to this melt results in the formation of a bidentate (C_{2v}) and a monodentate (C_{3v}) species. In the latter case, the Al^{3+} ion may also interact with a contiguous sulphate ion in a similar fashion to form a bridging C_{2v} species. Addition of Li^+ ions to the melt only produces the monodentate (C_{3v}) sulphate species. Solutions of Cr(III) , Fe(III) and Ni(II) ions have also been considered. Whereas Cr(III) ions are octahedrally coordinated by bidentate sulphato anions forming $[\text{Cr}(\text{SO}_4)_3]^{3-}$ complexes, Fe(III) ions form tetrahedrally coordinated $[\text{Fe}(\text{SO}_4)_4]^{5-}$ complexes containing monodentate sulphato anions; the situation for Ni(II) ions is complex, an octahedral $[\text{Ni}(\text{SO}_4)_3]^{4-}$ -tetrahedral $[\text{Ni}(\text{SO}_4)_4]^{6-}$ coordination equilibrium being established.⁸⁰

Electrochemical studies⁸¹ of molten Na_2SO_4 have shown that the dominant oxidant is the $\text{S}_2\text{O}_7^{2-}$ ion. Dissolved oxygen and SO_2 can also act as oxidants but their contributions are limited by their very low solubilities in molten Na_2SO_4 .

A group of Australian workers,^{82,83,84} have investigated the reactions of a number of oxygen-containing salts with molten $\text{K}_2\text{S}_2\text{O}_7$; investigatory techniques used in the study included mass spectroscopy of the vapour over the molten salt, Raman spectroscopy of quenched samples, thermogravimetry and chemical analysis. The reactions are summarised in Scheme 2; they are all Lux-Flood acid-base reactions in which the pyrosulphate anion abstracts an oxide anion from the oxyanions to form the sulphate anion.^{82,83}

Phase relationships in the $\text{Li}_2\text{S}_2\text{O}_7$ - $\text{Na}_2\text{S}_2\text{O}_7$ - $\text{K}_2\text{S}_2\text{O}_7$ ternary system have been investigated.⁸⁴ Solubility limits have been established for $\text{Li}_2\text{S}_2\text{O}_7$, $\text{Na}_2\text{S}_2\text{O}_7$, $\text{K}_2\text{S}_2\text{O}_7$, LiKS_2O_7 and NaKS_2O_7 and the existence of two quasi-binary systems, $\text{Li}_2\text{S}_2\text{O}_7$ - NaKS_2O_7 and LiKS_2O_7 - NaKS_2O_7 has been ascertained.⁸⁴



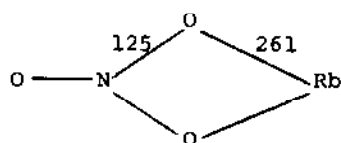
Scheme 2

1.4 SIMPLE COMPOUNDS OF THE ALKALI METALS

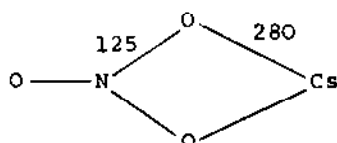
Data abstracted for this section are primarily associated with recent advances in the chemistry of simple binary and ternary compounds containing an alkali metal; by the very nature of these materials, structural and thermodynamic data predominate. In contrast to previous Reports, however, ion pairs are also included in this section.

1.4.1 Ion Pairs

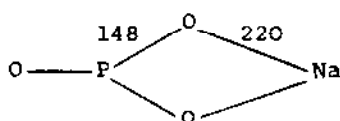
Ion pairs have been investigated both in the gas phase⁸⁵⁻⁸⁷ and in low temperature matrices.⁸⁸⁻⁹¹ Gas phase structures of $\text{Rb}^+[\text{NO}_3]^-$,⁸⁵ $\text{Cs}^+[\text{NO}_3]^-$,⁸⁶ and $\text{Na}^+[\text{PO}_3]^-$ ⁸⁷ have been elucidated by a group of Russian authors using electron diffraction methods. The diffraction data were considered within the context of the three most probable equilibrium geometries, all of which assumed D_{3h} symmetry for the anion: (a) a triangular pyramidal configuration with C_{3v} symmetry (b) a planar C_{2v} symmetry configuration with the Cs^+ cation in an axial monodentate arrangement and (c) a planar C_{2v} symmetry configuration with the Cs^+ cation in a dihedral bidentate arrangement. For all three ion pairs (1 - 3) the experimental data were consistent with geometry (c). Although bond distances could be determined with reasonable accuracy, bond angles could not be measured owing to the limitation of the experimental data and technique; structural data are included on the diagrams. Ab initio calculations of the equilibrium geometry of the $\text{Li}^+[\text{PO}_3]^-$ ion pair have also been undertaken.⁹² The difference in energy between the more stable configurations (b) and (c) was found to be very small ($< 17\text{kJ mol}^{-1}$).



(1)



(2)

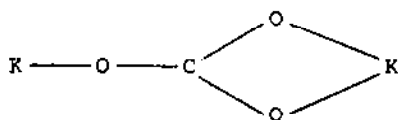


(3)

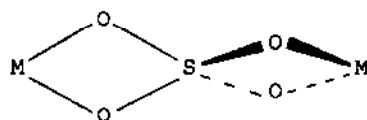
distances/pm.

and it is suggested that the moiety is non-rigid with respect to migration of the cation around the anion.⁹²

I.r. studies of $M_2^+[\text{CO}_3]^{2-}$ ($M=\text{K}, \text{Rb}, \text{Cs}$),⁸⁸ $M_2^+[\text{SO}_4]^{2-}$ ($M=\text{K}, \text{Rb}, \text{Cs}$)⁸⁹ and $\text{Cs}^+[\text{PF}_4]^-$,⁹⁰ isolated in various cryogenic matrices, have been completed. Analysis of the data indicate that $\text{K}_2^+[\text{CO}_3]^{2-}$ has a C_{2v} structure (4),⁸⁸ and that $M_2^+[\text{SO}_4]^{2-}$ has a D_{2d} structure (5).⁸⁹



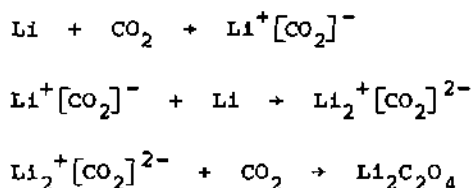
(4)



(5)

The equilibrium geometry of $\text{Cs}^+[\text{PF}_4]^-$ is more complex, the anion adopting a folded square C_{2v} structure for the anion (c.f. isoelectronic SF_4) with the Cs^+ cation in an axial monodentate arrangement.⁹⁰ The salt-molecule reaction technique used to prepare $\text{Cs}^+[\text{PF}_4]^-$ has also been successfully used in the preparation of $\text{Cs}^+[\text{PF}_3\text{Cl}]^-$ and $\text{Cs}^+[\text{PF}_2\text{Cl}_2]^-$; the synthesis of $\text{Cs}^+[\text{PFCl}_3]^-$ and of $\text{Cs}^+[\text{PCl}_4]^-$ has not been achieved using this method, thereby supporting the suggestion that PCl_3 is a weaker Lewis acid than PF_3 .⁹⁰

In a fascinating study⁹¹ of the reductive coupling of CO_2 by lithium atoms to give lithium oxalate, both $\text{Li}^+[\text{CO}_2]^-$ and $\text{Li}_2^+[\text{CO}_2]^{2-}$ ion pairs have been detected as reactive intermediates by i.r. matrix isolation spectroscopy. The results support scheme 3 as the mechanism of the dimerisation process which leads to oxalate formation.⁹¹



Scheme 3

1.4.2 Binary Compounds

There is a general paucity of data for binary compounds. Furthermore, those which are available are somewhat fragmented, relating to a number of diverse materials.

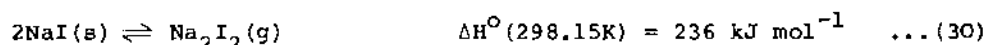
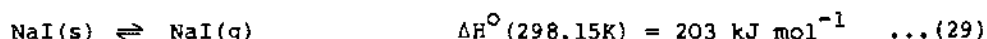
Ab initio calculations of the equilibrium geometries of the Li_2F_2 dimer⁹³ and of the $(\text{LiH})_n$ ($2 < n < 8$) oligomers⁹⁴ have been undertaken. The geometry of Li_2F_2 , which has D_{2h} symmetry, is best described by the results obtained using the DZRS basis set; on the other hand, the most realistic vibrational properties of this dimer were obtained using the DZHD basis set.⁹³ The equilibrium structures for $(\text{LiH})_n$ oligomers with odd values of n were found to be planar cyclic with D_{nh} molecular geometry; those for $(\text{LiH})_n$ oligomers with even values of n , however, were found to be three-dimensional precursors of the crystal structure. Stability calculations for these molecules confirm the strong tendency of LiH to oligomerise.⁹⁴

Rotational constants and cohesive energies of alkali metal hydrides, MH ($\text{M}=\text{Li}, \text{Na}, \text{K}, \text{Rb}, \text{Cs}$) have been computed⁹⁵ by replacing Woodcock's generalised pair potential with a combination of Morse-Kratzer potentials; the computed values are in accordance with available thermochemical data.

Various crystal properties of the alkali metal halides with the NaCl structure, MX ($\text{M}=\text{Li}, \text{Na}, \text{K}, \text{Rb}$; $\text{X}=\text{F}, \text{Cl}, \text{Br}, \text{I}$) have been evaluated using either the Born model formulation⁹⁶ (crystal binding energies) or Woodcock's generalised pair interaction potential energy function⁹⁷

(compressibilities and thermal expansion coefficients).

The vapourisation thermodynamics of NaI, equations (29,30),



have been derived from measurements of the vapour density of the saturated vapour over solid NaI.

Standard thermodynamic data for the formation of K_2S have been derived⁹⁹ from the results of bomb calorimetry studies of the combustion of K_2S in fluorine gas; the data are compiled in Table 3.

Single crystals of KHS have been prepared¹⁰⁰ by reaction of KNH_2 with H_2S in liquid NH_3 . The structure of KHS (Figure 2) has been solved by X-ray diffraction methods. Although it crystallises with rhombohedral symmetry, it is best considered in the alternative hexagonal setting (Figure 2a); the interatomic distances within the octahedral coordination polyhedra of both ions are $r(\text{K}\dots\text{S}) = 331$ or $r(\text{K}\dots\text{H}) = 287 \text{ pm}$.¹⁰⁰

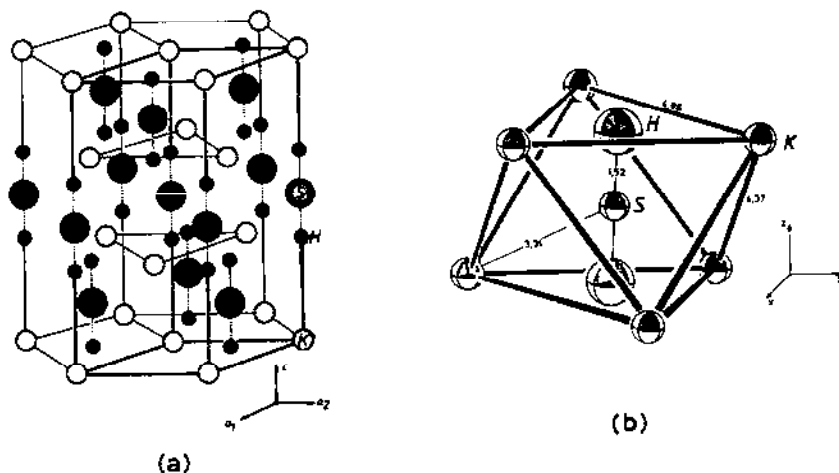


Figure 2. Aspects of the crystal structure of KHS; (a) the hexagonal unit cell and (b) the coordination polyhedron of the SH^- anion (reproduced by permission from Z. Anorg. Allg. Chem., 473(1981)125).

Table 3. Standard thermodynamic data for the formation of K_2S ,⁹⁹ $CsNO_3$,¹⁰⁵ $Na_2CO_3 \cdot 3NaHCO_3$ [Wegscheider's salt]¹⁰⁶ and of $Na_2CO_3 \cdot NaHCO_3 \cdot 2H_2O$ [Trona].¹⁰⁶

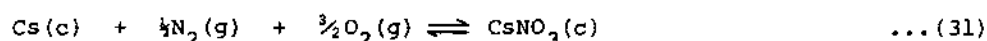
Compound	$-\Delta H_f^\circ(X, c, 298.15)$ kJ mol^{-1}	$-\Delta S_f^\circ(X, c, 298.15)$ $\text{J K}^{-1} \text{mol}^{-1}$	$-\Delta G_f^\circ(X, c, 298.15)$ kJ mol^{-1}
K_2S	406.2 ± 2.9	46.3 ± 16.7	392.4 ± 5.8
$CsNO_3$	505.8 ± 0.5	334.6 ± 0.5	406.0 ± 0.5
$Na_2CO_3 \cdot 3NaHCO_3$	3984.03 ± 0.80	-	-
$Na_2CO_3 \cdot NaHCO_3 \cdot 2H_2O$	2682.11 ± 0.44	-	-

Anhydrous $CsOH$ has been synthesised by reaction of $CsOH \cdot H_2O$ with $CsNH_2$ in supercritical NH_3 .¹⁰¹ Temperature dependent structural studies have shown that the orthorhombic modification ($a = 435.0$, $b = 1199$, $c = 451.6$ pm; anti- $NaOH$ type structure) is converted into a cubic modification ($a = 642.7$; $NaCl$ structure) at $497.5K$.¹⁰¹

2H -double resonance studies of various anhydrous and hydrated alkali metal (Li, Na, K) hydroxides have been undertaken;¹⁰² the 2H -quadrupole coupling constants of the OH^- anion are correlated with its stretching force constants. ^{23}Na -quadrupole resonance has also been detected in both $NaOH$ and $NaOH \cdot H_2O$.¹⁰²

The existence of orientational disorder in the CN^- anions of $NaCN \cdot 2H_2O$ suggested by van Rij and Britton¹⁰³ on the basis of a refinement of X-ray diffraction data has been confirmed spectroscopically by Falk.¹⁰⁴ Doubling of CN^- stretching fundamentals occurs. The ratios of doublet band areas are consistent with the energy of the $NC \dots Na$ orientation being higher than that of the $CN \dots Na$ orientation by $0.8 \pm 0.3 \text{ kJ mol}^{-1}$. The fraction of reversed CN^- groups at $295K$ is estimated by Falk¹⁰⁴ to be 0.33 ± 0.06 , somewhat greater than the previous estimate of 0.20 by van Rij and Britton.¹⁰³

Standard thermodynamic parameters for the formation of $CsNO_3$, according to equation (31), have been recommended¹⁰⁵ from an analysis of heat capacity data ($5 \leq T/K \leq 350$). Standard enthalpy of formation data for $Na_2CO_3 \cdot 3NaHCO_3$ and of $Na_2CO_3 \cdot NaHCO_3 \cdot 2H_2O$ have been



calculated¹⁰⁶ from enthalpy of solution data in excess aqueous NaOH. Data for the three salts are included in Table 3.

Weppner et al have published the results of a comprehensive study of phase equilibria in the quasi-binary systems $\text{Li}_3\text{N-LiX}$ ($\text{X} = \text{Cl, Br, I}$)¹⁰⁷ and LiOH-LiX ($\text{X} = \text{Br, I}$);¹⁰⁸ they have also reported free energy of formation for the ternary lithium nitride halides $\text{Li}_x\text{N}_y\text{X}_z$.¹⁰⁷ Salient properties of $\text{Li}_x\text{N}_y\text{X}_z$ are collected in Table 4.¹⁰⁷ With the exception of $\text{Li}_9\text{N}_2\text{Br}_3$, they have all been obtained previously and characterised crystallographically; $\text{Li}_9\text{N}_2\text{Br}_3$ crystallises in a body-centred tetragonal structure with $a = 1176.1$ and $c = 599.3$ pm.¹⁰⁷ Each of the LiOH-LiX ($\text{X} = \text{Br, I}$) systems contains two intermediate ternary compounds, $\text{Li}_2(\text{OH})\text{I}$, $\text{Li}_5(\text{OH})_4\text{I}$, $\text{Li}_2(\text{OH})\text{Br}$ and $\text{Li}_4(\text{OH})_3\text{Br}$, all of which decompose in

Table 4. Salient properties (melting points, T_m , peritectic decomposition temperatures, T_d , free energies of formation from the elements, $\Delta G_F^\circ(\text{X}, \text{c}, \text{T})$, and free energies of formation from Li_3N and LiX ($\text{X} = \text{Cl, Br, I}$), $\Delta G_X^\circ(\text{X}, \text{c}, \text{T})$) of the compounds formed in the quasi-binary $\text{Li}_3\text{N-LiX}$ ($\text{X} = \text{Cl, Br, I}$) systems.

Compound	T_m/K	T_d/K	T/K	$-\Delta G_F^\circ(\text{X}, \text{c}, \text{T})$ kJ (g. atom)^{-1}	$-\Delta G_X^\circ(\text{X}, \text{c}, \text{T})$ kJ (g. atom)^{-1}
$\text{Li}_9\text{N}_2\text{Cl}_3$	983	-	595	169±1	81
$\text{Li}_{11}\text{N}_3\text{Cl}_2$	978	-	595	154±2	95
Li_6NBr_3	-	873	573	135±2	30
$\text{Li}_9\text{N}_2\text{Br}_3$	-	783	573	118±2	37
$\text{Li}_{13}\text{N}_4\text{Br}$	-	757	573	66±3	29
Li_5NI_2	846	-	560	124±2	48
$\text{Li}_{6.67}\text{N}_{1.89}\text{I}$	1048	-	586	90±2	47

peritectic reactions at 452, 575, 518 and 564K, respectively.¹⁰⁸ With the exception of $\text{Li}_2(\text{OH})\text{Br}$, the X-ray powder diffraction patterns obtained are complex and could not be indexed unambiguously.

$\text{Li}_2(\text{OH})\text{Br}$ crystallises in a primitive cubic ($a = 405.6 \text{ pm}$, $\text{Pn}3\text{m}$ space group) antiperovskite type structure with statistical occupation of $2/3$ of the available Li^+ positions.¹⁰⁸

1.4.3 Ternary Pnictides

As in previous Reports, the range of ternary compounds considered in this and the subsequent sections is limited to those containing both an alkali and a transition metal; this restriction prevents unnecessary duplication with other Chapters of this review.

Schuster et al¹⁰⁹⁻¹¹¹ have prepared a series of ternary pnictides. They have been characterised primarily by X-ray diffraction methods; the compounds and their unit parameters are listed in Table 5. Schuster et al¹¹² have also measured ($80 \leq T/\text{K} \leq 290$) the magnetic susceptibilities of the ternary compounds Li_2LnX_2 ($\text{Ln} = \text{Ce}, \text{Pr}, \text{Nd}, \text{Tb}$; $\text{X} = \text{P}, \text{As}, \text{Sb}, \text{Bi}$); the data support the existence of the Ln^{3+} cation in the materials.

1.4.4 Ternary Oxides and Chalcogenides

Recent progress in the chemistry of ternary oxides¹¹³ and of ternary sulphides¹¹⁴ has been comprehensively reviewed; chemical, structural, magnetic and spectroscopic properties are considered in detail. The magnetic properties of the ternary oxides adopting

Table 5. Unit cell parameters for a number of ternary pnictides

Compound	Symmetry	Space Group	a/pm	b/pm	c/pm	Ref.
LiMnX ($\text{X} = \text{P}, \text{As}, \text{Sb}$)*	tetragonal	P4/nmm	413.3	-	595.7	109
NaMnX ($\text{X} = \text{P}, \text{As}, \text{Sb}, \text{Bi}$)*	tetragonal	P4/nmm	408.6	-	688.4	109
K_2PdP_2	orthorhombic	Cmcm	635.5	1389.8	590.0	110
K_2PtAs_2	orthorhombic	Cmcm	646.5	1410.6	609.6	110
KRh_2P_2	tetragonal	I4/mmm	388.4	-	1298.6	111
KM_2As_2 ($\text{M} = \text{Fe}, \text{Co}, \text{Rh}$)*	tetragonal	I4/mmm	384.2	-	1386.1	111

* The crystallographic data refer to the element listed first.

either the K_2NiF_4 or $\alpha-NaFeO_2$ structural types have also been reviewed;¹¹⁵ the relationship between structure and magnetic behaviour is stressed.

There has been a remarkable decrease in the number of papers published in which the synthesis and structural characterisation of ternary oxides is described. Those materials which have been prepared¹¹⁶⁻¹²⁰ are listed in Table 6 together with pertinent structural data. Although most of these data were obtained using X-ray diffraction methods,¹¹⁶⁻¹¹⁹ the structure of $Na_2CrO_4(II)$ was determined using neutron diffraction techniques;¹²⁰ the results obtained confirm the earlier X-ray diffraction structure. The ternary oxides were generally prepared by classical solid state methods (i.e., high temperature reactions between alkali metal oxides, carbonates or nitrates with transition metal oxides). The high pressure modification of $LiVO_2$ was obtained¹¹⁶ by treating the ambient pressure modification to 6.0-6.5 GPa at 1300K; it is metastable and has retained its structure for the past ten years.

As part of an extensive study of the processes occurring in solid state reactions in both inert and oxidising atmospheres, Fotiev et al have investigated the interaction of Na_2CO_3 with V_2O_3 ,¹²¹ FeO ,¹²² Fe_3O_4 ¹²² and FeV_2O_4 .¹²² In an inert atmosphere, interaction takes place as a direct redox process between the reagents; in an atmosphere of air, the Fe^{2+} and V^{3+} are initially oxidised to Fe^{3+} and V^{5+} and then there is successive interaction of the oxidation products with Na_2CO_3 . Fotiev et al¹²³ have also determined the formation conditions for the quaternary oxides $NaFe_3V_4O_{15}$ and $NaFeV_2O_7$.

A small number of quaternary oxides have been prepared and characterised, primarily by structural methods.¹²⁴⁻⁶ The majority of these materials are molybdates; they are listed together with pertinent unit cell parameters in Table 6. In another investigation of the chemistry of quaternary molybdates, Dion and Noel¹²⁷⁻⁹ have defined basic phase relationships in the pseudo-ternary $Na_2O-VO_3-MoO_3$ system and have studied the hydrogen reduction of a number of ternary and quaternary oxides formed in this system.

I.r. spectroscopic studies ($650 \leq \bar{\nu}/cm^{-1} \leq 1200$) have been undertaken for $Cs_xV_2O_5$ ($0 \leq x \leq 0.664$);¹³⁰ the data suggest, in agreement with earlier X-ray diffraction results, that the CsV_3O_8 phase appears at about $x = 0.008$.

Table 6. Crystallographic parameters for a number of ternary oxides, quaternary oxides and ternary selenides.

Compound	Symmetry	Space Group	a/pm	b/pm	c/pm	$\alpha/^\circ$	$\beta/^\circ$	$\gamma/^\circ$	Ref.
LiVO_2 (H.P.)	cubic	$\text{Fd}\bar{3}\text{m}$	822.7	-	-	-	-	-	116
NaCeO_2	tetragonal	$(\alpha\text{-LiFeO}_2)$	478	-	1099	-	-	-	117
NaLnO_2 (Ln=Nd, Sm, Eu, Gd)*	cubic		493	-	-	-	-	-	117
Na_4RuO_4	tetragonal	$\text{I4}_1/\text{amd}$	562.3	-	866	-	-	-	118
Na_2RuO_3	orthorhombic	-	545.4	937.7	3146	-	-	-	118
$\text{Na}_4\text{Ru}_3\text{O}_8$	cubic	$\text{Pm}\bar{3}$	889.0	-	-	-	-	-	118
$\text{Na}_2\text{Ru}_4\text{O}_9$	monoclinic	C2/m	2318	283.0	1100	-	104.5	-	118
NaRu_4O_8	tetragonal	I4/m	987.2	-	311.5	-	-	-	118
$\text{Na}_2\text{Ru}_9\text{O}_{19}$	orthorhombic	-	1245	380.8	765.0	-	-	-	118
Na_3RuO_4	monoclinic	-	1099.0	1275.4	568.1	-	109.9	-	118
$\text{Na}_6\text{Au}_2\text{O}_6$	tetragonal	$\text{P4}_2/\text{nnm}$	946.5	-	450.6	-	-	-	119
Na_2CrO_4 (II) 296K	orthorhombic	Cmcm	586.2	925.1	714.5	-	-	-	120
NaLiV_2O_6	monoclinic	C2/c	1018.7	907.4	584.0	-	108.95	-	124
$\text{Na}_2\text{M}_5\text{Mo}_6\text{O}_{24}$ (M=Mg, Co, Zn)*	triclinic	$\text{P}\bar{1}$	1057.5	861.7	695.1	103.42	102.67	112.37	125
$\alpha\text{-K}_5\text{VMoO}_4$ (H.T)	hexagonal	$\text{P}\bar{3}1\text{m}$	1045.3	-	410.4	-	-	-	126
Na_3FeSe_3	monoclinic	$\text{P2}_1/\text{n}$	745.2	717.6	1308.1	-	90.5	-	137
KAgSe	tetragonal	P4/nmm	452	-	759	-	-	-	138

* The crystallographic data refer to the element listed first.

Thermodynamic parameters have been reported for several ternary oxides;²⁰ interest in these data has been stimulated by the roles played by the oxides (Cs_3CrO_4 ,¹³¹ Cs_4CrO_4 ,¹³² MUO_3 ($\text{M} = \text{Li, Na, K, Rb}$),¹³³ Na_3UO_4 ,²⁰ $\beta\text{-Cs}_2\text{U}_2\text{O}_7$ ¹³⁴) in nuclear reactor technology. Whereas the thermodynamic data for Cs_3CrO_4 , Cs_4CrO_4 and MUO_3 ($\text{M} = \text{Li, Na, K, Rb}$) were determined from solution calorimetry studies (using either XeO_3 or $\text{Ce}(\text{SO}_4)_2$ as oxidant), those for Na_3UO_4 were derived from measurements of oxygen activities in equilibrium with UO_2 and Na_3UO_4 in the presence of liquid sodium. In the case of $\beta\text{-Cs}_2\text{U}_2\text{O}_7$, earlier data¹³⁵ have been revised in the light of the recent critical re-evaluation of thermochemical quantities for UO_2Cl_2 . The results for Cs_3CrO_4 and Cs_4CrO_4 have been used to derive thermochemical quantities for the reduction of caesium chromates.¹³² All the thermodynamic data are collected in Table 7.

The equilibrium phase diagram for the Na_2S - CdS system has been constructed from d.t.a and X-ray diffraction data.¹³⁶ Three ternary sulphides exist; two decompose in peritectic reactions, Na_6CdS_4 ($1123 \pm 5\text{K}$) and Na_2CdS_2 ($1173 \pm 5\text{K}$), the third melts congruently Na_4CdS_3 ($1113 \pm 5\text{K}$).

The ternary selenide Na_3FeSe_3 has been prepared by reaction of Na_2CO_3 with iron sponge at 1000K under a stream of hydrogen saturated with selenium.¹³⁷ An alternative chemical transport method, in which NaH -iron sponge-selenium mixtures were heated in a glass ampoule subjected to a 700-800K temperature gradient, has also been devised.¹³⁷ Structural parameters for Na_3FeSe_3 ¹³⁷ are included in Table 6 together with those for KAgSe .¹³⁸

1.4.5 Ternary Halides

Discussion in this section is restricted to the chemistry of anhydrous ternary halides; solvated halides are not considered. Recent progress in the chemistry of ternary fluorides has been comprehensively reviewed;¹¹³ chemical, structural, magnetic and spectroscopic properties are considered in detail.

Phase relationships in the RbBr - TmBr_3 ¹³⁹ and KI - ZrI_4 ¹⁴⁰ systems have been elucidated using d.t.a, X-ray diffraction and chemical analyses. Two compounds, Rb_3TmBr_6 and $\text{Rb}_3\text{Tm}_2\text{Br}_9$ are formed in the former system;¹³⁹ they undergo peritectic decomposition reactions to form $\text{Rb}_3\text{Tm}_2\text{Br}_9$ and RbBr (at 583K) and RbBr and TmBr_3 (at 733K), respectively. $\text{Rb}_3\text{Tm}_2\text{Br}_9$ undergoes a polymorphic transition at 613K. Only one compound, K_2ZrI_6 , was observed in

Table 7. Standard thermodynamic parameters for the formation of a number of caesium chromates and alkali metal uranates and for the reduction of caesium chromates.

Compound	$-\Delta H_f^\circ(X, c, 298)$ kJ mol ⁻¹	$-\Delta S_f^\circ(X, c, 298)$ J K ⁻¹ mol ⁻¹	$-\Delta G_f^\circ(X, c, 298)$ kJ mol ⁻¹	Reference
Cs ₃ CrO ₄	1543.13±2.7	393.4	1425.91±4.0	131
Cs ₄ CrO ₄	1588.5±3.2	-	-	132
LiUO ₃	1522.1±1.7	-	-	133
NaUO ₃	1494.6±1.6	-	-	133
KUO ₃	1522.9±1.6	-	-	133
RbUO ₃	1520.9±1.7	-	-	133
Na ₃ UO ₄	2050	448.0	1916	20
β-Cs ₂ U ₂ O ₇	3220.2±1.8	-	-	134
Reduction	$-\Delta H_r^\circ(298)$ kJ mol ⁻¹	$-\Delta S_r^\circ(298)$ J K ⁻¹ mol ⁻¹	$-\Delta G_r^\circ(298)$ kJ mol ⁻¹	
Cs ₂ CrO ₄ (c) + Cs(c) ⇌ Cs ₃ CrO ₄ (c)	113.1±3.3	17.6±1.6	107.8±3.3	132
Cs ₃ CrO ₄ (c) + Cs(c) ⇌ Cs ₄ CrO ₄ (c)	45.4±4.2	19.4±5.2	39.6±4.5	132

Table 8. Crystallographic parameters for a number of ternary halides.

Compound	Symmetry	Space Group	a/pm	b/pm	c/pm	$\beta/^\circ$	Reference
A_xVF_3	orthorhombic		~ 1300	~ 740	~ 750	-	143
KCoF ₃	cubic	Pm3m	406.88	-	-	-	144
α -CsCrCl ₃ (295K)	hexagonal	P6 ₃ /mmc	725.7	-	623.8	-	145
α -CsCrI ₃ (295K)	hexagonal	P6 ₃ /mmc	810.7	-	691.7	-	145
α -CsCuCl ₃ (430K)	hexagonal	P6 ₃ /mmc	721.2	-	614.1	-	146
NaFeF ₄	monoclinic	P2 ₁ /c	790.8	535.1	753.1	101.92	147
Li ₂ MnBr ₄ (298K)	tetragonal	-	777.6	-	1109.1	-	148
Li ₂ MnBr ₄ (673K)	cubic	-	1123	-	-	-	148
Li ₂ MnBr ₄ (773K)	cubic	-	563	-	-	-	148
Li ₂ CdBr ₄ (623K)	cubic	-	1134	-	-	-	148
Li ₂ CdBr ₄ (723K)	cubic	-	569	-	-	-	148
K ₂ CuF ₄	tetragonal	(K ₂ NiF ₄)	414.7	-	1273	-	149
Cs ₃ CoCl ₅	tetragonal	I4/mcm	923.15	-	1455.35	-	150
Cs ₃ CoBr ₅ (4.2K)	tetragonal	I4/mcm	946	-	1504	-	151
K ₃ UF ₉	orthorhombic	-	697.4	753.4	976.8	-	152
Rb ₃ UF ₉	orthorhombic	-	712.1	761.2	961.4	-	152
K ₃ Cu ₂ F ₇	tetragonal	I4/mmm	415.6	-	2052	-	149
Rb ₃ Cu ₂ Cl ₇	orthorhombic	Ccca	2484.3	721.6	721.6	-	153
Cs ₃ Y ₂ I ₉	hexagonal	P6 ₃ /mmc	840.6	-	2128.0	-	154
Cs ₃ ZrI ₉	hexagonal	P6 ₃ /mmc	826.9	-	1990.8	-	154

the latter system;¹⁴⁰ it melts congruently at 1220K and undergoes two polymorphic transitions at 843 and 912K.

Na_2MnF_5 has been prepared in quantitative yield by reduction of KMnO_4 with acetylacetone in the presence of NaHF_2 ;¹⁴¹ it was characterised by i.r., magnetic susceptibility and chemical analytical methods. Conditions for the preparation of single crystals of Cs_2CuCl_4 and of CsCuCl_3 from aqueous solution have been quoted in detail.¹⁴²

Numerous structural studies of ternary halides have been undertaken;¹⁴³⁻¹⁵⁴ crystallographic data are collected in Table 8. Although the majority of the data are derived from single crystal X-ray diffraction measurements, those for Cs_3CoBr_5 were obtained in a low temperature (4.2K) single crystal neutron diffraction study.¹⁵¹ Detailed analysis of the electron density distribution (derived from single crystal X-ray diffraction intensity data) in KCoF_3 showed that the high spin $(t_{2g})^5(e_g)^2$ electronic configuration is a good approximation for the Co^{2+} ion in this material.¹⁴⁴ Similarly the high spin $(t_{2g})^3(e_g)^1$ electronic configuration of Cr^{2+} in $\alpha\text{-CsCrX}_3$ ($X = \text{Cl}, \text{I}$)¹⁴⁵ and the $(t_{2g})^6(e_g)^3$ electronic configuration of Cu^{2+} in $\alpha\text{-CsCuCl}_3$ ¹⁴⁶ are held responsible for the Jahn-Teller distortion of the BaNiO_3 structure adopted by these materials.

Polymorphic transitions in Li_2MBr_4 ($M = \text{Mn}, \text{Cd}$) have been investigated in detail. Salient features are given in Table 8 and Scheme 4. At room temperature, Li_2MnBr_4 is tetragonal whereas Li_2CdBr_4 forms a mixture of CdBr_2 and cubic $\text{Li}_{1-x}\text{Cd}_{x/2}\text{Br}_2$ mixed

Li_2MnBr_4 : tetragonal $\xrightleftharpoons{543\text{K}}$ cubic-I $\xrightleftharpoons{733\text{K}}$ cubic-II

Li_2CdBr_4 : $\text{CdBr}_2/\text{Li}_{1-x}\text{Cd}_{x/2}\text{Br}_2$ $\xrightleftharpoons{513\text{K}}$ cubic-I $\xrightleftharpoons{633\text{K}}$ cubic-II
mixed crystals

crystals. Both halides form two high temperature cubic phases - a spinel phase (cubic-I) and a defect NaCl phase (cubic-II).

Boo et al.¹⁴³ have undertaken extensive studies of the structural and magnetic properties of the pseudo hexagonal M_xVF_3 ($M = \text{K}, \text{Rb}, \text{Cs}$) compounds. These materials, which are analogues of the hexagonal tungsten bronzes, M_xWO_3 (space group $\text{P6}_3/\text{mcm}$) undergo distortions

which lower their symmetry from hexagonal to orthorhombic in two unique ways. The distinction between the two is defined by the ratio of orthohexagonal dimensions, $|a|/\sqrt{3}|b|$, which is either greater than unity, M_xVF_3 -I, or less than unity, M_xVF_3 -II. In the K_xVF_3 and Rb_xVF_3 systems a transition occurs from M_xVF_3 -I to M_xVF_3 -II at $x = 0.26$ and 0.24 ; the Cs_xVF_3 system adopts the M_xVF_3 -II structure over its entire composition range. Evidence of atomic ordering has also been obtained; four stoichiometric phases were observed for compositions $x = 0.167$, 0.222 , 0.250 and 0.333 . Although all four phases which are designated $\alpha(x)$ and have unique modulated structures were found in the Rb_xVF_3 system, only three phases, $\alpha(0.167)$, $\alpha(0.222)$ and $\alpha(0.333)$, were found in the K_xVF_3 system; in the Cs_xVF_3 system the Cs^+ ions appear to be mostly random.¹⁴³

Single crystal spectroscopic studies have been effected on $NaMnF_3$,¹⁵⁵ $NaCoF_3$,¹⁵⁵ $CsCuCl_3$,¹⁵⁶ Cs_2CeCl_6 ,¹⁵⁷ and $Cs_3Ti_2Cl_9$;¹⁵⁸ aspects of the structural chemistry of these halides are inferred from the interpretation of the spectra.¹⁵⁵⁻⁷

Vapour pressure studies of $MF-ZrF_4$,¹⁵⁹ $NaCl-ZrCl_4$,¹⁶⁰ and $NaCl-HfCl_4$,¹⁶⁰ systems have been undertaken and thermodynamic data derived for the associated equilibria. Vapour pressure measurements of the exchange reactions, equation (32), have also been effected.¹⁶⁰ They indicate that the efficiency of the alkali

$$HfCl_4(g) + M_2ZrCl_6(s.s) \rightleftharpoons M_2HfCl_6(s.s) + ZrCl_4(g) \quad \dots(32)$$

($M = Li, Na, K$; s.s = solid solution)

metal halides in the separation of hafnium from zirconium (by a recently developed process based on the selective reactivity of $ZrCl_4$ and of $HfCl_4$ with alkali metal chlorides) increases in the sequence



The thermal stabilities of K_2TcI_6 ,¹⁶¹ and Cs_2CeCl_6 ,¹⁶² have been ascertained by d.t.a. and t.g.a. techniques. Whereas K_2TcI_6 decomposes via K_2TcI_3 to metallic technetium and KI ,¹⁶¹ Cs_2CeCl_6 decomposes directly to $CsCl$, $CeCl_3$ and chlorine gas.¹⁶² The thermal analysis data for Cs_2CeCl_6 were used to calculate the enthalpy of the decomposition reaction ($\Delta H_r^\circ(298) = 29.9 \pm 3.5 \text{ kJ mol}^{-1}$) and to estimate the enthalpy of formation of Cs_2CeCl_6

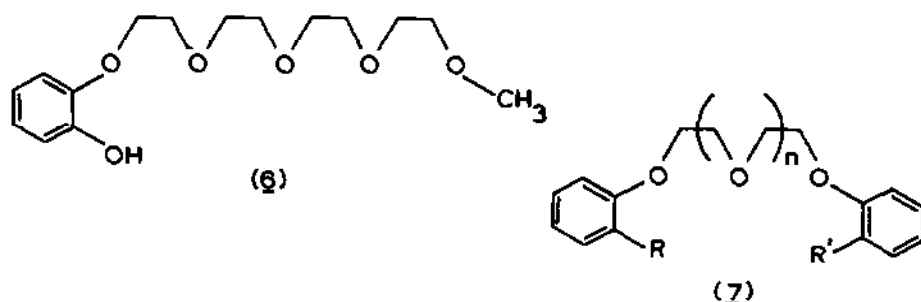
$(\Delta H_f^\circ(\text{Cs}_2\text{CeCl}_6, c, 298\text{K}) = -1974.09 \pm 8.37 \text{ kJ mol}^{-1})$. The enthalpies of fusion of KMCl_3 ($M = \text{Mg, Ca}$), K_2MCl_4 ($M = \text{Mg, Sr, Ba}$), K_2LaCl_5 , K_3LnCl_6 ($\text{Ln} = \text{Pr, Nd}$) and $\text{KLn}_3\text{Cl}_{10}$ ($\text{Ln} = \text{Gd, Dy}$) have been determined.¹⁶³

1.5 COMPOUNDS OF THE ALKALI METALS CONTAINING ORGANIC MOLECULES OR COMPLEX IONS.

The format adopted for this section is similar to that used for the 1980 Review.¹⁶⁴ Thus the text is simplified by incorporation of subdivisions for specialised topics currently of interest in bioinorganic chemistry. These include acyclic polyether, crown and cryptate complexes, together with derivatives of carboxylic acids, nucleotides, etc. Subdivisions for the individual alkali metals are also included; for these, data pertinent to several alkali metals are discussed once only, in the subdivision for the lightest element considered.

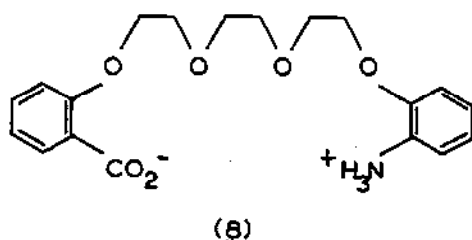
1.5.1 Acyclic Polyether Complexes

Complex formation between alkali and alkaline earth metal cations and acyclic polyethers, especially those with terminal groups containing donor atoms has been the subject of a small number of papers.¹⁶⁵⁻⁸ A comparative study of the complexing ability of (6), its conjugate base and its crown analogue, B18C6, for alkali (Li, Na, K, Rb, Cs) and alkaline earth metal (Ca, Sr, Ba) cations has been undertaken using spectroscopic methods.¹⁶⁵ The derived equilibrium constants indicate that B18C6 binds the cations more strongly than does its open chain sexadentate analogues, of which the conjugate base is the more effective. Complexation of the alkali (Na, K, Rb) and alkaline earth metal (Ca) cations by a series of acyclic polyethers with various end groups (7; $1 \leq n \leq 3$; $R = R' = \text{OH, OCH}_2\text{C}_6\text{H}_5, \text{OCH}_2\text{CH}_2\text{OH, OCH}_2\text{CO}_2\text{C}_2\text{H}_5, \text{OCH}_2\text{COOH}$) has been elucidated



by thermodynamic methods.¹⁶⁶ Stability constants increase as n is increased and as R and R' are varied through the series OH , $\text{OCH}_2\text{C}_6\text{H}_5$, $\text{OCH}_2\text{CH}_2\text{OH}$, $\text{OCH}_2\text{CO}_2\text{C}_6\text{H}_5$, $\text{OCH}_2\text{CO}_2\text{H}$. There is no evidence that internal hydrogen bonding contributes to the stability of these complexes.¹⁶⁶ Complex formation between Na^+ and a similar series of acyclic polyethers (7 ; $5 \leq n \leq 8$; $R = \text{NHCOCH}_3$, CONHCH_3) has been studied by multinuclear (^1H -, ^{13}C - and ^{23}Na -) nmr techniques. Derived thermodynamic data emphasise the significant role sometimes played by solvent participation during complex formation.¹⁶⁷

The molecular structure of $(8) \cdot \text{NaClO}_4$, a complex containing a linear polyether with terminal amino and carboxyl functions, has been determined from single crystal X-ray diffraction data.¹⁶⁸ There are two molecules per asymmetric unit (Figure 3) which are related to each other by an approximate non-crystallographic centre of symmetry. Both polyether ligands exist in the zwitterion configuration with ion pair attraction between the amino (NH_3^+) and carboxyl (COO^-) end groups. The Na^+ coordination sphere (Figure 3)



comprises four polyether oxygen atoms in an equatorial plane (the fifth polyether oxygen atom - the aminophenoxy end group oxygen atom - does not coordinate the Na^+ cation), together with a perchlorate oxygen atom and a translated carboxyl oxygen atom in the axial positions. Pertinent interatomic distances are included in Figure 3.

The complexing ability of a series of oligoethylene glycols, $\text{HO}(\text{CH}_2\text{CH}_2\text{O})_n\text{H}$ ($1 \leq n \leq 4$), for alkali ($\text{Li}, \text{Na}, \text{K}, \text{Cs}$) and alkaline earth metal ($\text{Mg}, \text{Ca}, \text{Sr}, \text{Ba}$) cations has been assessed in a study of the lipophilization in toluene of the otherwise insoluble 2-nitrophenolate salts.¹⁶⁹

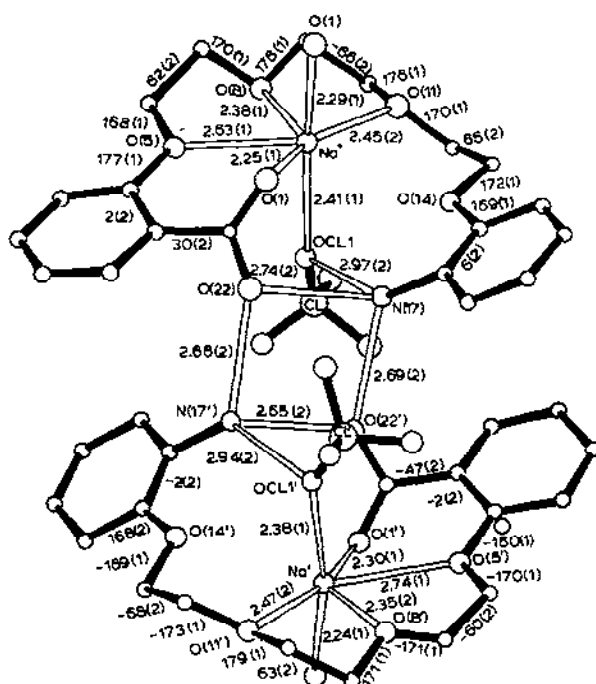


Figure 3. Molecular geometry of the asymmetric unit of (8).NaClO₄; giving pertinent interatomic distances/Å (reproduced by permission from Z. Naturforsch., 36b(1981)102).

1.5.2 Crown Complexes

Compared to previous Reports there has been a marked increase in the number of papers on alkali and alkaline earth metal complexes of crown and related macrocyclic ligands. Consequently this topic has been divided into two subsections in which complexes formed by 'classical' crown compounds and by novel macrocyclic ligands of unusual design are considered.

The template effect of alkali and alkaline earth metal cations in the synthesis of 12C4,¹⁷⁰ 15C5,¹⁷⁰ 18C6¹⁷⁰ and of B18C6¹⁷¹ has been studied quantitatively. The different catalytic abilities of the various cations was noted - optimum yields of 12C4, 15C5 and 18C6 were obtained with Li⁺, Na⁺ and K⁺, respectively¹⁷⁰ - and discussed¹⁷¹ in terms of the structural and electronic effects of the metal cations.

Structural studies have been undertaken on 15C5.NaSCN.4H₂O¹⁷²

(B15C5)₂.K[picrate],¹⁷³ (18C6)₂.K₂[phthalocyanine],¹⁷⁴ and DB18C6.KI.(NH₂)₂CS.¹⁷⁵ The sodium derivative contains two crystallographically distinct Na⁺ cations.¹⁷² Each cation is situated at the centre of a 15C5 crown ether cavity, $r(\text{Na}(1)\dots\text{O}) = 233\text{--}251$ pm, $r(\text{Na}(2)\dots\text{O}) = 235\text{--}250$ pm, the coordination sphere being completed in axial positions either by an N-bonded SCN⁻ anion, $r(\text{Na}(1)\dots\text{N}) = 226$ pm and a water oxygen atom, $r(\text{Na}(1)\dots\text{O}) = 246$ pm or by a single N-bonded SCN⁻ anion, $r(\text{Na}(2)\dots\text{N}) = 248$ pm. The difference in the two Na⁺ cations arises from the adoption by the 15C5 ligands of one of two disordered positions generated from the presence in the structure of statistical mirror planes.¹⁷²

The three potassium derivatives contain three different types of K⁺ coordination sphere; they are shown in Figure 4. In (B15C5)₂.K[picrate], (Figure 4a),¹⁷³ the cation is sandwiched between two B15C5 crown ether ligands, $r(\text{K}\dots\text{O}) = 281\text{--}296$ pm and has no interaction with the picrate ion. In (18C6)₂.K₂[phthalocyanine], (Figure 4b),¹⁷⁴ the K⁺ coordination sphere is atypical, the potassium being external to the 18C6 cavity; it is raised 160 pm from the mean plane of oxygen atoms. In fact two K⁺ ions are sandwiched separately between crown ether rings, $r(\text{K}\dots\text{O})_{\text{av}} = 339$ pm, and a phthalocyanine macrocycle, $r(\text{K}\dots\text{N})_{\text{av}} = 291$ pm in the trimacrocyclic sandwich complex illustrated in Figure 4b. In DB18C6.KI.(NH₂)₂CS, (Figure 4c),¹⁷⁵ the K⁺ ion is situated at the centre of the crown ether cavity and is in contact with all six ether oxygen atoms, $r(\text{K}\dots\text{O}) = 271\text{--}280$ pm; the sevenfold hexagonal pyramidal coordination is completed by the iodide anion, $r(\text{K}\dots\text{I}) = 357$ pm. The thiourea molecule neither participates in the complexation of K⁺ nor has it any contact with the polyether ligand; instead it forms polymeric chains by hydrogen bonding to sulphur atoms of adjacent thiourea molecules and to iodide anions (Figure 4c).¹⁷⁵

Field desorption mass spectrometry studies have been shown to be useful in the structural characterisation of crown ether complexes of alkali metal cations.¹⁷⁶ Strong peaks for the [crown ether.M]⁺ cationic moiety are invariably detected at low emitter currents for neutral or ionic complexes despite the general weakness of alkali metal-oxygen bonds. Analysis of the field desorption mass spectra of B15C5.NaI.H₂O (which is known to exist as [B15C5.Na.H₂O]⁺ I⁻), diMe-B15C5.NaBr ([diMe-B15C5.Na.Br]) DB30C10.KI ([DB30C10.K]⁺ I⁻) and (9).NaBr.xH₂O (which is of unknown structure), has led to the assignment of the ionic structure

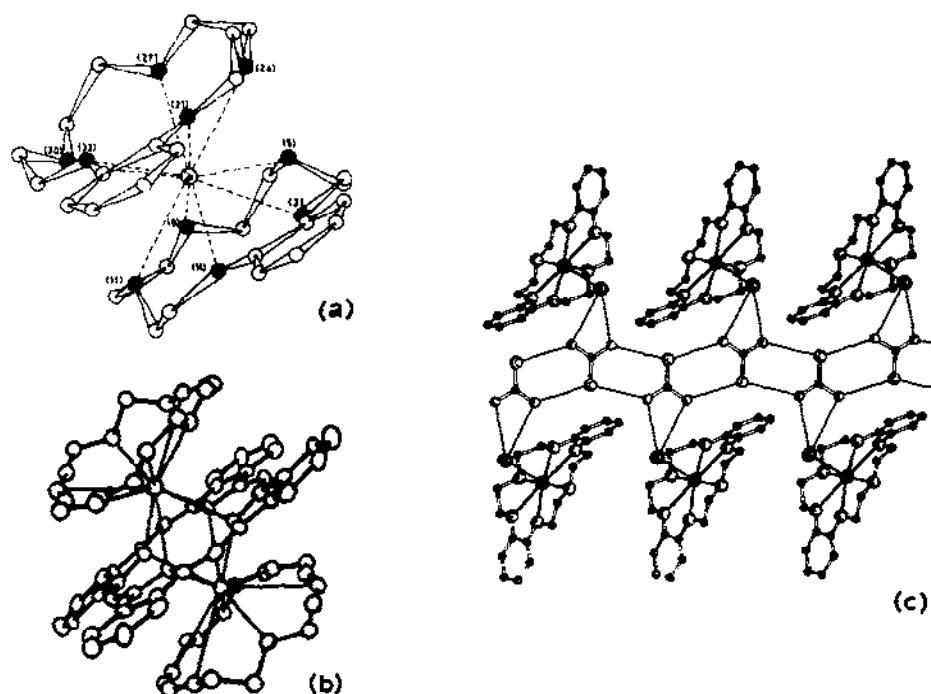
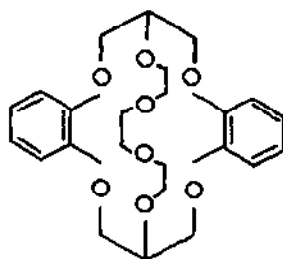


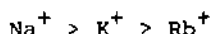
Figure 4. Perspective views of the K^+ coordination sphere in (a) $(B15C5)_2.K[picrate]$, (b) $(18C6)_2.K_2[phthalocyanine]$ and (c) $DB18C6.KI.(NH_2)_2CS$ (reproduced by permission from (a) *Inorg. Nucl. Chem. Letters*, 17(1981)207, (b) *J. Am. Chem. Soc.*, 103(1981)4629 and (c) *Angew. Chem. Int. Ed. Engl.*, 20(1981)1045).

$[(9).Na]^+Br^-.xH_2O$ for the latter complex.¹⁷⁶



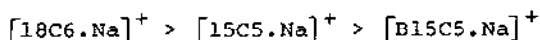
(9)

Field desorption mass spectrometry studies have also been used to derive stability data for DB18C6 complexes of alkali metal cations (Li-Cs) in the gas phase.¹⁷⁷ The ratio of the ion intensities $I_{[L.M]^+}/I_{M^+}$ decreases sharply in the series



for the $[DB18C6.M^+].I^-$ complexes, indicating the greater stability of the sodium complex. This sequence is somewhat unexpected since the greatest stability in aqueous solutions is found for the $[DB18C6.K^+].I^-$ complex. It is important to recall, however, that desolvation of the cation always occurs on formation of the $[L.M]^+$ complex.¹⁷⁷

The stabilities of sodium cation complexes with 15C5, B15C5 and 18C6 (as well as with C211, C221, C222 and C222B),¹⁷⁸ and of alkali metal cation (Na-Cs) complexes with 18C6¹⁷⁹ have been determined in both aqueous and non-aqueous solvents using multinuclear (¹³C-, ²³Na-) n.m.r.¹⁷⁸ and conductivity¹⁷⁹ techniques. The stabilities of the sodium ion complexes¹⁷⁸ varied in the order

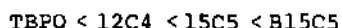


and those of the 18C6 complexes¹⁷⁹ varied in the order

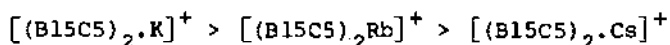
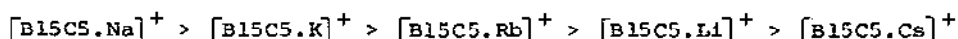


The selectivity of several small crown ethers (B12C4, B13C4, DB14C4, B15C5 and DB18C6) for a series of lithium salts has been assessed by solubility measurements.¹⁸⁰ B13C4 was found to be the most effective complexing agent for Li^+ . Indeed, both benzene and dichloromethane solutions of B13C4 selectively extract lithium salts from aqueous solutions.

Solvent extraction processes involving alkali metal salts in the presence of crown ethers have been investigated by four independent groups of authors.¹⁸¹⁻⁵ The distribution of alkali metal picrates (MX, M = Li-Cs) between water and benzene has been studied^{181,182} in the presence of tributylphosphate (TBPO), 12C4, 15C5, B15C5 and mixtures thereof. Extraction constants for rubidium and caesium picrates are determined in the presence of all four ligands; they increase in the sequence



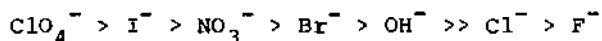
reflecting the increase in the number of donor oxygen atoms on the ligand. Extraction processes for all the alkali metal picrates in the presence of B15C5 have been elucidated.¹⁸² B15C5 extracted the salts as either $[\text{B15C5.M}]^+\text{X}^-$ or $[(\text{B15C5})_2.\text{M}]^+\text{X}^-$ complexes; in the presence of TBPO, B15C5 extracted rubidium and caesium picrates as $[\text{B15C5.M.TBPO}]^+\text{X}^-$ complexes. The sequence of extraction constants of these complexes are



The distribution of alkali metal picrates (MX ; $\text{M} = \text{Li}-\text{Cs}$) between water and polyurethane foam has been studied¹⁸³ in the presence of DCH18C6. The sequence of extraction constants for the $[\text{DCH18C6.M}]^+\text{X}^-$ complexes is



The effect of anions on the extraction of alkali metal salts from water into dichloroethane has been investigated in the presence of DCH18C6 and DCH24C8.¹⁸⁴ A significant effect is observed for DCH18C6, the extraction constants increasing in the sequence



This sequence is independent of the alkali metal, the extraction constants of the $[\text{DCH18C6.M}]^+\text{X}^-$ and $[\text{DCH24C8.M}]^+\text{X}^-$ complexes increasing in the same sequence as for the distribution of $[\text{DCH18C6.M}]^+\text{X}^-$ between water and polyurethane foam.¹⁸³ The effect of ionic strength on the extraction of potassium picrate into dichloromethane as $[\text{18C6.K}]^+\text{X}^-$ has also been assessed.¹⁸⁵

Several unusual anions have been stabilised by alkali metal-crown ether cations; compounds which have been isolated include $[\text{DB18C6.K}]^+[\text{Al}_2(\text{CH}_3)_6\text{O}_2]^-$,¹⁸⁶ $[\text{18C6.Na}]^+[\text{M}(\text{CO})_5\text{SH}]^-$ and

$[18C6.Na]^+[M_2(CO)_{10}(\mu-SH)]^-$ ($M = Cr, Mo, W$)^{187,188} and $[(18C6)_{14}Cs_9]^{9+}[Rh_{22}(CO)_{35}H_x]^{5-}[Rh_{22}(CO)_{35}H_{x+1}]^{4-}$; ¹⁸⁹ single crystal X-ray structural analysis of these salts has elucidated the molecular geometries of both the cations and the anions. The preliminary communication¹⁸⁶ in which the preparation and structural characterisation of $[DB18C6.K]^+[Al_2(CH_3)_6O_2]^-$ is reported gives details of the structure of the anion but not of the cation.

Structural analysis of $[18C6.Na]^+[W(CO)_5SH]^-$ and of $[18C6.Na]^+[W_2(CO)_{10}(\mu-SH)]^-$ has shown that both complexes are chain polymeric with sodium-carbonyl linkages between alternating cations and anions (Figure 5).^{187,188} The Na^+ cations are situated in a hexagonal bipyramidal coordination sphere in both complexes. In the former complex (Figure 5a), the Na^+ coordination geometry is slightly distorted with the six oxygen atoms of the 18C6 molecule occupying the equatorial plane, $r(Na...O) = 262-291$ pm, and the oxygen bonded carbonyl of one anion, $r(Na...O) = 241$ pm, and the thiolato sulphur atom of a second anion, $r(Na...S) = 301.4$ pm, occupying the two axial sites. In the latter complex (Figure 5b), however, the Na^+ coordination geometry is very distorted. As before, the equatorial plane comprises the six oxygen atoms of the 18C6 molecule, $r(Na...O) = 257.5-272.7$ pm, and the 8-fold coordination is completed by oxygen atoms on adjacent dinuclear anions, $r(Na...O) = 245.8, 247.1$ pm.

$[(18C6)_{14}Cs_9]^{9+}[Rh_{22}Co_{35}H_x]^{5-}[Rh_{22}Co_{35}H_{x+1}]^{4-}$ has been isolated from the reaction of $Rh(CO)_2acac$ with $PhCO_2Cs$ in 18C6 after 15-17 hours at 423-428K.¹⁸⁹ The complex, the largest discrete aggregate of metal atoms reported to date, has been characterised by low temperature (163K) single crystal X-ray diffraction studies. The overall composition of the cationic complex can be broken down into the three complexes: $[(18C6)Cs]^+$, $[(18C6)_2.Cs]^+$, $[(18C6)_3.Cs_2]^{2+}$; the asymmetric unit contains three 1:1, two 2:1 and two 3:2 complexes. Whereas the 1:1 complex is well known, the 2:1 and 3:2 complexes are novel, the 3:2 complex being an unprecedented species. The molecular geometries of the three complexes are shown in Figure 6. In the 1:1 complex (Figure 6a), the Cs^+ cation is external to the 18C6 cavity, $r(Cs...O) = 309-369$ pm, its coordination sphere being completed by two symmetry related bridging carbonyl ligands of the nearest cluster anion, $r(Cs...O) = 351$ pm. The Cs^+ cation in the 2:1 complex (Figure 6b) is sandwiched between two 18C6 moieties with $r(Cs...O)_{av} = 335$ and

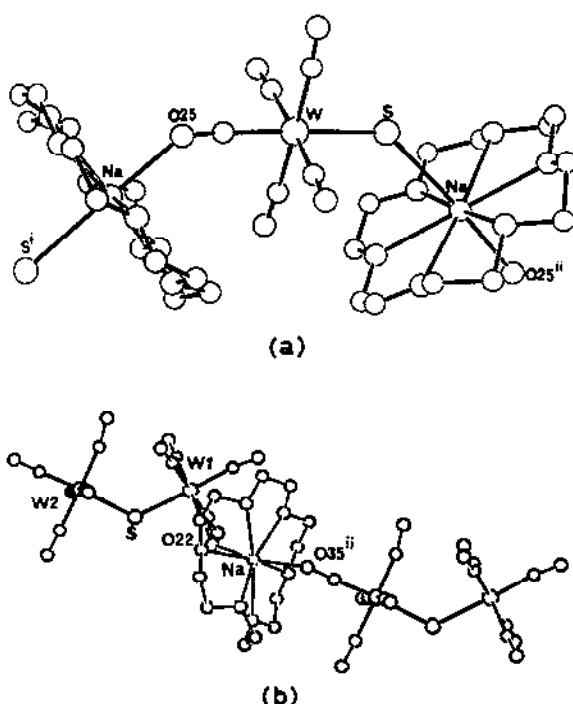


Figure 5. Molecular structures of (a) $[18C6.Na]^+[W(CO)_5SH]^-$ and (b) $[18C6.Na]^+[W_2(CO)_{10}(\mu-SH)]^-$ (reproduced by permission from J. Organomet. Chem., 212(1981)C10).

343 pm for the six oxygen atoms of crown(1) and crown(2), respectively (Figure 6b). The 3:2 complex, a so-called "club sandwich" complex, contains two Cs^+ cations sandwiched between three 18C6 moieties (Figure 6c). Average caesium-oxygen contacts are: 359 and 379 pm between Cs(3) and the six oxygen atoms of crown(3) and crown(4), respectively and 369 and 403 pm between Cs(4) and the six oxygen atoms of crown (4) and crown(5), respectively.¹⁸⁹

The complexation of $^{24}Na^+$ and $^{22}Na^+$ by crown ethers (and cryptands) has been investigated in chloroform-water systems in view of possible equilibrium isotope shifts.¹⁹⁰ With crown ethers $^{24}Na^+$ enhancement varied from insignificant values (for large crown ethers) up to $3.1 \pm 0.4\%$ (for 18C6). In the case of cryptands, $^{24}Na^+$ enrichment of $5.2 \pm 1.8\%$ (for C221) and $^{22}Na^+$ enrichment of $5.4 \pm 0.5\%$ (for C222) was achieved.¹⁹⁰

The formation of complexes of DB18C6 with $RMgX$ ($R = Me, Et$; $X = Br, I$) and $RCaX$ ($R = Me, Et, Ph$; $X = Br, I$) has been studied

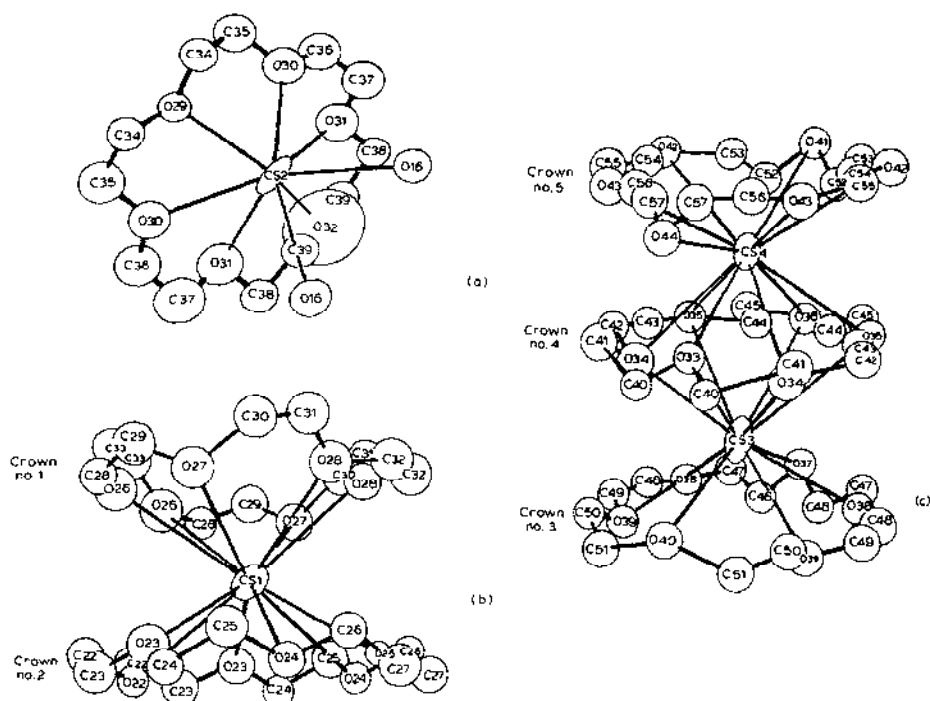


Figure 6. Ortep diagrams of the fragments of the $[(18C6)_4Cs_9]^{9+}$ cationic complex of $[(18C6)_4Cs_9]^{9+}[Rh_{22}(CO)_{35}H_x]^{5-}$, $[R_{22}(CO)_{35}H_{x+1}]^{4-}$: (a) $[(18C6)Cs]^{+}$, (b) $[(18C6)_2Cs]^{+}$, (c) $[(18C6)_3Cs_2]^{2+}$ (reproduced by permission from *Inorg. Chem.*, 20(1981)227).

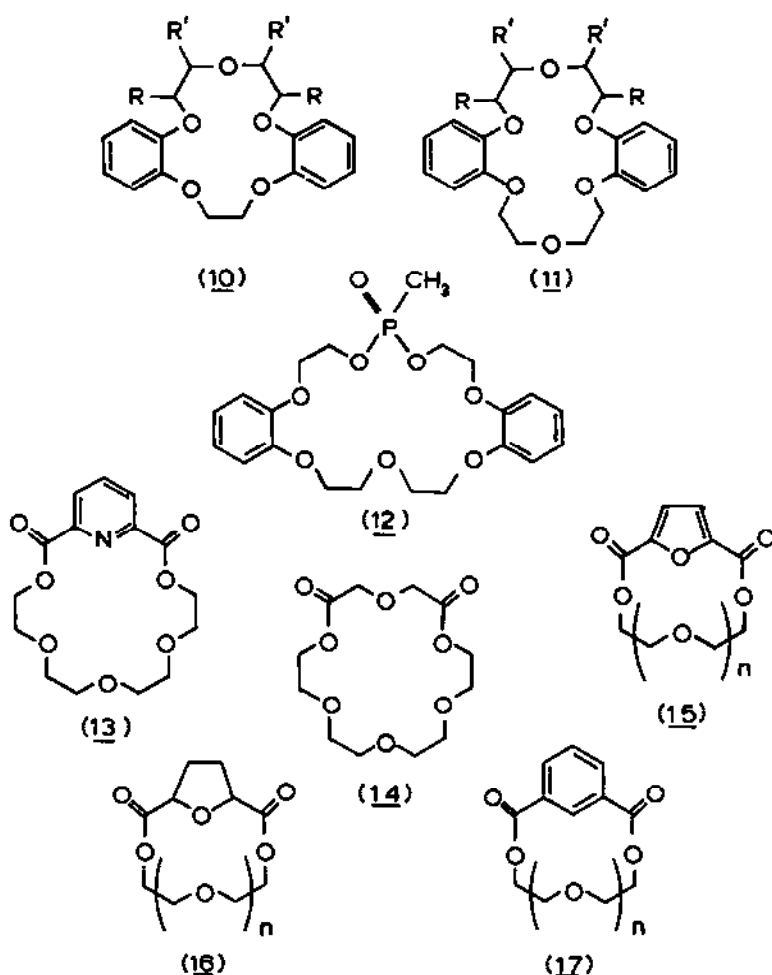
spectrophotometrically.¹⁹¹ Their reactions with aldehydes result in the formation of the corresponding alcohol with practically 100% specificity.¹⁹¹

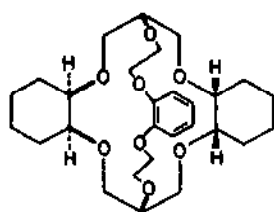
The facile transfer of $K_2S_2O_8$ into a variety of solvents (including hydrocarbons) in the presence of various crown ethers has been reported.¹⁹² The utilisation of these solutions for the initiation of the rapid polymerisation of acrylic and methacrylic monomers at temperatures close to ambient has also been described.¹⁹²

1.5.3 Complexes of Macrocyclic Polyethers of Novel Design

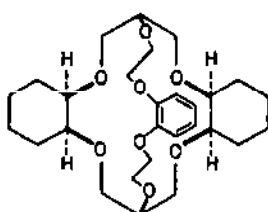
The desire to design and prepare macromolecular moieties, containing 3-D cavities of controlled geometry, capable of selectively binding specific substrates has led to a proliferation of macrocyclic polyethers. A large number of these materials

(10-27) have been shown to form complexes with either alkali or alkaline earth metal cations;¹⁹³⁻²⁰¹ the complexes have been identified in either solution¹⁹³⁻⁸ or solid state¹⁹⁹⁻²⁰¹ structural studies. Complex formation between (10), (11), (12) and alkali and alkaline earth metal cations has been studied spectrophotometrically. Though 1:1 (11): M^{n+} ($M = Na, K, Ca$) moieties are formed in the presence of the DB18C6 derivatives (11), 2:1 (10): K^+ and 1:1 (10): M^{n+} ($M = Na, Ca$) moieties are the major species present with the DB15C5 derivatives, (10).¹⁹³ Complexes with 1:1 (12): M^{n+} ($M = Li, Na, Mg-Ba$) molar ratios are formed with the phosphoryl containing macrocyclic ligand (12).¹⁹⁴

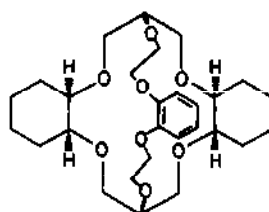




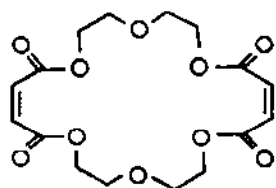
(18)



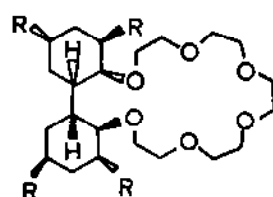
(19)



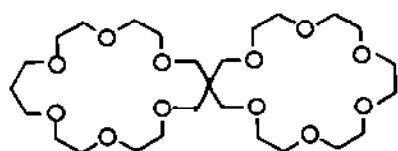
(20)



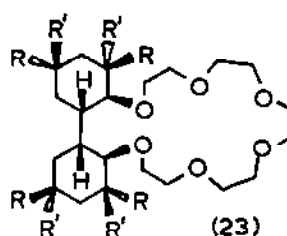
(21)



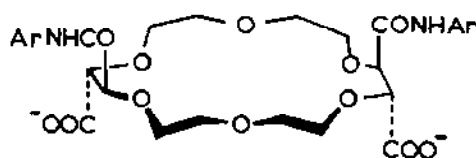
(22)



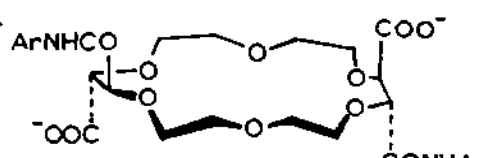
(24)



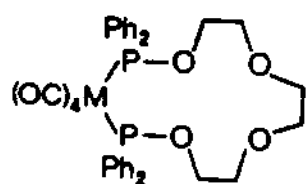
(23)



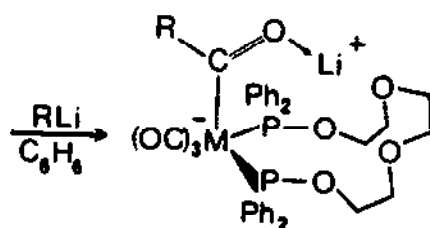
(25)



(26)



(27)



(28)

Formation constants for the 1:1 complexes between the macrocyclic polyether-diester ligands (13-17) and Na^+ , K^+ , Cs^+ and Sr^{2+} ions¹⁹⁵ and between the isomeric macrobicyclic polyethers (18-20) and Na^+ , K^+ , Rb^+ and Cs^+ ions¹⁹⁶ have been determined in methanol by thermodynamic methods. The values for the latter complexes show very significant differences between the isomeric ligands increasing from (20) through (18) to (19); the highest values occur for K^+ cations. This behaviour is consistent with the hypothesis that hydrogen atoms on cyclohexane junctions are somewhat electropositive, so that the cavity is most electronegative in (19), least electronegative in (20) and intermediate in (18).¹⁹⁶

Extraction constants¹⁹⁷ for a number of alkali metal (Li-Cs) and alkaline earth metal (Mg-Ba) picrates by macrocyclic polyether-ester ligands (21) have been determined; the selectivity of the macrocycles for the different cations is discussed in detail.¹⁹⁷ Ion selectivity studies¹⁹⁸ for alkali metal cations (Li-Cs) have been undertaken using macrocyclic polyether ligands containing the bicyclohexyl moiety (22,23); the selectivities of the ligands were similar to those of the analogous binaphthyl derivatives of 18C6.¹⁹⁸

Preliminary communications have been reported in which the structures of (24).2LiI.4H₂O,¹⁹⁹ the Ca^{2+} and Sr^{2+} complexes of (25) and (26),²⁰⁰ and the complex formed (28) on reaction of (27) with PhLi in benzene,²⁰¹ are described. The structure of the double loop complex¹⁹⁹ is unusual in that both of the rings bind one of the water molecules of solvation and a Li^+ cation in the same cavity (Figure 7). The metal cation is at the centre of a distorted trigonal bipyramid formed by three polyether oxygen atoms, the coordinated water oxygen atom and an oxygen atom from a solvating water molecule. In accord with the VSEPR theorem three shorter $\text{Li}^+\dots\text{O}$ contacts lie in the equatorial plane, $r(\text{Li}\dots\text{O}) = 193\text{-}198\text{ pm}$, while the two apical distances are somewhat longer, $r(\text{Li}\dots\text{O}) = 212, 223\text{ pm}$.¹⁹⁹

The complexing properties of the anti-(side discriminated) and syn-(face discriminated) tetrafunctional macrocycles (25) and (26), respectively, have been compared²⁰⁰ in their complexes with Ca^{2+} and Sr^{2+} , respectively. Although the syn-isomer wraps itself tightly around the cation, the anti-isomer adopts a more open structure. Thus, the carboxylate groups of the syn-isomer coordinate on the same side of the macrocycle, whereas those of

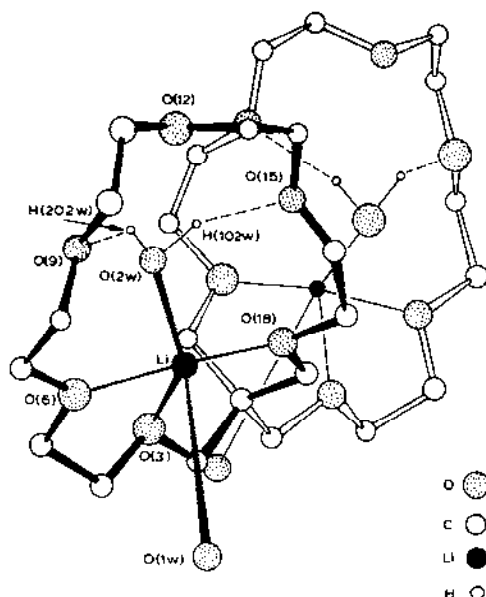


Figure 7. Perspective diagram of the molecular structure of the cation in (24).2LiI.4H₂O (reproduced by permission from J. Chem. Soc. Chem. Commun., (1981)472).

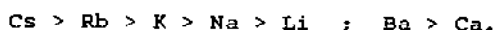
the anti-isomer coordinate on opposite sides of the macrocycle. The cations are nine-coordinate in both complexes. Although the coordination sphere of the syn-complex is completed by a chloride anion, the ninth position of the anti-complex is occupied by a water molecule.²⁰⁰

The structure of (28) contains a cavity with a radius of 200 pm in which the Li⁺ cation resides. The cavity is defined by the benzoate oxygen and the four oxygen atoms of the diposphinite-polyether ring; unfortunately details (bond distances and angles) of the Li⁺ coordination sphere are not quoted in the preliminary publication.²⁰¹

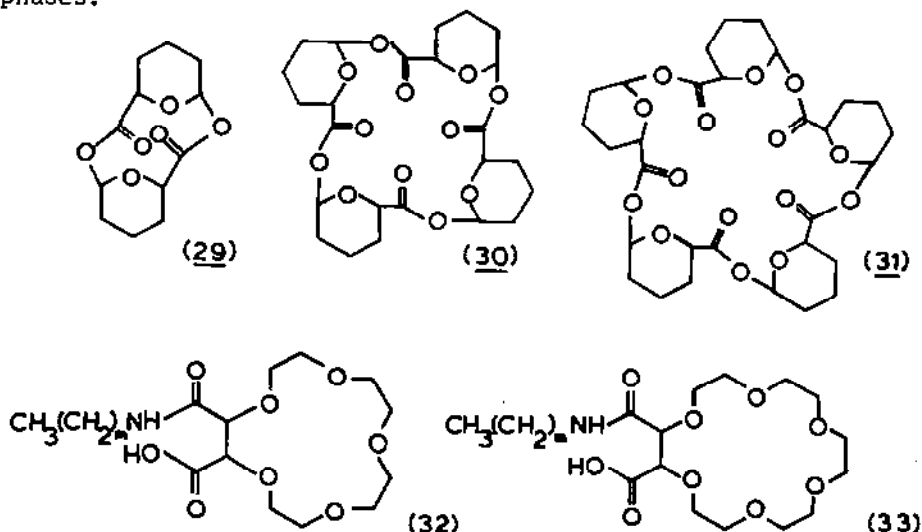
Ion transport mechanisms involving alkali metal cation complexes of macrocyclic polyether ligands have been studied in several laboratories.^{195,202-6} A correlation between the toxicity of crown ethers and their capability of transporting K⁺ ion has been noted;²⁰² it is based on the results of a study of the antibacterial activity of and ion (Li-Cs) transport efficiency and selectivity of 15C5, 18C6, B18C6 and DCH19C6.

The capacity of several macrolides, consisting of alternating

tetrahydropyran and ester moieties (29-31), for transporting and binding alkali (Li-Cs) and alkaline earth metal (Ca,Ba) picrates has been assessed.²⁰³ Whereas (29) was totally ineffective, (30) and (31) were found to be quite effective with ion selectivity sequences:



The observed properties are discussed in comparison with those of some natural and synthetic ionophores.²⁰³ The polyether-diester macrocycles (15) have also been found to be effective carriers of Cs^+ across a CHCl_3 liquid membrane separating aqueous phases.¹⁹⁵



Transport of alkali metal ions against their concentration gradients has been achieved using an artificial membrane system based on a series of 15C5 and 18C6 monoamides bearing long chain alkyl groups (32,33).^{204,205} Under the influence of a proton gradient the carriers move alkali metal cations from basic to acidic solution through a chloroform membrane as depicted in Figure 8a; transport occurs against the concentration gradient as a result of a coupled counterflow of protons. Carriers derived from 18C6 transport K^+ selectively and all ions more rapidly than 15C5 derivatives which are, however, selective for Na^+ .²⁰⁵

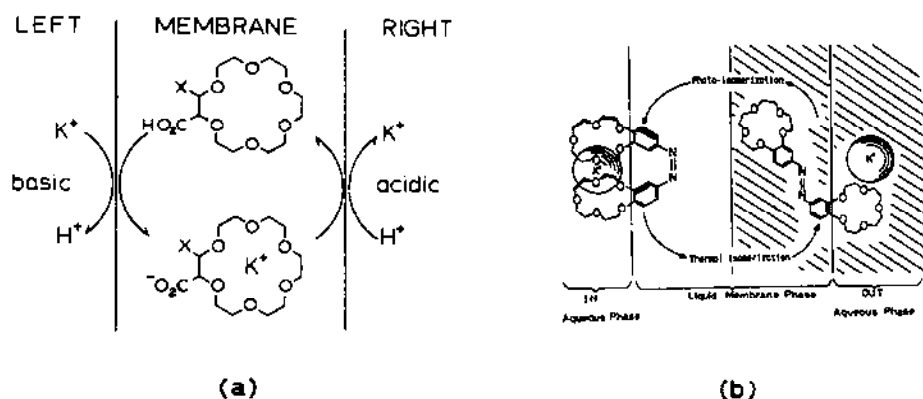
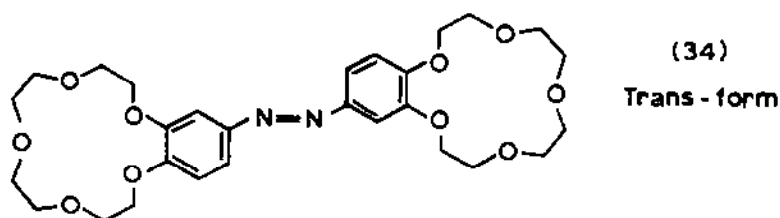


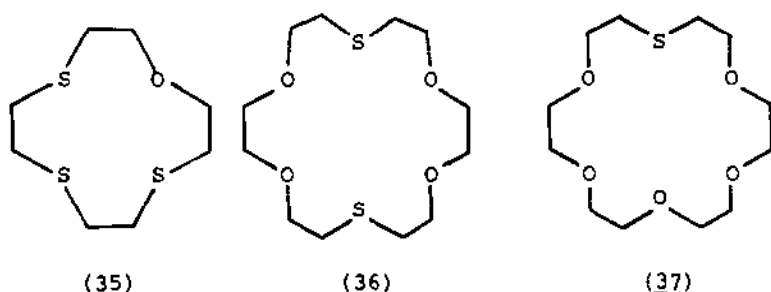
Figure 8. Schematic mechanisms for (a) carrier mediated counter-transport of a metal ion and a proton and (b) light driven ion transport (reproduced by permission from (a) *Canad. J. Chem.*, 59(1981)1734 and (b) *J. Am. Chem. Soc.*, 103(1981)111).

A photoresponsive bis(crown ether) with an azo-linkage (34), capable of transporting alkali metal cations across a liquid o-dichlorobenzene membrane has been synthesised.²⁰⁶ The trans-cis isomerism of (34) is photosensitive, whereas the cis-trans isomerism is thermally sensitive; the interconversion is reversible such as



the motion of a butterfly. Ion transport studies showed that the transport phenomenon was light sensitive, the transport velocity of the cation being accelerated when the liquid membrane in contact with the 1N aqueous phase was partially photoirradiated. This was thought to imply that ion transport can be facilitated by the interconversion between cis-(34) and trans-(34) occurring in the membrane phase as depicted in Figure 8b.²⁰⁶

Complexes of polyether sulphides with alkali metal cations have been investigated by two independent groups of authors.²⁰⁷⁻²¹¹ Complex formation between (35) and (36) and Li^+ , Na^+ and Cs^+ has



been studied by multinuclear (^7Li -, ^{23}Na -, ^{137}Cs -) n.m.r. techniques.²⁰⁷ The stabilities of the complexes have been compared with those of the corresponding polyethers 12C4 and 18C6; in all cases, substitution of the oxygen atoms by sulphur atoms results in a substantial decrease in complex stability.²⁰⁷

The results of a comprehensive series of crystal structure analyses of the polyether sulphide (37)²⁰⁸ and its complexes with NaSCN ,²⁰⁹ KSCN ,²¹⁰ and RbSCN ²¹¹ have been reported by Dalley et al. In all three complexes the cation coordinates to all five oxygen atoms of the polyether sulphide. The sulphur-cation interaction, however, depends on the cation; although there is no interaction for the Na^+ cation, there is a weak interaction for K^+ and Rb^+ cations.²⁰⁸ The Na^+ cation sits in a cavity formed by the five oxygen atoms to which it is coordinated. The nitrogen atom of the NCS^- anion completes the sixfold coordination of the Na^+ cation; the sulphur atom of the NCS^- anion translated a unit cell in the c direction interacts weakly with the Na^+ cation on the other side of the macrocycle.²⁰⁹ The K^+ cation sits in the cavity formed by the six heteroatoms of the macrocyclic ligand and is coordinated to all six atoms. The SCN^- ions interact but weakly with the K^+ ion in axial positions and link adjacent molecules.²¹⁰ The Rb^+ cation is located above the mean plane of, and coordinates to, all the heteroatoms of the macrocycle. It also coordinates in axial positions to the SCN^- anion (which exhibit an 80% preference for coordination through the nitrogen atom) and a sulphur atom from

an adjacent ligand.²¹¹ With the exception of this latter interatomic distance, $r(\text{Rb}\dots\text{S}) = 347.0$ pm, all salient structural data are summarised in Table 9.

Table 9. Salient interatomic distances/pm in the structures of (37).NaNCS,²⁰⁹ (37).KCNS²¹⁰ and (37).RbNCS.²¹¹

Compound	$\text{M}^+\dots\text{S}$	$\text{M}^+\dots\text{O}$	$\text{M}^+\dots\text{N}(\text{CS})$	$\text{M}^+\dots\text{S}(\text{CN})$	Distance of M^+ from mean plane of heteroatoms
(37).NaNCS	448.6	247.9-257.6	239.6	320.7	23*
(37).KCNS	328.4	276.8-287.4	304.3	336.6	20
(37).RbNCS	337.4	286.0-304.3	317.1	343.1	120

* This distance is that from the mean plane of the five oxygen atoms.

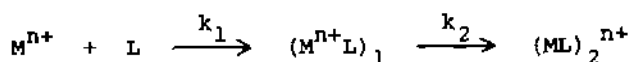
1.5.4 Cryptates and Related Complexes

Surprisingly few papers describing the chemistry of cryptates and related complexes have been published during the period of the Review. A combination ambient temperature X-ray and low temperature (20K) neutron diffraction study of $[\text{K-C222}]^+[\text{Cr}_2(\text{CO})_{10}(\mu\text{-H})]^-$ has been undertaken to determine the influence of the lattice environment and the K^+ ion on the anion's metal carbonyl framework and the ordered Cr-H-Cr bond.²¹² The K^+ ion is within the cryptate moiety and is coordinated to six oxygen, $r(\text{K}\dots\text{O}) = 278\text{-}289$, and two nitrogen, $r(\text{K}\dots\text{N}) = 298, 302$, donor atoms. Comparison of these distances with corresponding data for $[\text{K-C222}]^+\text{I}^-$ indicates that interaction with the $[\text{Cr}_2(\text{CO})_{10}(\mu\text{-H})]^-$ anion leads to an elongation of the cryptate moiety ($r(\text{N}\dots\text{N})$ increases by ~ 27 pm and $r(\text{K}\dots\text{N})$ increases by ~ 15 pm).²¹²

Several studies of the solution chemistry of cryptate complexes have been undertaken.²¹³⁻⁷ Volumes of complexation of C211, C221 and C222 with $\text{Li}^+\text{-Cs}^+$ in methanol and of C222 with, inter alia $\text{Ca}^{2+}\text{-Ba}^{2+}$ in water have been determined at 298K using a flow digital densitometer.²¹³ The interactions show a discontinuity when the radius of the cation is equal to the radius of the cavity of the undistorted cryptate.

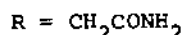
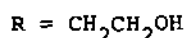
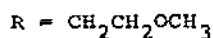
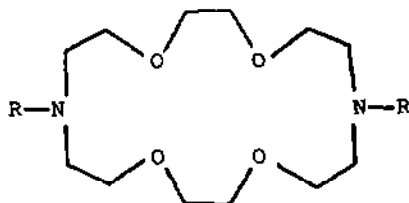
The kinetics of complexation of Li^+ and Ca^{2+} by C211 have been

measured in water at 298K using a stopped flow calorimeter.²¹⁴
 The complexation reaction exhibited a minimum of two relaxations;
 the following reaction mechanism was proposed:

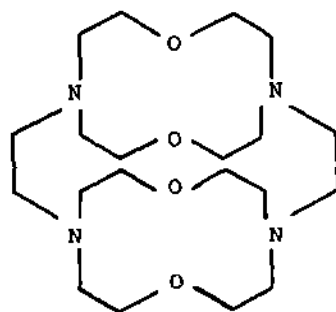


Cox, Schneider et al have undertaken a kinetic and thermodynamic study of the complexation of Li^+ - Cs^+ and of Ca^{2+} by C211, C221 and C222 in various solvents (aqueous and non-aqueous)^{215,216} and of Li^+ - Cs^+ by $C2_{D22}$ and $C2_{B2B2}$.²¹⁷ The stability constants of the $[M-C2_{D22}]^+$ and $[M-C2_{B2B2}]^+$ moieties were compared with previous results for $[M-C222]^+$ and $[M-C2_{B22}]^+$ complexes; the substituents cause a reduction in the stability of the cryptates and an increase in the dissociation rates.²¹⁷

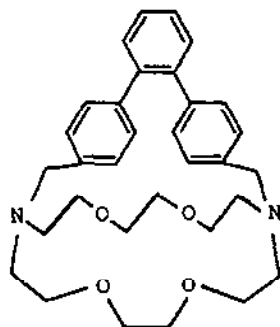
The stability constants of N,N'-disubstituted diaza-crown ether complexes (38) with Na^+ , K^+ , Mg^{2+} , Ca^{2+} have been obtained in aqueous solution at 298K.²¹⁸ They are discussed in terms of metal ion hydration, metal ion/cavity size, type of donor atom and the



(38)



(40)



(39)

topology of the ligand; comparisons are made with C22, C21, C222 and C221.²¹⁸

The molecular structures of the diaza-crown ether complexes, (39).NaNCS.CH₃OH,²¹⁹ and of (40).NaBF₄,²²⁰ have been elucidated. The pseudo crown section of the ligand in the former complex adopts the 'boat' configuration, thereby allowing all six heteroatoms to coordinate the Na⁺ ion in a biapical square pyramidal arrangement, $r(\text{Na}\cdots\text{O}) = 240.7\text{--}247.6$ pm, $r(\text{Na}\cdots\text{N}) = 268.5, 269.8$ pm, whilst the terphenyl residue folds away (Figure 9a). There is no direct contact between Na⁺ and NCS⁻; the anion is hydrogen bonded to a

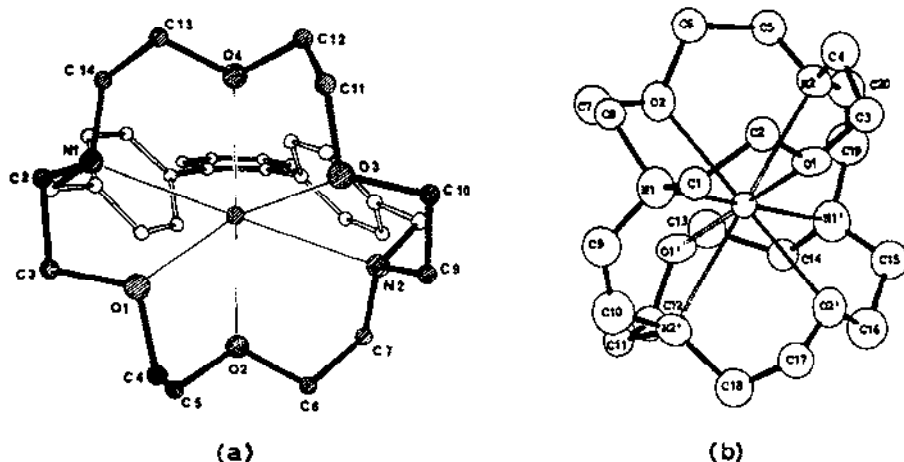


Figure 9. Perspective views of the cationic structure in (a) (39).NaNCS.CH₃OH and (b) (40).NaBF₄ (reproduced by permission from (a) Acta Crystallogr., B37(1981)1832 (b) Acta Chem. Scand., A35(1981)717).

methanol molecule.²¹⁹ In the latter complex, the Na⁺ ion is enveloped by the tricyclic ligand, (40) such that it is coordinated by all eight heteroatoms, $r(\text{Na}\cdots\text{O}) = 247, 250$ pm, $r(\text{Na}\cdots\text{N}) = 264, 265$ pm (Figure 9b); there is no interaction between Na⁺ and BF₄⁻.²²⁰

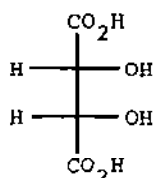
1.5.5 Salts of Carboxylic Acids

As in the 1980 Review, interest in these salts has centred on their structural chemistry. The crystal and molecular structures of lithium hydrogen acetylenedicarboxylate monohydrate²²¹ and of lithium hydrogen phthalate monomethanol solvate²²² have been determined by X-ray and neutron diffraction methods respectively; although the Li⁺ cations are effectively four-coordinate in both

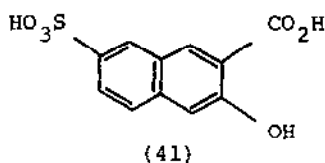
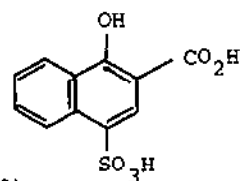
molecules, one of the two crystallographically distinct Li^+ ions in the latter has two more distant neighbours. The Li^+ cation in the acetylene dicarboxylate salt is approximately tetrahedrally surrounded by four oxygen atoms from three anions, $r(\text{Li}\dots\text{O}) = 192.6\text{--}197.9$ pm and from the water molecule, $r(\text{Li}\dots\text{O}) = 187.1$ pm.²²¹

One of the Li^+ cations in the phthalate salt, is sited in a fairly regular tetrahedral coordination sphere comprised of four oxygen atoms from four anions, $r(\text{Li}\dots\text{O}) = 192.1\text{--}194.1$ pm; the other Li^+ ion is sited in a grossly distorted tetrahedral coordination sphere comprised of four oxygen atoms from two phthalate anions, $r(\text{Li}\dots\text{O}) = 205.2, 205.6$ pm, and two solvate molecules, $r(\text{Li}\dots\text{O}) = 192.2, 194.4$ pm, with two more distant phthalate oxygen atoms, $r(\text{Li}\dots\text{O}) = 268.2, 282.3$ pm.²²² The electron distribution in the D_2O solvate of lithium formate has been studied²²³ by difference methods using experimental X-ray structural data and theoretical quantum-mechanical calculations.

The structures of seven sodium salts, viz, sodium oxalate,²²⁴ sodium dihydrogen triacetate,²²⁵ sodium 1,1-dihydroxyacetate,²²⁶ dextrarotatory (+) sodium ammonium tartrate tetrahydrate and racemic (\pm) sodium ammonium tartrate monohydrate,²²⁷ sodium 3-hydroxy-7-sulphonato-2-naphthoic acid trihydrate²²⁸ and sodium 1-hydroxy-4-sulphonato-2-naphthoic acid dihydrate,²²⁸ have been either refined²²⁴ or elucidated²²⁵⁻⁸ during the period of this Review. The refined structure of sodium oxalate²²⁴ is substantially the same as that determined earlier²²⁹ with some minor modifications to bond lengths. The Na^+ ion is in a distorted octahedral environment; this is also the case in the other six salts.²²⁵⁻⁸ In the acetate,²²⁵ the Na^+ ion is surrounded by oxygen atoms from two acetate anions, $r(\text{Na}\dots\text{O}) = 231.6, 232.6$ pm, and four acetic acid molecules, $r(\text{Na}\dots\text{O}) = 244.8\text{--}258.0$ pm; $r(\text{Na}\dots\text{O})$ are shorter for the acetate anions owing to the greater electrostatic attraction between these moieties and the Na^+ ion.²²⁵ The six oxygen atoms surrounding the Na^+ ion in the dihydroxyacetate²²⁶ come from two monodentate and two bidentate anions, $r(\text{Na}\dots\text{O}) = 232.9\text{--}245.8$ pm. The Na^+ coordination sphere in the dextrarotatory tartrate tetrahydrate is composed of six oxygens from three anions, $r(\text{Na}\dots\text{O}) = 239.6\text{--}250.6$ pm, and three water molecules, $r(\text{Na}\dots\text{O}) = 235.3\text{--}237.3$ pm; that in the racemic tartrate monohydrate, however, is composed of six oxygen atoms from two monodentate and one bidentate anion, $r(\text{Na}\dots\text{O}) = 229.0\text{--}248.9$ pm, and two water molecules, $r(\text{Na}\dots\text{O}) = 244.3, 263.9$ pm.²²⁷



Tartaric acid

3-hydroxy-7-sulphonato-
2-naphthoic acid.1-hydroxy-4-sulphonato-
2-naphthoic acid.

The major difference in the structures of the two naphthoic acid derivatives is in the extent of the distortion of the octahedral Na^+ coordination sphere.²²⁸ For (41), the distortion is only slight, the six oxygen atoms coming from a bidentate sulphonato group, $r(\text{Na}\dots\text{O}) = 235.3, 245.0$ pm, and a carboxyl group, $r(\text{Na}\dots\text{O}) = 237.6$ pm of separate anions and three water molecules, $r(\text{Na}\dots\text{O}) = 245.2-249.3$ pm. For (42), however, gross distortion occurs, the six oxygen atoms coming from two monodentate sulphonato groups, $r(\text{Na}\dots\text{O}) = 230.4, 262.0$ pm, a hydroxyl group, $r(\text{Na}\dots\text{O}) = 262.7$ pm, and a carboxyl group, $r(\text{Na}\dots\text{O}) = 247.1$ of four separate anions and two water molecules, $r(\text{Na}\dots\text{O}) = 234.6, 239.6$ pm.²²⁸

The structure of $\text{KHC}_2\text{O}_4 \cdot \text{H}_2\text{C}_2\text{O}_4 \cdot 2\text{H}_2\text{O}$ has been redetermined in space group $\text{P}1$ as opposed to the earlier $\text{P}\bar{1}$;²³⁰ the refinement was undertaken to analyse the hydrogen bonding in the structure.

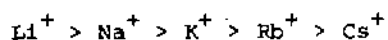
Single crystal X-ray diffraction studies of the methyloxanthates $\text{M}[\text{SOCOCH}_3]$ ($\text{M} = \text{K},$ ²³¹ Rb ²³²) have shown that whereas the K^+ ion is surrounded by four oxygen, $r(\text{K}\dots\text{O}) = 276.4-307.5$ pm, and four sulphur atoms, $r(\text{K}\dots\text{S}) = 331.7-367.4$ pm from five anions, the Rb^+ ion is surrounded by five oxygen, $r(\text{Rb}\dots\text{O}) = 286.5-353.3$ pm, and three sulphur atoms, $r(\text{Rb}\dots\text{S}) = 340.9-353.4$ pm, from six anions. In neither salt is the cation in a regular coordination sphere; that of the K^+ ion consists of two interpenetrating distorted O_4 and S_4 tetrahedra,²³¹ whereas that of the Rb^+ ion is a distorted bicapped trigonal prism.²³²

In the structure of the α -cyclodextrin (α -CD) inclusion complex with the potassium salt of γ -aminobutyric acid (GABA), $\alpha\text{-CD} \cdot \text{GABA}^- \cdot \text{K}^+ \cdot 10\text{H}_2\text{O}$, the anions are inserted in the cavities of the α -CD molecules and do not coordinate the K^+ ion.²³³ The K^+ ion is coordinated to six oxygen atoms in a distorted octahedral arrangement; four atoms, two from water molecules, $r(\text{K}\dots\text{O}) = 273, 300$ pm, and two from glucose moieties, $r(\text{K}\dots\text{O}) = 296, 304$ pm, form

a rough plane and the other two atoms, one from a water molecule, $r(K...O) = 277$ pm, and one from a glucose moiety, $r(K...O) = 277$ pm, occupy the apices.²³³

Field desorption mass spectra of sodium acetate, sodium propionate, labelled analogues and mixtures have been measured.²³⁴ In particular, hydrogen and alkyl group exchange accompanying the desorption process was investigated. Unfortunately a simple mechanistic scheme cannot be formulated owing to the complexity of the intermolecular reactions.²³⁴ ^{39}K quadrupole resonance signals have been detected in a number of potassium salts at room temperature;²³⁵ these include potassium hydrogen oxalate, potassium hydrogen maleate, dipotassium maleate, potassium hydrogen chloromaleate and potassium hydrogen phthalate.

Aqueous solution behaviour of alkali metal (Li-Cs) citrates²³⁶ and sodium cholate²³⁷ has been investigated using n.m.r. techniques. The formation constants of the alkali metal citrate complexes decrease in the sequence



Although the cholate anion is monomeric at low concentrations (< 0.01 mol dm⁻³), tetramer formation occurs at higher concentrations; it is complete at very high concentrations (> 0.11 mol dm⁻³).²³⁷

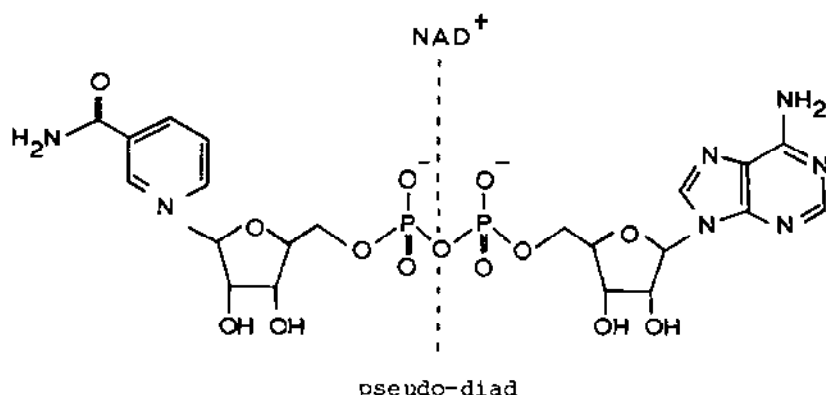
A group of Russian authors have reported the results of a comprehensive study of the thermal decomposition of the phthalates, $M_2X \cdot 2H_2O$,^{238,239} MHX ,^{238,239} $RbH_3X_2 \cdot 2H_2O$ ²⁴⁰ and CsH_3X_2 ²⁴¹ ($M=Rb, Cs$; $X=phthalate$). The normal phthalate dihydrates $M_2X \cdot 2H_2O$ initially undergo total dehydration, the rubidium salt via the monohydrate, $Rb_2X \cdot H_2O$, the caesium salt via the hemihydrate, $Cs_2X \cdot \frac{1}{2}H_2O$. Subsequently the anhydrous salts decompose to M_2CO_3 , CO_2 and carbon. At very high temperatures combustion of carbon and decomposition of M_2CO_3 occurs. The anhydrous hydrogen phthalates, MHX , decompose directly to the normal phthalate and phthalic acid; subsequent decomposition is as for the anhydrous normal phthalate. Thermal decomposition of $RbH_3X_2 \cdot 2H_2O$ and of CsH_3X_2 proceeds in a series of distinct steps. The initial step in both cases leads to formation of the anhydrous hydrogen phthalate, MHX and phthalic acid; subsequent decomposition is as for the anhydrous hydrogen phthalate.

1.5.6 Salts of Nucleotides and Moieties of Biological Significance

Several papers have been published²⁴²⁻⁶ in which various aspects of complex formation between alkali metal cations and nucleotides or related species are discussed. Although the majority of the papers are structurally based, complex formation between Na^+ or K^+ and adenosine-5'-triphosphate(ATP) has been studied in solution using potentiometric and calorimetric methods.²⁴² The formation constants of $[\text{M}(\text{ATP})]^{3-}$ complexes agree with those previously reported and indicate a high stability. No evidence for the formation of $[\text{MH}(\text{ATP})]^{2-}$ or $[\text{M}_2(\text{ATP})]^{2-}$ complexes was obtained under the conditions of the experiment ($C_M \leq 0.1 \text{ mol dm}^{-3}$).²⁴²

Structural data have been obtained for the disodium salt of guanosine-5'-monophosphate (GMP) hydrate,²⁴³ the monosodium salt of cytidine-5'-diphosphoethanolamine (CDPE) hydrate,²⁴⁴ and the lithium salt of the coenzyme nicotinamide adenine dinucleotide (NAD^+) dihydrate.²⁴⁵

There are four crystallographically independent Na^+ ions, each of which is six-coordinate, in the structure of the GMP derivative (Figure 10a). $\text{Na}(1)$ has four water oxygen atoms, $r(\text{Na}(1) \dots \text{O}) =$



nicotinamide-5'-ribonucleotide

adenylic acid

236.5-249.5 pm, and two N(7) atoms of separate guanosine bases, $r(\text{Na}(1) \dots \text{N}) = 241.9, 261.1 \text{ pm}$, as neighbours. $\text{Na}(2)$ and $\text{Na}(3)$ are completely surrounded by water oxygen atoms, $r(\text{Na}(2) \dots \text{O}) = 239.6-275.8 \text{ pm}$ and $r(\text{Na}(3) \dots \text{O}) = 233.8-261.8 \text{ pm}$, $\text{Na}(4)$ coordinates to four water oxygen atoms, $r(\text{Na}(4) \dots \text{O}) = 227.1-282.8 \text{ pm}$ and the two hydroxyl oxygen atoms of a ribose moiety, $r(\text{Na}(4) \dots \text{O}) = 231.4, 247.1 \text{ pm}$.²⁴³ The Na^+ coordination sphere in the CPDE derivative is complex.²⁴⁴ The ion is surrounded by four oxygen atoms, two

from the ribose moiety, $r(\text{Na}\dots\text{O}) = 238.7, 238.9$ pm, one phosphate oxygen, $r(\text{Na}\dots\text{O}) = 222.0$ pm and one water oxygen, $r(\text{Na}\dots\text{O}) = 229.3$ pm, and a single nitrogen atom from the cytosine base, $r(\text{Na}\dots\text{N}) = 245.5$ pm; a sixth coordination position is occupied by a more remote cytosine oxygen atom, $r(\text{Na}\dots\text{O}) = 297.0$ pm.²⁴⁴

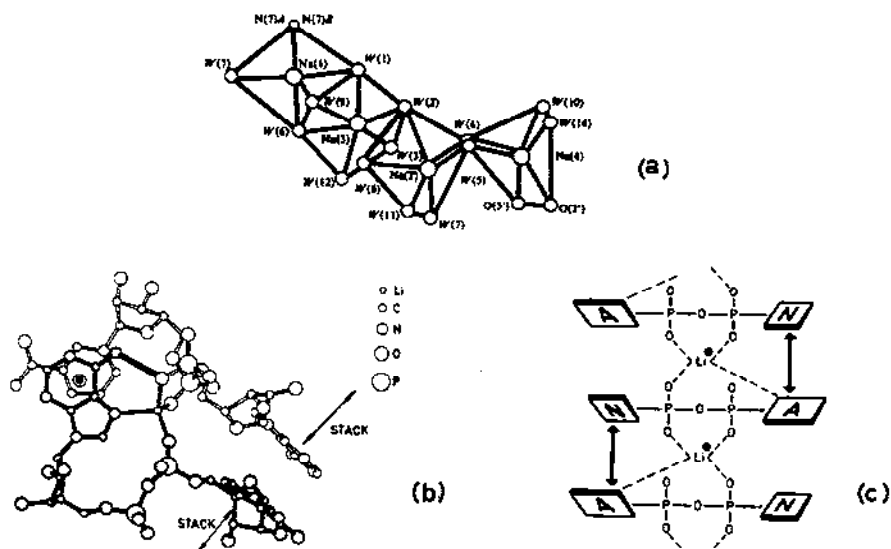


Figure 10. Coordination polyhedra of (a) Na^+ in $[\text{GMP}]\text{Na}_2\cdot\text{H}_2\text{O}$ and (b) Li^+ in $\text{Li}^+\cdot\text{NAD}^+\cdot 2\text{H}_2\text{O}$. Schematic diagram (c) of the stacking in $\text{Li}^+\cdot\text{NAD}^+\cdot 2\text{H}_2\text{O}$ (reproduced by permission from (a) *Acta Crystallogr.*, B37(1981)1825 and (b,c) *J. Am. Chem. Soc.*, 103(1981)907).

As might be expected the structure of $\text{Li}^+\cdot\text{NAD}^+\cdot 2\text{H}_2\text{O}$ is very complex.²⁴⁵ The role played by the Li^+ ion in the molecular stacking in the unit cell is shown in Figure 10c; it links the NAD^+ molecular units, which adopt an extended form with nicotinamide and adenine nearly perpendicular to each other at 1200 pm separation, in an antiparallel fashion with alternating adenine and nicotinamide residues on adjacent molecules. The coordination geometry of the Li^+ ion (Figure 10b) is approximately tetrahedral and comprises N(7) of the adenine moiety, $r(\text{Li}\dots\text{N}) = 213$ pm, the nicotinamide phosphate oxygen, $r(\text{Li}\dots\text{O}) = 186$ pm, and the pyrophosphate free oxygens, $r(\text{Li}\dots\text{O}) = 188, 192$ pm.²⁴⁵

Structural studies have been undertaken for the sodium salt of phosphoenolpyruvate ($\text{HO}_2\text{C}\cdot\text{CH}(\text{CH}_3)\cdot\text{O}\cdot\text{PO}_3\text{H}_2$)²⁴⁶ and for the monosodium

and disodium salts of N-formyl, N-hydroxyglycine (hadacidin - $\text{HO}_2\text{C} \cdot \text{CH}_2 \cdot \text{N}(\text{OH}) \cdot \text{CHO}$).²⁴⁷ Two crystallographically independent Na^+ ions exist in the phosphoenolpyruvate salt.²⁴⁶ $\text{Na}(1)$ has six oxygen nearest neighbours, four contributed by phosphate residues of different anions, $r(\text{Na} \dots \text{O}) = 236.3\text{--}265.8$ pm, and two by water molecules, $r(\text{Na} \dots \text{O}) = 240.9, 249.0$ pm. $\text{Na}(2)$ is coordinated to five oxygen atoms, three from independent anions, $r(\text{Na} \dots \text{O}) = 230.9\text{--}255.8$ pm, and two from water molecules, $r(\text{Na} \dots \text{O}) = 233.5, 241.8$ pm. In the monosodium salt of hadacidin,²⁴⁷ which is an L-aspartate antagonist for the enzyme adenylosuccinate synthetase, the Na^+ ion resides in a distorted octahedral environment of oxygen atoms, four of which are provided by three anions, $r(\text{Na} \dots \text{O}) = 233.5\text{--}258.6$ pm, and two by water molecules, $r(\text{Na} \dots \text{O}) = 228.3, 238.1$ pm. The Na^+ ion coordination is much more complex in the disodium salt of hadacidin, there being three crystallographically independent cations.²⁴⁷ $\text{Na}(1)$ is in a distorted trigonal bipyramidal coordination sphere of oxygen atoms, four of which come from three anions, $r(\text{Na} \dots \text{O}) = 231.8\text{--}236.1$ pm, and one from a water molecule, $r(\text{Na} \dots \text{O}) = 233.6$ pm. $\text{Na}(2)$ is octahedrally coordinated by two oxygen atoms from symmetry related anions, $r(\text{Na} \dots \text{O}) = 245.4$ pm, and four oxygen atoms from symmetry related water molecules, $r(\text{Na} \dots \text{O}) = 239.2, 254.0$ pm. $\text{Na}(3)$ is octahedrally coordinated by four oxygen atoms from symmetry related anions, $r(\text{Na} \dots \text{O}) = 233.0, 267.9$ pm and by two oxygen atoms from symmetry related water molecules, $r(\text{Na} \dots \text{O}) = 244.1$ pm. The distortion of the coordination octahedra around $\text{Na}(2)$ and $\text{Na}(3)$ of the disodium salt is much less than that around the cation in the monosodium salt of hadacidin.²⁴⁷

Structural features of the hydrated forms of sodium²⁴⁸ and potassium²⁴⁹ sucrose octasulphate, $\text{C}_{12}\text{H}_{14}\text{O}_{11} \cdot (\text{SO}_3\text{M})_8 \cdot n\text{H}_2\text{O}$ ($\text{M} = \text{Na}, \text{K}$), have been elucidated. Although the potassium salt²⁴⁹ is crystalline, the sodium salt²⁴⁸ is amorphous. Thus, whereas the structure of the potassium salt has been determined by conventional methods, that of the sodium salt has been elucidated from X-ray scattering intensity data using the radial distribution function together with the correlation method. Each of the eight K^+ ions is surrounded by five to seven oxygen atoms forming irregular coordination polyhedra. On average each K^+ ion (except for $\text{K}(7)$) is surrounded by 4.7 oxygen atoms from sulphato groups and 1.7 oxygen atoms from water molecules, $r(\text{K} \dots \text{O})_{\text{av}} = 283.2$ pm. $\text{K}(7)$ is

surrounded by seven oxygen atoms from sulphato groups, $r(K...O)_{av} = 281.4$ pm.²⁴⁹ The model which best fitted the scattering intensity data for the amorphous sodium salt was based on the structure of the potassium salt. Each sulphur atom is tetrahedrally surrounded by oxygen atoms, $r(S...O)_{av} = 150$ pm, while each Na^+ ion is octahedrally surrounded by oxygen atoms, $r(Na...O)_{av} = 242$ pm.²⁴⁸

The crystal structure of a complex of valinomycin (a cyclic dodecadepsipeptide containing D-valine, D- α -hydroxyvaleric acid, L-valine and L-lactic acid in the sequence $cyclo(L\text{-Val-D-Hyv-D-Val-L-Lac})_3$) with potassium picrate has been determined by single crystal methods.²⁵⁰ The K^+ ion resides inside the valinomycin cavity, $r(K...O) = 267\text{--}281$ pm, and has a weak but definite interaction with an oxygen atom of the para-nitro group of the picrate anion, $r(K...O) = 386$ pm.²⁵⁰

1.5.7 Multimetal Complexes Containing Alkali Metals

Structural studies have been undertaken on a small number of multimetal complexes including lithium; both methyl($-Li(\mu\text{-Me})_2M-$) and chloro($-Li(\mu\text{-Cl})_2M-$) bridging units have been studied. Three compounds containing methyl bridging units have been structurally characterised.^{151,152} $[Li(tmen)(\mu\text{-Me})_2Mg(\mu\text{-Me})_2Li(tmen)]$ and $[Li(tmen)(\mu\text{-Me})_2Mg(\mu\text{-Me})_2Mg(\mu\text{-Me})_2Li(tmen)]$ have been prepared by reaction of $(MeLi)_4$ with (Me_2Mg) in dry ether containing tmen.²⁵¹ The structure of the former has been elucidated by single crystal methods. The Mg atom is tetrahedrally surrounded by methyl groups, $r(Mg...C) = 223.1\text{--}229.5$ pm, which form bridges to the crystallographically distinct Li atoms, $r(Li(1)...C) = 227.5, 229.5$ pm, $r(Li(2)...C) = 226.1, 230.4$ pm, which are chelated by tmen ligands $r(Li(1)...N) = 209.4, 210.0$ pm, $r(Li(2)...N) = 209.3, 211.5$ pm. The Li^+ coordination polyhedra is distorted tetrahedral. The structure of the latter complex is assumed by inference.²⁵¹ $[Li_3(tmen)_3ErMe_6]$ has been crystallised from a solution of $ErCl_3$ and $(MeLi)_4$ in dry ether containing tmen.²⁵² Structural analysis has shown that the Er atom is surrounded in a distorted octahedral configuration by six methyl groups, $r(Er...C) = 257$ pm, which form three bridges to lithium atoms, $r(Li...C) = 222$ pm, chelated by tmen molecules, $r(Li...N) = 221$ pm. Once again the Li^+ coordination polyhedron is distorted tetrahedral.²⁵²

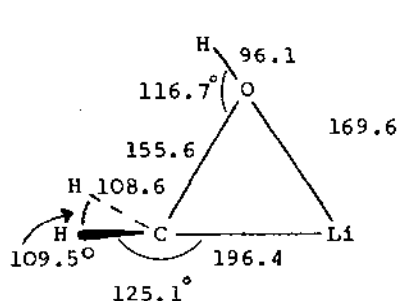
A plethora of complexes containing chloro bridging units have been prepared and characterised.²⁵³ They include

(a) $[\text{Ln}(\text{h}^5\text{-C}_5\text{H}_3(\text{SiMe}_3)_2)]_2(\mu\text{-Cl})_2\text{LiL}_2$ ($\text{Ln} = \text{Sc, Y, La, Ce, Pr, Nd}$ or Yb ; $\text{L} = \text{thf}$ or $\text{Ln} = \text{Y, La}$; $\text{L}_2 = \text{tmen}$ or $\text{Ln} = \text{Y, Nd}$; $\text{L}_2 = \text{dme}$),
 (b) $[\text{LnCl}_{2-n}(\text{OAr}^{\text{Me}})_n(\mu\text{-Cl})_2\text{Li}(\text{thf})_2]$ ($\text{OAr}^{\text{Me}} = \text{OC}_6\text{H}_2\text{Bu}_2^{\text{t-2,6-Me-4}}$; $\text{Ln} = \text{Y, La, Er, Yb}$; $n = 1$ or $\text{Ln} = \text{Y}$, $n = 2$) and (c)
 $[\text{ErCl}(\text{N}(\text{SiMe}_3)_2)(\mu\text{-Cl})_2\text{Li}(\text{thf})_2]$. Structural analysis of the compound $[\text{Nd}(\text{h}^5\text{-C}_5\text{H}_3(\text{SiMe}_3)_2)]_2(\mu\text{-Cl})_2\text{Li}(\text{thf})_2$ has shown that both metal atoms are in distorted tetrahedral environments; detailed structural parameters are not quoted in this preliminary communication.²⁵³

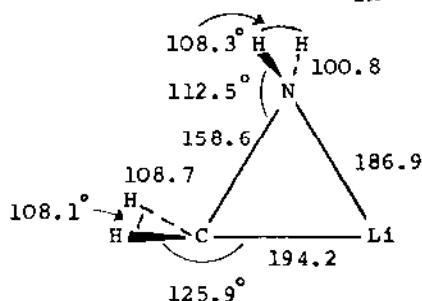
1.5.8 Lithium Derivatives

Although there are a vast number of publications dealing with lithium chemistry, the majority have been ignored since they deal with organolithium chemistry which is reviewed elsewhere. The only papers which have been abstracted for this Review are those involving either theoretical studies of small molecules or experimental studies of inorganic derivatives.

The results of several ab initio MO calculations on small organolithium moieties have been presented.²⁵⁴⁻⁸ Of the many isomeric forms considered for LiCH_2OH and LiCH_2NH_2 , the most stable structures are the bridged species, (43) and (44), respectively;²⁵⁴ they correspond to the most stable isomer of LiCH_2F discussed in the 1979 review.²⁵⁹ Similarly the most stable structure of $\text{LiCH}_2\text{CH}_2\text{Li}$ was found to be the C_{2h} molecule (45) with a trans conformation (dihedral angle $\angle\text{LiCCLi} = 180^\circ$) but an unusual partially bridged geometry ($\angle\text{LiCC} = 73.2^\circ$).²⁵⁵ However, the D_{2h} symmetrically

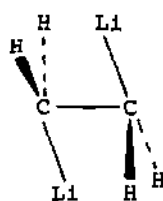


(43)

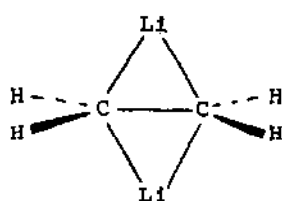


(44)

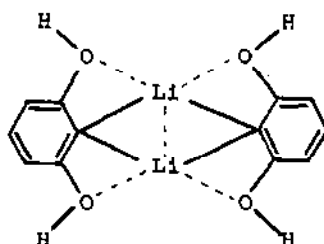
distances / pm.



(45)



(46)



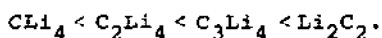
(47)

trans doubly bridged structure (46), a transition state for dyotropic rearrangement is only 7.9 kJ mol^{-1} higher in energy.²⁵⁵

Theoretical studies²⁵⁶ of 2,6-substituted phenyl lithium dimers (planar tetraco-ordinate carbon candidates) have shown that although the dimer of phenyl-lithium has an intrinsic preference for a planar geometry at the carbon atom ($\Delta H_f^O(\text{calc}) = -141.0 \text{ kJ mol}^{-1}$) vis-a-vis a tetrahedral geometry at the carbon atom ($-116.3 \text{ kJ mol}^{-1}$), the introduction of two water molecules is sufficient to reverse the stability order of planar ($-669.4 \text{ kJ mol}^{-1}$) and tetrahedral ($-725.4 \text{ kJ mol}^{-1}$) isomers.²⁵⁶ For the dimer of 2,6-dihydroxyphenyl-lithium, however, the intrinsic preference for the phenyl-lithium dimer unit to adopt a planar geometry (47) is reinforced through 'intramolecular solvation'. It is thought that the large difference in stability between the planar isomer ($-942.1 \text{ kJ mol}^{-1}$) and the tetrahedral isomer ($-820.0 \text{ kJ mol}^{-1}$) may be sufficient to stabilise the planar isomer vis-a-vis a solvated tetrahedral isomer.²⁵⁶

Ab initio calculations of the relationship between the energies of carbanions, R^- and their lithiated counterparts, RLi ²⁵⁷ and of hydride abstraction from ethyl, n-butyl and s-butyl lithium²⁵⁸ have also been undertaken.

Studies²⁶⁰ of the thermal rearrangements of the lithiated compounds CLi_4 , CH_2Li_2 and C_3Li_4 have produced the following thermal stability sequence

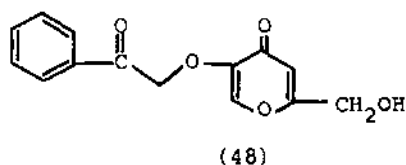


It has also been shown that flash vacuum heating of these compounds results in vapour transport with no more than 10% decomposition (normal heating results in 100% decomposition to Li_2C_2); this observation illustrates that it may be possible to structurally

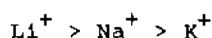
characterise gas phase polyolithium organic moieties.²⁶⁰

Earlier assignments of the structures of $\text{CH}_2=\text{CH}-\text{CH}_2\text{X}$ ($\text{X} = \text{Li}, \text{K}, \text{Cs}, \text{MgBr}$) have been confirmed in a high resolution ^{13}C -n.m.r. study of terminally monodeuterated derivatives in thf.²⁶¹ Thus, allyl lithium forms a distorted π -complex, allyl potassium and allyl caesium are perfectly symmetrical or slightly asymmetrical π -complexes and allyl magnesium bromide exists in a σ -covalent structure which rapidly and reversibly converts into its 'metallomeric' mirror image.²⁶¹

Complexation of alkali metal cations by 1,2-dimethoxyethane²⁶² by the dicarbonyl ligands, $\text{CH}_3\text{CO}(\text{CH}_2)_n\text{COCH}_3$ ($0 \leq n \leq 2$),²⁶³ by phenacyl kojate (48)²⁶⁴ and by 2,2'-bipyridine²⁶⁵ has been



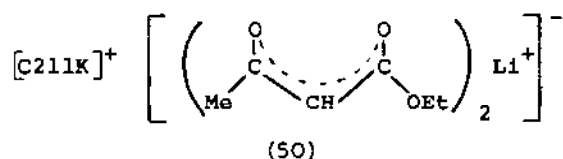
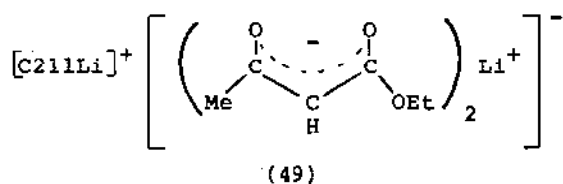
investigated in a variety of aqueous and non-aqueous solvents. Dielectric relaxation studies²⁶² of solutions of MClO_4 ($\text{M} = \text{Li}, \text{Na}$) in dme indicate that solvation of Li^+ and Na^+ by dme cannot be described as for thf or ethylacetate for which the assumption of rigidly bound solvating molecules is acceptable, but must allow for some freedom in the orientation of the solvating dme molecules. Multinuclear (^7Li , ^{23}Na , ^{39}K) n.m.r. studies²⁶³ of the interaction of alkali metal cations with $\text{CH}_3\text{CO}(\text{CH}_2)_n\text{COCH}_3$ have shown that the chemical shifts can be regarded as a semi-quantitative measure of the strength of the ion-ligand interaction, at least within a series of homologous ligands. Conductometric studies²⁶⁴ have been applied in an attempt to ascertain synthesis conditions for a series of complexes of alkali metal cations with phenacyl kojate. Complex formation between alkali metal cations ($\text{Li}, \text{Na}, \text{K}, \text{Cs}$) and 2,2'-bipyridine has been investigated²⁶⁵ by multinuclear (^7Li -, ^{13}C -, ^{23}Na -, ^{39}K -, ^{133}Cs -) n.m.r. techniques. The stabilities of the complexes fall in the sequence



and vary inversely with the solvating abilities of the solvents; no complexes were detected in solutions containing Cs^+ .²⁶⁵

Complexation of secondary butyl lithium by tmen has been examined²⁶⁶ by n.m.r. spectroscopic techniques at low temperatures ($203 \leq T/K \leq 253$); evidence for an endothermic disproportionation of the 1:1 sec-BuLi:tmen complex to the 1:2 complex is reported.

⁷Li n.m.r. spectra²⁶⁷ of the (Li^+ , Li^+ triple ion) couple (49) in CH_2Cl_2 and Me_2SO exhibits two sharp signals; the



corresponding spectra of the (K^+ , Li^+ triple ion) couple (50) shows only one absorption with the same shift as the lower field signal of (49). It is concluded that the lower field signal belongs to the triple ion and the high field signal to the cryptate cation. Although the chemical shift of the high field signal is independent of solvent that of the low field signal is strongly affected by solvent; it is assumed that the structure of the triple ion can be distorted to permit solvation by a basic solvent.²⁶⁷

⁷Li and ¹³C n.m.r. studies²⁶⁸ of thf solutions of lithium salts of picolyl (pyridylmethyl)-type delocalised anions suggest that they form tight ion pairs in which the cation-anion interaction occurs primarily at the ring nitrogen atom.

The molecular structures of lithium pentakis(methoxycarbonyl)cyclopentadiene monohydrate²⁶⁹ and of the 1:1:1 adduct of 2-lithio-2-phenyl-1,3-dithiane with thf and tmen²⁷⁰ have been determined from single crystal X-ray diffraction studies. The Li^+ ion is tetrahedrally coordinated in both complexes. In the former complex it is surrounded by four oxygen atoms, two from one anion, one from a second anion and the fourth from a water molecule.²⁶⁹ In the latter complex, however, it is surrounded by the two nitrogen atoms of the tmen molecule, $r(\text{Li} \dots \text{N}) = 211.0, 214.8 \text{ pm}$, the oxygen atom of the thf molecule, $r(\text{Li} \dots \text{O}) = 197.0 \text{ pm}$ and the

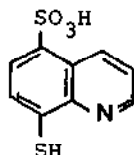
The remaining papers²⁷⁵⁻⁷ abstracted for this section pertain to single crystal X-ray diffraction studies of four diverse sodium derivatives. The structures of two p-terphenyl(tp) ion pairs have been determined;²⁷⁵ whereas that of the complex $[\text{Na}_2\text{tp}(\text{thf})_6]$ is a contact ion pair structure, that of $[\text{Na}_2\text{tp}_3(\text{dme})_6]$ is a solvent separated ion pair structure. The structure of $[\text{Na}_2\text{tp}(\text{thf})_6]$ is built up of $[\text{Na}(\text{thf})_3]^+$ cations and of p-terphenyl anions; the Na^+ ions are located above and below the centre of the central ring of the anion, $r(\text{Na}\dots\text{C}) = 278\text{--}286$ pm, the other side of the Na^+ coordination sphere being filled by three thf molecules, $r(\text{Na}\dots\text{O}) = 229\text{--}231$ pm. The oxygen atoms of the three thf molecules lie at the corners of an equilateral triangle which is almost parallel to the plane of the anion. The structure of $[\text{Na}_2\text{tp}_3(\text{dme})_6]$ consists of $[\text{Na}(\text{dme})_3]^+$ cations, p-terphenyl anions and p-terphenyl molecules. The Na^+ coordination sphere is disordered. Unfortunately a suitable disorder model for the $[\text{Na}(\text{dme})_3]^+$ cations could not be developed; the quoted coordinates of the dme molecules represent small peaks in a dense electron density cloud about the Na^+ ion with a chemically acceptable geometry.²⁷⁵

The structure of sodium methanesulphonate²⁷⁶ contains three crystallographically independent Na^+ ions. Two Na^+ ions are each surrounded by six oxygen atoms from six different anions forming distorted octahedral configurations with $r(\text{Na}\dots\text{O}) = 227.6\text{--}266.9$ pm. The third Na^+ ion is surrounded by eight oxygen atoms from two unidentate, $r(\text{Na}\dots\text{O}) = 231.8\text{--}246.9$ pm and three bidentate, $r(\text{Na}\dots\text{O}) = 241.8\text{--}309.9$ pm, anions.²⁷⁶ In the structure of sodium scylloinositol diborate decahydrate²⁷⁷ each Na^+ ion is octahedrally coordinated by the oxygen atoms of six water molecules, $r(\text{Na}\dots\text{O}) = 236\text{--}244$ pm; the Na^+ ions are situated in parallel columns close to the screw axes with $r(\text{Na}\dots\text{Na}) = 342$ pm.

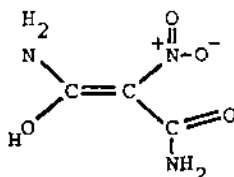
1.5.10 Potassium, Rubidium and Caesium Derivatives

The papers abstracted for this section deal almost exclusively with crystal-chemical studies; in all, the crystal and molecular structures of five potassium²⁷⁸⁻²⁸² and of two rubidium^{283,284} derivatives have been elucidated. A variety of K^+ coordination numbers and geometries occur in the 1:1 adduct of KF with deuterated succinic acid, $\text{KF}(\text{CH}_2\text{COOD})_2$,²⁷⁸ the monopotassium salts of quinoline-8-thiol-5-sulphonic acid (54)²⁷⁹ and nitromalonamide (55)²⁸⁰ and the tetra-thf solvate of the dipotassium salt of

phthalocyanine.²⁸¹ The K^+ ion is six coordinate in the 1:1 KF : succinic acid adduct, the irregular coordination polyhedra being composed of two fluorine atoms, $r(K...F) = 268.5, 287.4$ pm and four carboxyl oxygen atoms, $r(K...O) = 281.8-285.2$ pm. Seven coordinate K^+ ions are found in the two monopotassium salts. In the quinoline derivative,²⁷⁹ the K^+ ion is surrounded by seven



(54)



(55)

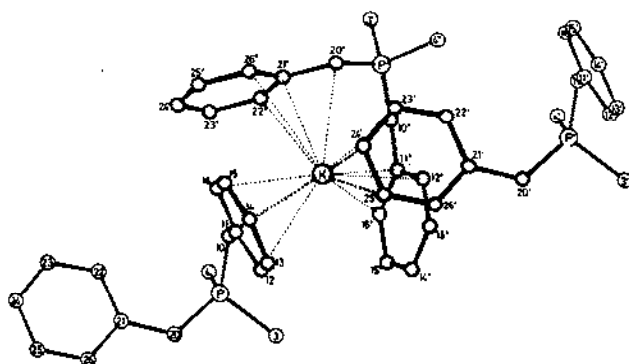
oxygen atoms from four different anions, $r(K...O) = 273-289$ pm; in the nitromalonamide derivative,²⁸⁰ however, it is surrounded by seven oxygen atoms from five different anions, $r(K...O) = 272-306$ pm. The coordination of the K^+ ion in the phthalocyanine derivative is quite unusual.²⁸¹ The K^+ ions are effectively sandwiched between a 4N-isoindeole plane, provided by the phthalocyanine dianion, $r(K...N)_{av} = 278.3$ pm and a 4O-plane, generated by four dmf molecules, $r(K...O)_{av} = 284.7$ pm. The overall coordination polyhedron is a distorted cubic arrangement.

The ylides, $R_2P(CH_2C_6H_5)=CHC_6H_5$, react with lithium alkyls, sodium amide and potassium hydride in thf to yield the corresponding alkali metal complexes, $K^+[(C_6H_5CH)_2P(CH_3)_2]^-$. The products have been characterised by chemical and spectroscopic methods and in the case of the potassium complex by single crystal X-ray diffraction studies. The structure (Figure 11a) is complex; the K^+ ion resides in the space between three anions, there being one carbon atom within 300 pm, 10 within 350 pm and 17 within 400 pm.

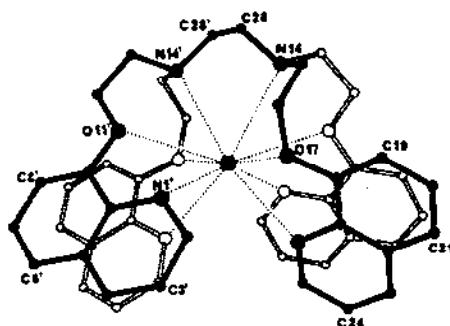
The crystal structure of $Rb.tcnq.(II)$ has been redetermined.²⁸³ The Rb^+ cation is surrounded by eight nitrogen atoms, $r(Rb...N) = 305-327$ pm, in a distorted coordination geometry. The interplanar spacing between the neighbouring tcnq anions is 325 pm, which is markedly lower than that reported earlier.²⁸⁵

Ten coordinate Rb^+ occurs in the structure of NNN'N'-tetrakis-[2-(8-quinolyloxy)ethyl]ethylene diamine, rubidium iodide.²⁸⁴ The wrapping of the decadentate tetrapod ligand around the Rb^+ ion is

shown in Figure 11b; it is best described as spherical with $r(\text{Rb}\dots\text{O}) = 280.6, 323.1$ and $r(\text{Rb}\dots\text{N}) = 302.6-319.1$ pm.



(a)



(b)

Figure 11. Coordination of the cations in (a) potassium phosphonium bis(benzylide) and (b) the NNN'N'-tetrakis[2-(8-quinolyloxy)ethyl]ethylene diamine-rubidium iodide complex (reproduced by permission from (a) Chem. Ber., 114(1981)608, and (b) Inorg. Chim. Acta, 54(1981)L185).

REFERENCES

- 1 P.Hubberstey, Coord. Chem. Rev., 40(1982)1.
- 2 Various articles in Proc. 2nd. Int. Conf. on 'Liquid Metal Technology in Energy Production', USDOE CONF-800401-P1/P2, (1980).
- 3 Various articles in J. Electrochem. Soc., 128(1981).
- 4 R.T.Myers, J. Inorg. Nucl. Chem., 43(1981)3083.
- 5 R.N.Newman and J.F.B.Payne, Proc. 2nd. Int. Conf. 'Liquid Metal Technology in Energy Production', USDOE CONF-800401-P1, 4-1(1980).
- 6 M.Reuillon, H.Mellottee and R.Delbourgo, J. Chem. Res. (S), (1981)128.
- 7 M.Reuillon and H.Mellottee, J. Chem. Res(S), (1981)326.
- 8 A.J.Borgers, M.J.Jongerius, W.J.Ventevoegel, T.Hollander and C.T.J.Alkemade, J. Chem. Soc. Faraday Trans. I, 77(1981)1083.
- 9 A.J.Borgers, M.J.Jongerius, T.Hollander and C.T.J.Alkemade, J. Chem. Soc. Faraday Trans. I, 77(1981)1075.
- 10 A.Sanjurjo, L.Nanis, K.Sancier, R.Bartlett and V.Kapur, J. Electrochem. Soc., 128(1981)179.
- 11 L.V.Coulter, S.H.Lee-Bechtold, V.Madhvaraja and J.K.Gibson, J. Chem. Thermodyn., 13(1981)815.
- 12 R.J.Pulham, P.Hubberstey, A.E.Thunder, A.Harper and A.T.Dadd, Proc. 2nd. Int. Conf. 'Liquid Metal Technology in Energy Production', USDOE CONF-800401-P2, 18-1(1980).
- 13 M.G.Barker, G.A.Fairhall and S.A.Frankham, Proc. 2nd. Int. Conf. 'Liquid Metal Technology in Energy Production', USDOE CONF-800401-P2, 18-41(1980).
- 14 P.Hubberstey, A.Harper, A.T.Dadd, D.J.Knight and K.Maughan, Proc. 2nd. Int. Conf. 'Liquid Metal Technology in Energy Production', USDOE CONF-800401-P2, 18-27(1980).
- 15 H.Migge, Proc. 2nd. Int. Conf. 'Liquid Metal Technology in Energy Production', USDOE CONF-800401-P2, 18-9(1980).
- 16 W.F.Galaway, Proc. 2nd. Int. Conf. 'Liquid Metal Technology in Energy Production', USDOE CONF-800401-P2, 18-18(1980).
- 17 H.R.Konvicka, P.F.Sattler and I.E.Schreinlechner, Proc. 2nd. Int. Conf. 'Liquid Metal Technology in Energy Production', USDOE CONF-800401-P2, 19-65(1980).
- 18 R.A.Sharma and T.G.Bradley, J. Electrochem. Soc., 128(1981)1835.
- 19 A.T.Dadd and P.Hubberstey, J. Chem. Soc. Faraday Trans. I, 77(1981)1865.
- 20 A.C.Whittingham, C.A.Smith, P.A.Simm and R.J.Smity, Proc. 2nd. Int. Conf. 'Liquid Metal Technology in Energy Production', USDOE CONF-800401-P2, 16-38(1980).
- 21 M.R.Hobdell, E.A.Trevillion and A.C.Whittingham, Proc. 2nd. Int. Conf. 'Liquid Metal Technology in Energy Production', USDOE CONF-800401-P2, 18-47(1980).
- 22 W.P.Stanaway and R.Thompson, Proc. 2nd. Int. Conf. 'Liquid Metal Technology in Energy Production', USDOE CONF-800401-P2, 18-54(1980).
- 23 R.W.Caputi and M.G.Adamson, Proc. 2nd. Int. Conf. 'Liquid Metal Technology in Energy Production', USDOE CONF-800401-P2, 18-62(1980).
- 24 J.Jung, A.Reck and R.Zeigler, Proc. 2nd. Int. Conf. 'Liquid Metal Technology in Energy Production', USDOE CONF-800401-P1, 4-8(1980).
- 25 W.Becker, G.Schwitzgebel and H.Ruppersberg, Z. Metallk., 72(1981)186.
- 26 F.E.Neale, N.E.Cusack and A.Rais, J.Phys. F: Metal Phys., 11(1981)L201.

- 27 T.Ishiguro and S.Tamaki, *J. Phys. F: Metal Phys.*, 11(1981)L199.
- 28 K.Hoshino and W.H.Young, *J. Phys. F: Metal Phys.*, 11(1981)L7.
- 29 C.Holzhey, F.Brouers and J.R.Franz, *J. Phys. F: Metal Phys.*, 11(1981)1047.
- 30 K.Hoshino, S.Tamaki and Y.Waseda, *J. Phys. F: Metal Phys.*, 11(1981)L179.
- 31 C.J.Wen and R.A.Huggins, *J. Electrochem. Soc.*, 128(1981)1636.
- 32 C.J.Wen and R.A.Huggins, *J. Electrochem. Soc.*, 128(1981)1181.
- 33 J.Stohr and H.Schafer, *Z. Anorg. Allg. Chem.*, 474(1981)221.
- 34 R.G.Ling and C.Belin, *Z. Anorg. Allg. Chem.*, 480(1981)181.
- 35 C.Belin, *Acta Crystallogr.*, B37(1981)2060.
- 36 H.-O.Cullmann, H.-W.Hinterkeuser and H.-U.Schuster, *Z. Naturforsch.*, 36b(1981)917.
- 37 H.-D.Sinnen and H.-U.Schuster, *Z. Naturforsch.*, 36b(1981)833.
- 38 R.W.Rudolph, W.L.Wilson and R.C.Taylor, *J. Am. Chem. Soc.*, 103(1981)2480.
- 39 M.J.Rothman, L.S.Bartell and L.L.Lohr, *J. Am. Chem. Soc.*, 103(1981)2482.
- 40 S.C.Critchlow and J.D.Corbett, *J. Chem. Soc. Chem. Commun.*, ; (1981)236.
- 41 P.Hubberstey, *Coord. Chem. Rev.*, 40(1982)10.
- 42 H.Ohno and K.Furukawa, *J. Chem. Soc. Faraday Trans. I*, 77(1981)1981.
- 43 J.Zarzycki, *J. Phys. Radium*, 19(1958)13A.
- 44 F.G.Edwards, J.E.Enderby, R.A.Howe and D.I.Page, *J. Phys.*, C, 8(1975)3483.
- 45 M.Itoh, T.Sasamoto and T.Sata, *Bull. Chem. Soc. Japan*, 54(1981)3391.
- 46 E.W.Dewing, *Metall. Trans.*, 12B(1981)705.
- 47 R.Roumieu and A.D.Pelton, *J. Electrochem. Soc.*, 128(1981)50.
- 48 B.Cristol, J.Houriez and D.Balesdent, *J. Chem. Thermodyn.*, 13(1981)937.
- 49 H.Bloom and M.S.White, *Austral. J. Chem.*, 34(1981)479.
- 50 T.Foosnaes and H.A.Oye, *Acta Chem. Scand.*, A35(1981)81.
- 51 W.C.Child, G.M.Begun and D.H.Smith, *J. Chem. Soc. Faraday Trans. II*, 77(1981)2237.
- 52 D.H.Smith, G.M.Begun and W.C.Child, *J. Chem. Soc. Faraday Trans. II*, 77(1981)1399.
- 53 M.Miyake, K.Okada, S.Iwai, H.Ohno and K.Furukawa, *J. Chem. Soc. Faraday Trans. I*, 75(1979)1169.
- 54 K.Ichikawa and K.Kawamura, *Bull. Chem. Soc. Japan*, 54(1981)3583.
- 55 M.L.Deanhardt and K.H.Stern, *J. Electrochem. Soc.*, 128(1981)2577.
- 56 M.Sorlie and H.A.Oye, *Inorg. Chem.*, 20(1981)1384.
- 57 S.V.Volkov, V.I.Shapoval, N.I.Buryak and V.G.Lutsenko, *Russ. J. Inorg. Chem.*, 25(1980)1645.
- 58 N.M.Sinitayn, V.N.Pichkov, A.S.Kozlov, G.C.Novitskii, A.A.Sidorov and I.A.Khartonik, *Russ. J. Inorg. Chem.*, 25(1980)1438.
- 59 Z.Tomczuk, S.K.Preto and M.F.Roche, *J. Electrochem. Soc.*, 128(1981)760.
- 60 Z.Tomczuk, M.F.Roche and D.R.Vissers, *J. Electrochem. Soc.*, 128(1981)2255.
- 61 G.Zwilling, D.M.Bailey and K.A.Gschneidner, *J. Less Common Metals*, 78(1981)109.
- 62 I.Uchida, J.Niikura and S.Toshima, *J. Inorg. Nucl. Chem.*, 43(1981)549.
- 63 W.H.Smyrl, *J. Electrochem. Soc.*, 128(1981)89.
- 64 R.Fehrmann, J.H. von Barner, N.J.Bjerrum and O.F.Nielsen, *Inorg. Chem.*, 20(1981)1712.
- 65 G.Brautigam, H.-H.Emons and I.Gunther, *Z. Anorg. Allg. Chem.*, 472(1981)205.

- 66 G.Brautigam, H.-H.Emons and I.Gunther, *Z. Anorg. Allg. Chem.*, 472(1981)213.
- 67 V.E.Norvell, K.Tanemoto, G.Mamantov and L.N.Klatt, *J. Electrochem. Soc.*, 128(1981)1254.
- 68 K.Tanemoto, G.Mamantov and R.Marassi, *J. Inorg. Nucl. Chem.*, 43(1981)1779.
- 69 G.Picard, F.Seon and B.Tremillon, *Bull. Soc. Chim. France*, (1981)I-353.
- 70 R.A.Carpis and L.A.King, *J. Electrochem. Soc.*, 128(1981)1510.
- 71 M.Sorlie and G.P.Smith, *J. Inorg. Nucl. Chem.*, 43(1981)931.
- 72 P.J.Iredale and A.Thompson, *J. Inorg. Nucl. Chem.*, 43(1981)2667.
- 73 M.Hassanein and N.S.Youssef, *Indian J. Chem.*, 20A(1981)501.
- 74 S.V.Volkov, V.I.Shapoval, N.I.Buryak and V.G.Lutsenko, *Russ. J. Inorg. Chem.*, 26(1981)286.
- 75 H.C.Egghart, *J. Inorg. Nucl. Chem.*, 43(1981)1390.
- 76 B.Holmberg, *J. Inorg. Nucl. Chem.*, 43(1981)5.
- 77 B.Holmberg and G.Thome, *J. Chem. Soc. Faraday Trans. I*, 77(1981)101.
- 78 K.W.D.Verma, R.K.Gupta and H.C.Gaur, *Indian J. Chem.*, 20A(1981)547,1093.
- 79 J.Winnick and P.N.Ross, *J. Electrochem. Soc.*, 128(1981)991.
- 80 T.R.Griffiths and K.King, *J. Chem. Soc. Faraday Trans. I*, 77(1981)2763.
- 81 D.A.Shores and W.C.Fang, *J. Electrochem. Soc.*, 128(1981)346.
- 82 A.N.Ford and S.A.Tariq, *Austral. J. Chem.*, 34(1981)647.
- 83 A.N.Ford and S.A.Tariq, *Austral. J. Chem.*, 34(1981)885.
- 84 M.Colombier, P.Leclercq and J.Said, *Bull. Chim. Soc. France*, (1981)I-419.
- 85 V.A.Kulikov, V.V.Ugarov and N.G.Rambidi, *J. Struct. Chem.*, 22(1981)310.
- 86 V.A.Kulikov, V.V.Ugarov and N.G.Rambidi, *J. Struct. Chem.*, 22(1981)448.
- 87 K.P.Petrov, V.V.Ugarov and N.G.Rambidi, *J. Struct. Chem.*, 22(1981)609.
- 88 J.S.Ogden and S.J.Williams, *J. Chem. Soc., Dalton Trans.*, (1981)456.
- 89 A.A.Belyaeva, M.I.Dvorkin and L.D.Shcherba, *J. Struct. Chem.*, 21(1980)738.
- 90 P.Wermer and B.S.Ault, *Inorg. Chem.*, 20(1981)970.
- 91 R.H.Hauge, J.L.Margrave, J.W.Kauffman, N.A.Rao, M.M.Konerski, J.P.Bell and W.E.Billups, *J. Chem. Soc. Chem. Commun.*, (1981)1258.
- 92 V.G.Zakzhevskii, A.I.Boldyrev and O.P.Charkin, *Russ. J. Inorg. Chem.*, 25(1980)1443.
- 93 A.I.Boldyrev, V.G.Solomonik, V.G.Zakzhevskii and O.P.Charkin, *Russ. J. Inorg. Chem.*, 25(1980)1277.
- 94 H.Kato, K.Hirao and K.Akagi, *Inorg. Chem.*, 20(1981)3659.
- 95 A.M.Ghodgaonkar and K.Ramani, *J. Chem. Soc. Faraday Trans. II*, 77(1981)209.
- 96 J.Shanker and K.Singh, *J. Inorg. Nucl. Chem.*, 43(1981)1445.
- 97 J.D.Pandey and R.P.Pandey, *J. Chem. Soc. Faraday Trans. II*, 77(1981)419.
- 98 D.E.Work, *J. Chem. Thermodyn.*, 13(1981)491.
- 99 G.K.Johnson and W.V.Steele, *J. Chem. Thermodyn.*, 13(1981)985.
- 100 H.Jacobs and C.Erten, *Z. Anorg. Allg. Chem.*, 473(1981)125.
- 101 H.Jacobs and B.Harbrecht, *Z. Naturforsch.*, 36b(1981)270.
- 102 I.J.F.Poplett and J.A.S.Smith, *J. Chem. Soc. Faraday Trans. II*, 77(1981)235.
- 103 C. van Rij and D.Britton, *Acta Crystallogr.*, B34(1978)2080.
- 104 M.Falk, *Canad. J. Chem.*, 59(1981)1267.

- 105 H.E.Floto, P.A.G.O'Hare and J.Boerio-Coates, J. Chem. Thermodyn., 13(1981)477.
- 106 C.E.Vanderzee and D.A.Wigg, J. Chem. Thermodyn., 13(1981)573.
- 107 P.Hartwig, A.Rabenau and W.Weppner, J. Less Common Metals, 80(1981)81.
- 108 P.Hartwig, A.Rabenau and W.Weppner, J. Less Common Metals, 78(1981)227.
- 109 G.Achenbach and H.-U.Schuster, Z. Anorg. Allg. Chem., 475(1981)9.
- 110 S.Rozsa and H.-U.Schuster, Z. Naturforsch., 36b(1981)1666.
- 111 S.Rozsa and H.-U.Schuster, Z. Naturforsch., 36b(1981)1668.
- 112 G.Zwiener, H.Neumann and H.-U.Schuster, Z. Naturforsch., 36b(1981)1195.
- 113 R.Hoppe, Angew. Chem. Int. Ed. Engl., 20(1981)63.
- 114 W.Bronger, Angew. Chem. Int. Ed. Engl., 20(1981)52.
- 115 G.LeFlem, P.Courbin, C.Delmas and J.-L.Soubeyrou, Z. Anorg. Allg. Chem., 476(1981)69.
- 116 C.Chich, B.L.Chamberland and A.F.Wells, Acta Crystallogr., B37(1981)1813.
- 117 M.G.Barker, S.A.Frankham and P.G.Gadd, J. Inorg. Nucl. Chem., 43(1981)2815.
- 118 I.S.Shaplygin and V.B.Lazarev, Russ. J. Inorg. Chem., 25(1980)1837.
- 119 H.Klassen and R.Hoppe, Z. Naturforsch., 36b(1981)1395.
- 120 J.K.Nimmo, Acta Crystallogr., B37(1981)431.
- 121 A.A.Fotiev and V.L.Kozhevnikov, Russ. J. Inorg. Chem., 25(1980)1411.
- 122 A.A.Fotiev and V.V.Strelkov, Russ. J. Inorg. Chem., 26(1981)942.
- 123 B.V.Slobodin, S.F.Blinova, A.A.Fotiev and N.P.Tugova, Russ. J. Inorg. Chem., 26(1981)660.
- 124 R.S.Bubnova, S.K.Filatov, V.S.Grunin and Z.N.Zonn, Sov. Phys. Crystallogr., 25(1980)734.
- 125 R.F.Klevtsova, V.G.Kim and P.V.Klevtsov, Sov. Phys. Crystallogr., 25(1980)657.
- 126 B.I.Lazoryak and V.A.Efremov, Sov. Phys., Crystallogr., 26(1981)263.
- 127 C.Dion and A.Noel, Bull. Soc. Chim. France, (1981)I-185.
- 128 C.Dion and A.Noel, Bull. Soc. Chim. France, (1981)I-371.
- 129 C.Dion and A.Noel, Bull. Soc. Chim. France, (1981)I-413.
- 130 Y.Kera, Bull. Chem. Soc. Japan, 54(1981)1693.
- 131 K.-Y.Kim, G.K.Johnson, C.E.Johnson, H.E.Floto, E.H.Appelman, P.A.G.O'Hare and B.A.Phillips, J. Chem. Thermodyn., 13(1981)333.
- 132 K.-Y.Kim, G.K.Johnson, P.A.G.O'Hare and B.A.Phillips, J. Chem. Thermodyn., 13(1981)695.
- 133 E.H.P.Cordfunke and W.Ouweltjes, J. Chem. Thermodyn., 13(1981)187.
- 134 P.A.G.O'Hare, H.E.Floto and H.R.Hoekstra, J. Chem. Thermodyn., 13(1981)1075.
- 135 P.A.G.O'Hare and H.R.Hoekstra, J. Chem. Thermodyn., 7(1975)831.
- 136 I.R.Polyvyannyi, V.A.Lata, L.P.Ivakina and V.I.Antonyuk, Russ. J. Inorg. Chem., 26(1981)561.
- 137 P.Muller and W.Bronger, Z. Naturforsch., 36b(1981)646.
- 138 G.Savelsberg and H.Schafer, J. Less Common Metals, 80(1981)F59.
- 139 A.K.Molodkin, A.M.Karagodina, A.G.Dudareva and A.B.Strekachinskii, Russ. J. Inorg. Chem., 26(1981)1219.
- 140 V.V.Chibrikov, A.V.Nevzorov, Z.B.Mikhmetshina, V.P.Seleznev and G.A.Yagodin, Russ. J. Inorg. Chem., 26(1981)1216.
- 141 M.N.Bhattacharjee, M.K.Chaudhuri, H.S.Dasgupta and D.T.Khathing, J. Chem. Soc. Dalton Trans., (1981)2587.

- 142 L.V.Soboleva, L.M.Belyaev, V.V.Ogadzhanova, M.G.Vasil'eva, *Sov. Phys. Crystallogr.*, 26(1981)462.
- 143 Y.S.Hong, R.F.Williamson and W.O.J.Boo, *Inorg. Chem.*, 20(1981)403.
- 144 N.Kijima, K.Tanaka and F.Marumo, *Acta Crystallogr.*, B37(1981)545.
- 145 W.J.Crama and H.W.Zandbergen, *Acta Crystallogr.*, B37(1981)1027.
- 146 W.J.Crama, *Acta Crystallogr.*, B37(1981)2133.
- 147 J.M.Dance, A.Tressaud, W.Massa and D.Babel, *J. Chem. Research (S)*, (1981)202.
- 148 H.D.Lutz, W.Schmidt and H.Haueseler, *Naturwiss.*, 68(1981)328.
- 149 E.Herdtwack and D.Babel, *Z. Anorg. Allg. Chem.*, 474(1981)113.
- 150 P.A.Reynolds, B.N.Figgis and A.H.White, *Acta Crystallogr.*, B37(1981)508.
- 151 B.N.Figgis and P.A.Reynolds, *Austral. J. Chem.*, 34(1981)2495.
- 152 M.Iwasaki, N.Ishikawa, K.Ohwada and T.Fujino, *Inorg. Chim. Acta*, 54(1981)L193.
- 153 W.J.Crama, *Acta Crystallogr.*, B37(1981)662.
- 154 D.H.Guthrie, G.Meyer and J.D.Corbett, *Inorg. Chem.*, 20(1981)1192.
- 155 H.A.Brown-Acquaye and A.P.Lane, *J. Inorg. Nucl. Chem.*, 43(1981)3143.
- 156 L.M.Belyaev, M.G.Vasil'eva and L.V.Soboleva, *Sov. Phys. Crystallogr.*, 26(1981)212.
- 157 A.Brandt, Y.M.Kiselev and L.I.Martynenko, *Z. Anorg. Allg. Chem.*, 474(1981)233.
- 158 B.Briat, O.Kahn, I.Morgenstern-Badarau and J.C.Rivoal, *Inorg. Chem.*, 20(1981)4193.
- 159 L.N.Sidorov, N.M.Karasev and Y.M.Korenev, *J. Chem., Thermodyn.*, 13(1981)915.
- 160 G.J.Kipouros and S.N.Flengas, *Canad. J. Chem.*, 59(1981)990.
- 161 I.V.Vinogradov, M.I.Konarev and L.L.Zaitseva, *Russ. J. Inorg. Chem.*, 26(1981)852.
- 162 A.Brandt, Y.M.Kiselev and L.I.Martynenko, *Russ. J. Inorg. Chem.*, 26(1981)499.
- 163 T.Hattori, K.Igarashi and J.Mochinaga, *Bull. Chem. Soc. Japan*, 54(1981)1883.
- 164 P.Hubbersley, *Coord. Chem. Rev.*, 40(1982)29.
- 165 G.Ercolani, L.Mandolini and B.Maschi, *J. Am. Chem. Soc.*, 103(1981)7484.
- 166 D.G.Parsons, M.R.Truter and J.N.Wingfield, *Inorg. Chim. Acta*, 51(1981)93.
- 167 J.Grandjean, P.Lazlo, W.Offermann and P.L.Rinaldi, *J. Am. Chem. Soc.*, 103(1981)1380.
- 168 K.K.Chacko and W.Saenger, *Z. Naturforsch.*, 36b(1981)102.
- 169 N.S.Poonia, G.C.Kumar, A.Jayakumar, P.Bagdi and A.V.Bajaj, *J. Inorg. Nucl. Chem.*, 43(1981)2159.
- 170 B.R.Bowsher and A.J.Rest, *J. Chem. Soc. Dalton Trans.*, (1981)1157.
- 171 G.Ercolani, L.Mandolini and B.Maschi, *J. Am. Chem. Soc.*, 103(1981)2780.
- 172 P.Groth, *Acta Chem. Scand.*, A35(1981)721.
- 173 V.W.Bhagwat, H.Manochar and N.S.Poonia, *Inorg. Nucl. Chem. Letters*, 17(1981)207.
- 174 R.F.Ziolo, W.H.H.Gunther and J.M.Troup, *J. Am. Chem. Soc.*, 103(1981)4629.
- 175 K.Hilgenfeld and W.Saenger, *Angew. Chem. Int. Ed. Engl.*, 20(1981)1045.
- 176 D.E.Games, L.A.P.Kane-Maguire, D.G.Parsons and M.R.Truter, *Inorg. Chim. Acta.*, 49(1981)213.
- 177 K.B.Yatsimirskii, V.G.Golovaty, E.N.Korol', V.A.Bidzilya and G.G.Talanova, *Doklady Chem.*, 255(1980)576.
- 178 J.D.Lin and A.I.Popov, *J. Am. Chem. Soc.*, 103(1981)3773.
- 179 Y.Takeda, *Bull. Chem. Soc. Japan*, 54(1981)3133.

- 180 U.Olsher and J.Jagur-Grodzinski, *J. Chem. Soc. Dalton Trans.*, (1981)501.
- 181 Y.Takeda, *Bull. Chem. Soc. Japan*, 54(1981)526.
- 182 Y.Takeda, Y.Wada and S.Fujiwara, *Bull. Chem. Soc. Japan*, 54(1981)3727.
- 183 A.S.Khan, W.G.Baldwin and A.Chow, *Canad. J. Chem.*, 59(1981)1490.
- 184 V.V.Yakushin, V.M.Abashkin and B.N.Laskorin, *Doklady Chem.*, 252(1980)239.
- 185 I.M.Kolthoff, *Canad. J. Chem.*, 59(1981)1548.
- 186 D.C.Hrncir, R.D.Rogers and J.L.Atwood, *J. Am. Chem. Soc.*, 103(1981)4277.
- 187 M.K.Cooper, P.A.Duckworth, K.Henrick and M.McPartlin, *J. Organometal. Chem.*, 212(1981)C10.
- 188 M.K.Cooper, P.A.Duckworth, K.Henrick and M.McPartlin, *J. Chem. Soc. Dalton Trans.*, (1981)2357.
- 189 J.L.Vidal, R.C.Schoening and J.M.Troup, *Inorg. Chem.*, 20(1981)227.
- 190 A.Knochel and R.-D.Wilken, *J. Am. Chem. Soc.*, 103(1981)5707.
- 191 A.V.Bogatskii, T.K.Chumachenko, N.G.Luk'yanenko, L.N.Lyamtseva and I.A.Starovoit, *Doklady Chem.*, 251(1980)105.
- 192 J.K.Rasmussen and H.K.Smith, *J. Am. Chem. Soc.*, 103(1981)730.
- 193 D.G.Parsons, M.R.Truter and J.N.Wingfield, *Inorg. Chim. Acta*, 47(1981)81.
- 194 V.A.Bidzilya, L.P.Golovkova and K.B.Yatsimirskii, *Russ. J. Inorg. Chem.*, 26(1981)664.
- 195 J.S.Bradshaw, S.L.Baxter, J.D.Lamb, R.M.Izatt and J.J.Christensen, *J. Am. Chem. Soc.*, 103(1981)1821.
- 196 J.A.Bandy, D.G.Parsons and M.R.Truter, *J. Chem. Soc. Chem. Commun.*, (1981)729.
- 197 A.V.Bogat-skii, N.G.Luk'yanenko, M.U.Mamina, V.A.Shapkin and D.Taubert, *Doklady Chem.*, 250(1980)82.
- 198 T.W.Bell, *J. Am. Chem. Soc.*, 103(1981)1163.
- 199 M.Czugler and E.Weber, *J. Chem. Soc. Chem. Commun.*, (1981)472.
- 200 J.P.Behr, J.M.Lehn, D.Moras and J.C.Thierry, *J. Am. Chem. Soc.*, 103(1981)701.
- 201 J.Powell, A.Kuksis, C.J.May, S.C.Nyburg and S.J.Smith, *J. Am. Chem. Soc.*, 103(1981)5941.
- 202 W.-W.Tso and W.-P.Fung, *Inorg. Chim. Acta*, 55(1981)129.
- 203 I.Tajima, M.Okada and H.Sumitomo, *J. Am. Chem. Soc.*, 103(1981)4096.
- 204 L.A.Frederick, T.M.Fyles, N.P.Gurprasad and D.M.Whitfield, *Canad. J. Chem.*, 59(1981)1724.
- 205 T.M.Fyles, V.A.Malik-Diemer and D.M.Whitfield, *Canad. J. Chem.*, 59(1981)1734.
- 206 S.Shinkai, T.Nakaji, T.Ogawa, K.Shigematsu and O.Manabe, *J. Am. Chem. Soc.*, 103(1981)111.
- 207 G.Rounaghi and A.I.Popov, *J. Inorg. Nucl. Chem.*, 43(1981)911.
- 208 M.L.Campbell, N.K.Dalley, R.M.Izatt and J.D.Lamb, *Acta Crystallogr.*, B37(1981)1664.
- 209 M.L.Campbell, S.B.Larson and N.K.Dalley, *Acta Crystallogr.*, B37(1981)1741.
- 210 M.L.Campbell, S.B.Larson and N.K.Dalley, *Acta Crystallogr.*, B37(1981)1744.
- 211 M.L.Campbell, N.K.Dalley and S.H.Simonsen, *Acta Crystallogr.*, B37(1981)1747.
- 212 J.L.Petersen, R.K.Brown and J.M.Williams, *Inorg. Chem.*, 20(1981)158.
- 213 N.Morel-Desrosiers and J.-P.Morel, *J. Am. Chem. Soc.*, 103(1981)4743.
- 214 G.W.Liesegang, *J. Am. Chem. Soc.*, 103(1981)953.

- 215 B.G.Cox, J.Garcia-Rosas and H.Schneider, J. Am. Chem. Soc., 103(1981)1054.
- 216 B.G.Cox, J.Garcia-Rosas and H.Schneider, J. Am. Chem. Soc., 103(1981)1384.
- 217 B.G.Cox, P.Firman, I.Schneider and H. Schneider, Inorg. Chim. Acta, 49(1981)153.
- 218 S.Kulstad and L.A.Malmsten, J. Inorg. Nucl. Chem., 43(1981)1299.
- 219 G.Weber, Acta Crystallogr., B37(1981)1832.
- 220 P.Groth, Acta Chem. Scand., A35(1981)717.
- 221 R.Mattes and G.Plescher, Acta Crystallogr., B37(1981)697.
- 222 H.Kuppers, A.Kvick and I.Olovsson, Acta Crystallogr., B37(1981)1203.
- 223 R.P.Ozerov, V.G.Tirel'son, A.A.Korkin, S.P.Ionov, V.E.Zavodnik and E.B.Fornicheva, Sov. Phys. Crystallogr., 26(1981)20.
- 224 D.A.Reed and M.M.Olmstead, Acta Crystallogr., B37(1981)938.
- 225 A.Perotti and V.Tazzoli, J. Chem. Soc. Dalton Trans., (1981)1768.
- 226 R.Mattes and G.Uckelmann, Acta Crystallogr., B37(1981)2071.
- 227 R.Kuroda and S.F.Mason, J. Chem. Soc. Dalton Trans., (1981)1268.
- 228 L.H.J.Lajunen, M.Leskela and J.Valkonen, Acta Chem. Scand., A35(1981)551.
- 229 G.A.Jeffrey and G.S.Parry, J. Am. Chem. Soc., 76(1954)5283.
- 230 J.Emsley, D.J.Jones and R.Kuroda, J. Inorg. Nucl. Chem., 43(1981)2243.
- 231 K.Klaeser, G.Kiel and G.Gattow, Z. Anorg. Allg. Chem., 483(1981)114.
- 232 K.Klaeser, G.Kiel and G.Gattow, Z. Anorg. Allg. Chem., 483(1981)95.
- 233 R.Tokuoka, M.Abe, K.Matsumoto, K.Shirakawa, T.Fujiwara and K.-I.Tomita, Acta Crystallogr., B37(1981)445.
- 234 G.W.Wood and W.F.Sun, Canad. J. Chem., 59(1981)2218.
- 235 I.J.F.Poplett and J.A.S.Smith, J. Chem. Soc. Faraday Trans. II, 77(1981)1155.
- 236 V.Cucinotta, C.Rigano, P.G.Daniele and S.Sammartano, Inorg. Chim. Acta, 56(1981)L45.
- 237 W.B.Smith and C.D.Barnard, Canad. J. Chem., 59(1981)1602.
- 238 B.M.Nirsha, G.M.Serebrennikova, Y.V.Oboznenko, L.M.Avdonina, B.V.Zhadanov, Y.A.Velikodnyi, G.R.Allakhverdov and A.S.Lomov, Russ. J. Inorg. Chem., 26(1981)173.
- 239 B.M.Nirsha, G.M.Serebrennikova, L.M.Avdonina, Y.V.Oboznenko, B.V.Zhadanov, G.R.Allakhverdov, G.M.Dobryakova and I.A.Kifarova, Russ. J. Inorg. Chem., 26(1981)320.
- 240 B.M.Nirsha, G.M.Serebrennikova, L.M.Avdonina and Y.V.Oboznenko, Russ. J. Inorg. Chem., 26(1981)757.
- 241 B.M.Nirsha, G.M.Serebrennikova, L.M.Avdonina and Y.V.Oboznenko, Russ. J. Inorg. Chem., 26(1981)909.
- 242 R.Cali, S.Musumeci, C.Rigano and S.Sammartano, Inorg. Chim. Acta, 56(1981)L11.
- 243 S.K.Katti, T.P.Seshadri and M.A.Viswamitra, Acta Crystallogr., B37(1981)1825.
- 244 S.K.Katti and M.A.Viswamitra, Acta Crystallogr., B37(1981)1058.
- 245 B.S.Reddy, W.Saenger, K.Muhlegger and G.Weimann, J. Am. Chem. Soc., 103(1981)907.
- 246 S.K.Katti, M.V.Hosur and M.A.Viswamitra, Acta Crystallogr., B37(1981)834.
- 247 D.L.Eng-Wilmot, M.B.Hossain and D. van der Helm, Acta Crystallogr., B37(1981)1207.
- 248 H.Morikawa, M.Miyake, S.-I.Iwai, Y.Nawata and M.Shiba, J. Chem. Soc. Faraday Trans. I., 77(1981)629.
- 249 Y.Nawata, K.Ochi, M.Shiba, K.Morita and Y.Iitaka, Acta Crystallogr., B37(1981)246.

- 250 J.A.Hamilton, M.N.Sabesan and L.K.Steinrauf, *J. Am. Chem. Soc.*, 103(1981)5881.
- 251 T.Geiser, J.Kopf, D.Thoennes and E.Weiss, *Chem. Ber.*, 114(1981)209.
- 252 H.Schumann, J.Pickardt and N.Bruncks, *Angew. Chem. Int. Ed. Engl.*, 20(1981)120
- 253 M.F.Lappert, A.Singh, J.L.Atwood and W.E.Hunter, *J.Chem. Soc. Chem. Commun.*, (1981)1191.
- 254 T.Clark, P. von R.Schleyer, K.N.Houk and N.G.Rondan, *J. Chem. Soc. Chem. Commun.*, (1981)579.
- 255 A.J.Kos, E.D.Jemmis, P. von R.Schleyer, R.Gleiter, U.Fischbach and J.A.Pople, *J. Am. Chem. Soc.*, 103(1981)4996.
- 256 J.Chandrasekhar and P. von R.Schleyer, *J. Chem. Soc. Chem. Commun.*, (1981)260.
- 257 P. von R.Schleyer, J.Chandrasekhar, A.J.Kos, T.Clark and G.W.Spitznagel, *J. Chem. Soc. Chem. Commun.*, (1981)882.
- 258 M.T.Reetz and W.Stephan, *J. Chem. Research (S)*, (1981)44.
- 259 P.Hubberstey, *Coord. Chem. Rev.*, 34(1981)33.
- 260 L.A.Shimp, J.A.Morrison, J.A.Gurak, J.W.Chinn and R.J.Lagow, *J. Am. Chem. Soc.*, 103(1981)5951.
- 261 M.Stahle and M.Schlosser, *J. Organomet. Chem.*, 220(1981)277.
- 262 H.Cachet, M.Fekir and J.-C.Lestrade, *Canad. J. Chem.*, 59(1981)1051.
- 263 H.C.Kraft, P.Peringer and B.M.Rode, *Inorg. Chim. Acta*, 48(1981)135.
- 264 N.S.Poonia, A.K.Arora and A.V.Bajaj, *J. Inorg. Nucl. Chem.*, 43(1981)2165.
- 265 E.Schmidt, A.Hourdakis and A.I.Popov, *Inorg. Chim. Acta*, 52(1981)91.
- 266 J.M.Catala, G.Clouet and J.Brossas, *J. Organomet. Chem.*, 219(1981)139.
- 267 C.Cambillau and M.Ourevitch, *J. Chem. Soc. Chem. Commun.*, (1981)996.
- 268 K.Konishi, A.Yoshino, M.Katoh, K.Takahashi, Y.Kawada, T.Sugawara, and H.Iwamura, *Bull. Chem. Soc. Japan*, 54(1981)3117.
- 269 M.I.Bruce, J.K.Walton, M.L.Williams, B.W.Skelton and A.H.White, *J. Organomet. Chem.*, 212(1981)C35.
- 270 R.Amstutz, J.D.Dunitz and D.Seebach, *Angew. Chem. Int. Ed. Engl.*, 20(1981)465.
- 271 P.S.Braterman and A.E.Leslie, *J. Organomet. Chem.*, 214(1981)C45.
- 272 P.P.Edwards, S.C.Guy and D.M.Holton, *J. Chem. Soc. Chem. Commun.*, (1981)1185.
- 273 E.I.Sinyavskaya, S.A.Pisareva, N.I.Tsokur, T.I.Ignat'eva, and M.P.Komarova, *Russ. J. Inorg. Chem.*, 26(1981)686.
- 274 R.Appel and K.Wald, *Z. Naturforsch.*, 36b(1981)127.
- 275 J.H.Noordik, H.M.Doesburg and P.A.J.Prick, *Acta Crystallogr.*, B37(1981)1659.
- 276 C.H.Wei and B.E.Hingerty, *Acta Crystallogr.*, B37(1981)1992.
- 277 C.T.Grainger, *Acta Crystallogr.*, B37(1981)563.
- 278 J.Elmsley, D.J.Jones and R.Kuroda, *J. Chem. Soc. Dalton Trans.*, (1981)2141.
- 279 A.Ozola, J.Ozols and J.Aoaks, *J. Struct. Chem.*, 21(1980)790.
- 280 O.Simonson, *Acta Crystallogr.*, B37(1981)344.
- 281 R.F.Ziolo and M.Extine, *Inorg. Chem.*, 20(1981)2709.
- 282 H.Schmidbaur, U.Deschler, B.Milewski-Mahrla and B.Zimmer-Gasser, *Chem. Ber.*, 114(1981)608.
- 283 H.Kobayashi, *Bull. Chem. Soc. Japan*, 54(1981)3669.
- 284 G.Weber, J.Riecke, W.Saenger and G.M.Sheldrick, *Inorg. Chim. Acta*, 54(1981)L185.
- 285 I.Shirotni and H.Kobayashi, *Bull. Chem. Soc. Japan*, 46(1977)2595.